POLITECNICO DI TORINO

Master Degree in Biomedical Engineering

Biomedical Instrumentation

Master Thesis

Event-related potentials' jitter compensation for Brain-Computer Interfaces applications

Candidate:
Marika Loglisci

Supervisors:
Prof. Gabriella Olmo
Prof. Vito De Feo

Academic Year 2019/2020

Abstract

Electroencephalogram (EEG) is a measure of brain activity that contains abundant information about human brain function. For this reason, recent clinical brain researches and Brain-Computer Interface (BCI) studies use EEG signals in many applications.

We studied a particular Event-related Potential, named *Readiness Potential*, connected to volitional motor intention, to explore cognitive functions in patients with *Disorders of Consciousness* as *Coma*, *Vegetative State*, and *Minimally Consciousness State*.

We studied the neural correlates of intention to move to investigate the self-awareness and of the environment.

In the early 1980s, B. Libet found that RP starts about *550 ms* before freely voluntary acts, but the consciousness of the act occurs about *200 ms* before the EMG onset. The *Readiness Potential* or *Bereitschaftpotential* (BP) can be distinguished into two segments: the *"early BP"*, related to the intention to move, and the *"late BP"* related to the movement itself. The BP is maximum in correspondence of the contralateral motor area to the movement, thus, it is possible to understand whether a subject is going to move the left or the right limb.

We carried out an experimental session in healthy volunteers under different experimental conditions. We detected RPs to distinguish between voluntary, semi-voluntary, and involuntary movements. We used EEGLAB, its plug-in MRCPLAB particularly, to analyse the EEG and EMG recordings. The RP is obtained by averaging the EEG over many trials, aligning the epochs by using the onset of the movement as a trigger.

Averaging is very sensitive to latency jitter, which is a timing misalignment of the epochs used to compute the RP. The misalignment is due to small changes in the brain times across all the trials and movements' onsets timing detection.

The goal of this thesis work is to implement a Matlab algorithm, based on Woody's method to compensate the jitter between trials, realigning the

epochs. This algorithm improves the averaging and enhances the RP signal quality.

To verify the reliability of the algorithm, the SNR (signal-to-noise ratio) is calculated. The algorithm about jitter compensation is added as a function of MRCPLAB.

Contents

List of figures

List of acronyms

- *BCI: Brain-Computer Interface*
- *RP: Readiness Potential*
- *BP: Bereitschaftpotential*
- *ERPs: Event-Related Potentials*
- *EEG: Electroencephalogram*
- *EMG: Electromyogram*
- *EOG: Electrooculogram*
- *ERD: Event-Related desynchronization*
- *ERS: Event-Related synchronization*
- *NCCs: Neuronal Correlates of Consciousness*
- *DOCs: Disorders of Consciousness*
- *VS: Vegetative State*
- *MCS: Minimally Consciousness State*
- *LIS: Locked-in Syndrome*
- *UWS: Unresponsive Waking Syndrome*
- *GCS: Glasgow Coma Scale*
- *CRS-R: Coma Recovery Scale-Revised*
- *SMART: Sensory Modality Assessment Technique*
- *WHIM: Wessex Head Injury Matrix*
- *DOCS: Disorder of Consciousness Scale*
- *CNC: Coma/Near Coma Scale*
- *fMRI: Functional Magnetic Resonance Imaging*
- *PET: Positron Emission Tomography*
- *SPECT: Single Photon Emission Computed Tomography*
- *TMS: Transcranial Magnetic Stimulation*

- *sp-TMS: Single-pulse Transcranial Magnetic Stimulation*

- *r-TMS: Repetitive Transcranial Magnetic Stimulation*

- *rCBF: Regional Cerebral Blood Flow*

- *PPA: Parahippocampal gyrus*

- *PMP: Pre-Motion Positivity*

- *MP: Motor Potential*

- *MRCPs: Movement-Related Cortical Potentials*

- *LRP: Lateralized Readiness Potential*

- *CNV: Contingent Negative Variation*

- *M1: Primary Motor Cortex*

- *pre-SMA: pre-Supplementary Motor Area*

- *SMA: Supplementary Motor Area*

- *PD: Parkinson's disease*

- *GUI: Graphic User Interface*

- *SCCN: Swartz Center For Computational Neuroscience*

- *ICA: Independent Component Analysis*

- *SNR: Signal-to-noise Ratio*

Introduction

The purpose of this work is to explore cognitive functions in unresponsive patients, suffering from Disorders of Consciousness such as Coma, Vegetative State (VS), and Minimally Consciousness State (MCS) through a reproducible motor command, to show a sign of awareness. Particularly, the focus was on the analysis of a specific *Event-Related Potential*, named *Readiness Potential (RP)*, connected to the voluntary motor intention. Thus, the study of this thesis is based on a better understanding of the contribution of this potential during the performance of the voluntary, semi-voluntary, and involuntary movements.

At the "Centro Puzzle" in Turin, we carried out intense research in neurophysiology and neuroscience fields. The project aims to carefully analyze the Readiness Potentials in healthy volunteers according to an experimental protocol to distinguish the three types of movements: voluntary, semi-voluntary, and involuntary, acquired by the EMG signal. The main objective of this project is to create a Brain-Computer Interface to identify Readiness Potentials, submerged in EEG signals. Brain-Computer Interfaces applications would provide patients with VS or MCS diagnosis, a means of communication with the outside world.

To calculate the Readiness Potential, we use the averaging technique. This technique consists of averaging the EEG signal on many trails, dividing the signal into epochs, which have a time window between *-5000 ms* and *3000 ms*, aligning them to the onset of the movement considered as a trigger. The averaging technique is sensitive to latency jitter, which is a timing misalignment of the epochs when calculating RPs.

A mentioned above, we create the epochs to be aligned with the EMG onset. This involves two problems: a *computational problem* is because the EMG onset is calculated roughly, so its detection does not reflect what happens at the neuronal level for different epochs, and a *biological problem* concerns the brain's response to the onset of the movement, as it can be different from movement to movement, resulting in different neuronal correlates.

The goal of this thesis is to implement an algorithm, based on Woody's method, to compensate for jitter across the trails, realigning the epochs.

The algorithm is based on the correlation among the epochs. We calculate the Pearson's linear correlation, and we assume that the brain is a linear system. So, we compute all correlations over time through the cross-correlation function.

The cross-correlation function measures the correlation between one signal and another, holding the first still, and shifting the second forward or backward in time. Our problem hypothesizes that the epochs are not perfectly aligned, so we calculate the cross-correlation function between the two generic epochs, considering as correlation the maximum of this function, which corresponds to the correlation between two signals with the best alignment.

The algorithm, therefore, implements Woody's method to improve the calculation of the RP by selecting the most correlated epochs where the final RP is obtained by the average of all the realigned epochs. We implement three methods, which develop Woody's methods, but they have some differences. *The first method* is the standard of Woody's method. This method may have a problem, namely the presence of a large artifact. What can happen is that the epoch, which most correlates with all the others, may not contain the signal but only a large artifact. So, it is not the most appropriate choice. For this reason, we choose as the initial template, the RP obtained by the average of all the not yet realigned epochs. This variation involves the realization of *the second method*. We can think that this method could be useful for patients' recordings. Although this problem was not the subject of this work, we added a further variant to the method, thus proposing *a third method*. Since patients' recordings are quite noisy, to find the RP within the EEG signal, we could use as the initial template, a signal with the typical waveform of the RP imposed by the user. Both the second method and the third method differ only from the standard one in the initial part to better calculate the most correlated epoch with the others, the rest of the algorithm proceeds in an identical way.

The thesis is divided into *five chapters*. In *the first chapter*, we explained an introduction about the basic concept of consciousness, to the point of detailing the *global disorders of consciousness*, those concerning brain dysfunctions that lead to a change in the overall level of consciousness. Their diagnosis is mainly based on behavioral assessments, considering specific assessment scales. To avoid misdiagnosis, behavioral observations are integrated with neuroimaging and neurophysiological techniques. In *the second chapter*, we illustrated the characteristics of Readiness Potential, and then we described the experimental phase that we dealt with during this thesis work. In *the third chapter*, we introduced the software used in the course of the work and the datasets taken into consideration. Finally, we explained Woody's method theoretically, and then we detailed the steps of the algorithm implemented. In *the fourth chapter*, we reported the results after computing the algorithm about the jitter compensation, with corresponding comments for each dataset examined. In *the fifth chapter*, finally, we presented the conclusions, also referring to future developments.

Chapter 1

Disorders of Consciousness

1.1 – What consciousness is

Many researchers have looked for identifying the brain's preparation action connected with a philosophical concept: *"free will"*. In European culture, since the 19th century, Descartes's fundamental own principle *"cogito ergo sum"* consisted of recognition of the primacy of consciousness about ontology and to epistemology: the perception of the world can be misleading as well as the way to know it, but you can be sure of your conscience. So, Descartes proposed that the mind selects between alternative actions, and then causes the body, through the brain, to perform the selected action. We found this concept of action in many modern societies and is a key issue of our folk psychology. However, it is incompatible with modern neuroscience, because of the dualism between mind-body [1]. The main question is: *"What is consciousness?"*. We could say that consciousness is everything that can be experienced: its absence is noted when one slips into a dreamless sleep at night and its gradual reappearance upon awakening the next day. Without consciousness, one could say, would not be an external world or awareness: perhaps nothing would exist [2]. Despite the intimate experience with consciousness, this remains difficult to explain today [3]. The term consciousness is ambiguous, associated with many different phenomena. Amid the heterogeneity of the different meanings, that are attributed to the concept, it is possible to identify common characteristics as well as a subdivision through criteria: *consciousness as a function* and *consciousness as experience.* Consciousness can be reduced to a physical and neurobiological process obtained by the interaction between the brain, the environment, and the body due to the actions among groups of neurons. In other

perspectives, consciousness becomes an irreducible and fundamental property, which cannot be a simple physical epiphenomenon [4]. The scientific community, therefore, finds it difficult to get a common and comprehensive agreement on the conceptual definition of consciousness. Nevertheless, consciousness is also divided into various phenomena, which range from relatively simple problems *"easy problems"* such as global disturbances of consciousness, which are easy to interpret for problems concerning experience *"hard problems"*, that is, how activations of neurons give life to subjective experience in the brain [3]. The simplest problems only are accessible through tools of cognitive science. There are several cognitive orientations, which deal with the concept of consciousness; they are divided into models based on theories of neural networks and theories of information processing.

The first models explain consciousness, in fact, through particular processing about information flows in modules or a process of controlling the action. On the other hand, models, based on neural networks, observe consciousness as the result of connectionist systems and networks. These theories concern models about analysis at a microscopic level, taking as their assumptions to neural architectures and, also, they propose descriptions about the activity, that is supposed to take place in the brain, at a purely functional level. From these previous theories, combing information processing with neural network theories, global approaches arise.

Over the past two decades, the role of consciousness, in neuropsychological architecture, evolved. Generally, consciousness works as a distributed and flexible system that guarantees the distribution to different non-conscious complex systems and the global access to information, that is of high value and essential for the organism.

Although consciousness is not itself an executive system, its property makes it a unifying function and has obvious utility for executive control [5].

1.1.1– Neuronal correlates of consciousness

The meaning of consciousness is not, however, the only concept that notes ambiguity and difficulty in researches for a standardized definition approved by the scientific community. Even if we try to define consciousness conceptually and devise reference models to study its functionality, another question immediately arises: *"What is the neural substrate of conscious experience?"*. The whole brain can be considered an NCC because it generates daily experience. But the site of consciousness can be further delimitated [6]. Clinical neurology observes consciousness as two major components: *the level of consciousness* (i.e., arousal, wakefulness, or vigilance) and *the content of consciousness* (i.e., awareness of the environment and the self). The area of the brain responsible for wakefulness consists of brainstem neuronal populations, previously called the reticular activating system, that directly project to both thalamic and cortical neurons. Depression of either brainstem or global hemispherical function may cause reduced wakefulness, for that matter. Awareness, conversely, involves the activity of the areas of the cerebral cortex and its reciprocal subcortical connections [7]. However, awareness necessarily requires wakefulness, but the mere latter's presence cannot guarantee awareness; despite eyes opening or the recovery of breathing function and blood circulation control, the brainstem regulation of the reticular ascending system is not sufficient, in case of severe trauma, for improvement of consciousness [2].
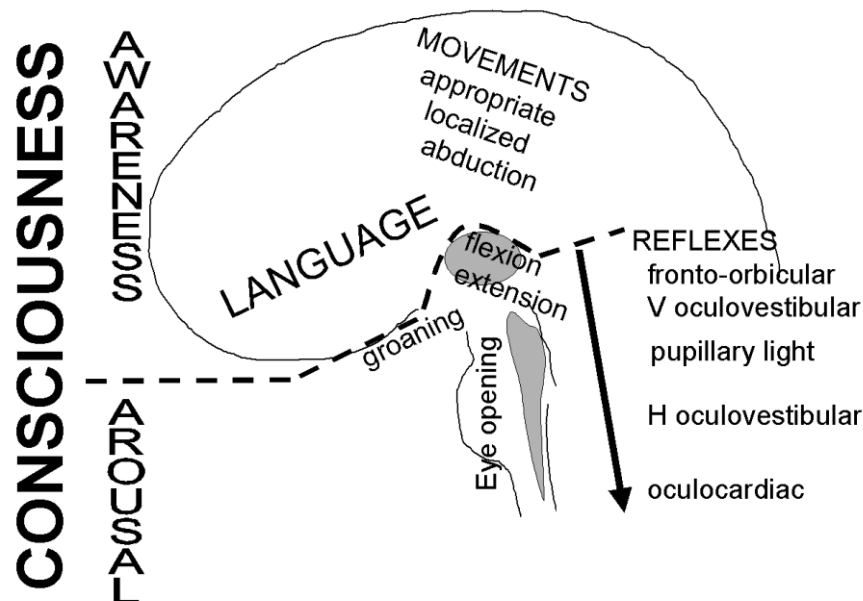
Figure 6 – A further simplified scheme of consciousness with its two main components: Arousal and Awareness. The gray area represents the reticular activating system that includes the brainstem and the thalamus; the arrow denotes the progressive disappearance of brainstem reflexes [7].

Conscious experience is the synthesis of multiple brain regions cooperation, so NCCs have been defined as the minimal neural mechanisms that are necessary and sufficient for experiencing any conscious percept, it is possible to guess the importance of the visual system corresponding to the primary visual cortex V1.

The key to consciousness functioning is to try to produce the available information of the visual scene for executive functions, then area V1 should not be part of NCCs [8]. Cognitive processes are associated with frontal lobes and area V1 has not direct projections with premotor or prefrontal regions.

1.2 – Disorders of consciousness

Disorders of consciousness (DOCs) are clinical conditions in which alterations or loss of consciousness occur, by causing a deficit of awareness of the environment and the self.

Disorders of consciousness are divided into two categories: *focal disorders* and *global disorders.* Focal disorders mean a reduction or a

loss of some particular classes of consciousness contents. Some examples of them are *neglect* that concerns the attention area, *anosognosia* for awareness and blindsight, and prosopagnosia for the visual perception area.

Whereas global disorders are observed in conditions of widespread brain dysfunction that lead to modify the general level of consciousness rather than affecting particular contents. Among these disorders, we find delirium, anaesthesia, brain damage, where consciousness can fade or dissolve in more serious conditions [9].

A DOC diagnosis is based on the presence or the absence of intentional motor reactivity, which are situations characterizing Coma, Vegetative State (VS) or Unresponsive Waking Syndrome (UWS) and Minimally Consciousness State (MCS). These disorders must be distinguished from Locked-in Syndrome (LIS) and brain death, although there are similarities between these conditions and DOCs [10].

1.2.1 – Coma

Coma is defined as a pathological state characterized by severe and long-term dysfunction of vigilance and consciousness. It is an immutable state of unconsciousness and absence of responsiveness, a transient nature normally. This disorder results from global brain dysfunction due to diffuse axonal injury after traumatic brain injury or from a lesion limited to brainstem structures involving the reticular activating system [10]. The patient in a coma lies motionless most of the time, with always eyes closing and without any awareness of the external world and self. The sleep-wake cycle is absent and behavioral responses are restricted to reflex activity only. Prolonged coma is rare as awareness usually returns within 2-4 weeks, most often evolving into VS or MCS.

1.2.2 – Vegetative state

A vegetative state is a clinical condition characterized by the complete absence of behavioral responses, which describe the presence of self-awareness (consciousness) and the environment (vigilance), with the concomitant reappearance of the sleep-wake cycle and complete or partial reactivation of hypothalamic automatic functions (e.g. cardiovascular, respiratory, thermoregulation functions) and the brainstem ones. VS derives from trauma-induced bi-hemispheric injury or bilateral lesions in the thalamus without damaging the brainstem, hypothalamus, and basal ganglia.

Patients in a vegetative state are usually not immobile; simple motor responses and fragments of spontaneous behavior can be observed, but movements are devoid of intentionality and not aimed at communication and interaction with the external world. Behaviorally, verbal intelligible responses do not occur but only moaning. Occasionally, some behaviors such as inappropriate smiling, crying, grimacing and even randomly produced single words have been reported in VS patients.

When this state lasts one month or more, VS is *persistent,* so it is a transient condition where a high rate of recovery of consciousness after one month occurs. When VS lasts more than three months after non-traumatic brain injury, and one year following traumatic etiologies, VS can be considered *permanent* [10].

1.2.3 – Minimally Consciousness State

Patients, who manage to evolve from Coma or Vegetative State, can go through a more or less transient condition: Minimally Consciousness State. It is distinguished from VS based on clear behavioral signs of consciousness at least, as the minimal ability of cognitive processing is conserved.

Command-following, recognizable yes-no responses, and understandable speeches represent the important evidence of conscious awareness. Episodes of crying or smiling, in MCS, occur concerning appropriate environmental stimuli.

Regarding prognosis, the probability of functional recovery at one year after traumatic injury is considered VS. Unlike VS, a defined temporal recovery does not exist for patients in MCS and some of them get slowly back while others remain in a permanent manner [10]. The patient is diagnosed with MCS when he can reliably communicate through verbal or gestural yes-no responses or can use two or more objects in a functional manner [11].

1.2.4 – Brain function and physiology

To differentiate VS from MCS is very difficult because both conditions are specific to unresponsive patients. Functional neuroimaging has fundamental importance to distinguish activation patterns of brain areas in the two clinical conditions objectively. Furthermore, the study of activation networks gives pieces of evidence about neuronal correlations between consciousness and the areas that are responsible for its maintenance.

Vegetative State can be assessed as a disjunction syndrome because of the detection of "functional disconnections" in the cortico-cortical areas, between the lateral frontal and median posterior areas. The recovery is also accompanied by a functional restoration of the frontoparietal region and some of its cortico-thalamus-cortical connections [12].

In contrast to VS, recent studies have been showing large-scale network activation in MCS patients when complex stimuli are administered. The functional magnetic resonance imaging (fMRI) technique was used to study two patients in MCS, discovering a cortical reaction linked to language [13].

MCS Patients show a higher rate of metabolism (55%) than VS patients in all cortical areas, although there is a significant decrease in glucose

rate in central metabolism for those with severe DOCs. The most consistent differences were found in the frontoparietal areas, including the occipitotemporal, the temporoparietal, and the frontoparietal junctions [14].

1.3 – Behavioral assessment methods

Until now, consciousness cannot be measured really by any machine. The behavioral examination is the "gold standard" for detecting symptoms of consciousness in severely brain-injured patients [10]. As noted above, consciousness is a multifaceted concept that can be reduced to two main categories: level of arousal (activation or vigilance) and awareness, based on subjective perceptions, feelings, and thoughts.

Many scoring systems have been developed to assess the level of consciousness and establish the diagnosis. The most used rating scale remains the *Glasgow Coma Scale (GCS)* in case of acute or sub-acute trauma, followed by the *Coma Recovery Scale-Revised (CRS-R)*, that is the best criteria of global DOCs evaluation. Other recommended scales are the *Sensory Modality Assessment Technique (SMART)*, the *Wessex Head Injury Matrix (WHIM)*, the *Disorder of Consciousness Scale (DOCS)*, and the *Coma/Near Coma Scale (CNC)*, with greater reservations.

Briefly below, these main rating behavioral evaluations are explained [15]:

- GCS has been developed as a support of the clinical evaluation of post-traumatic unconsciousness and is based on three components: visual response (E), verbal response (V), and motor response (M) to external stimuli.
- CRS-R was created for characterizing and monitoring patients completely diagnosed with VS or MCS. It was made up of arranged twenty-five elements hierarchically, which include six sub-scales: auditory, visual, and motor processes, motor process related to facial, language, and arousal areas.

- SMART gives a gradual assessment of sensorial, motor, and verbal responses of the patient related to a structured and regulated program of "sensory investigation". The aim of this scale is not only to optimize the brainstem activation and the level of awareness but to solicit positive and meaningful reactions in patients.
- WHIM had the objective of achieving an evaluation method, whose data could be collected by observing and testing daily life activities; support in evaluation and monitoring of all treated patients, in clinical rehabilitation. This scale effectively divides trauma moments from clinical recovery to assess progress when the patient emerges from post-traumatic amnesia.
- CNC scale measures small clinical changes in patients with severe, traumatic, and non-traumatic brain injury, characterizing VS or MCS. Its development was necessary to cope with the increase of patients in VS in long-term rehabilitation. However, CNC is not a recommended scale and can be used with greater care than previously illustrated scales.
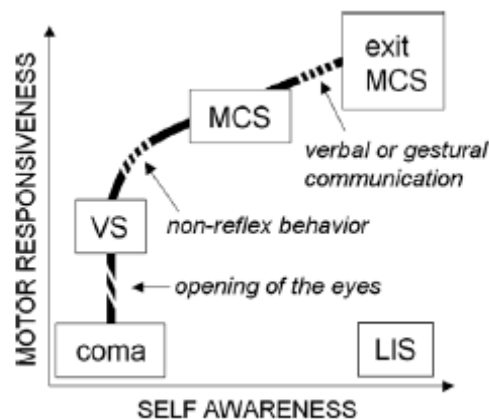
Figure 7 – Evaluation of self-awareness is based on motor responsiveness. With spontaneous or elicited eye-opening and the absence of voluntary motor activity, it has the transition from Coma to VS. The transition from VS to MCS is represented by reproducible evidence of non-reflex behavior. Exit from MCS is reported by the return of verbal or gestural communication. The Locked-in Syndrome (LIS) is an extreme example of intact self-awareness but with a nearly complete motor deficit, communicating only with eye-code [15].

1.4 – Instrumental assessment methods

The clinical assessment is based on the patient's clinical history supported by his behavioral observations. This allows clinicians to have peculiar problems to understand whether a certain behavior, which might be inconsistent or incomplete, produces a conscious or unconscious process. In fact, in a higher number of cases, this decision-making has been noticed some misdiagnoses in VS, MCS, and LIS patients. Objective behavioral assessment of minimal cognitive function can be demanding in patients with DOCs to identify motor responses or might be undetectable because no cognitive output is evident.

To address this problem, recent studies suggest a multimodal approach, which includes *functional neuroimaging techniques*, such as fMRI, PET, TMS, and others, and also *electrophysiological method* by measuring EEG signal and Evoked Potentials (ERP), with traditional behavioral scales. This approach can be used to assess cognitive functions in altered states of consciousness without having the dependency on the patient to move or speak to reveal awareness of self and the environment. It will be essential to improve clinician's ability for decreasing diagnostic errors among these conditions [16],[17].

In several cases, fMRI has been used to point out aspects of speech perception, emotional processing, language comprehension, and even conscious awareness to demonstrate that some patients retained it even if they meet all of the criteria that define VS [19]. Whilst until recently, in VS patients, either fluorodeoxyglucose PET or SPECT are used to measure resting cerebral blood flow, glucose metabolism and regional cerebral blood flow (rCBF) changes in response to auditory stimuli and visual stimuli. Most previous PET studies of VS patients have been measured resting brain metabolism and have demonstrated a mean global reduction in cerebral metabolic rate for glucose ranging from 40 % to 60% below normal [19],[20].

Although brain imaging studies were useful to explore residual cognitive function, it was unclear if the utility of these screenings would extend to groups of patients [16].

The use of electrophysiological (EEG) or brain neuroimaging (PET, fMRI) techniques are not yet included in formal diagnostic criteria of VS and MCS and is not required in the routine clinical care of patients. Several studies of brain activity and neurophysiological examinations have shown, in a subgroup of patients in VS and MCS, brain activation or neurophysiological patterns in response to stimuli-induced, despite the absence of responses to behavioral assessment [9].

1.4.1 – Brain neuroimaging techniques

For patients who retain peripheral motor function, rigorous behavioral assessment is usually able to indicate a patient's level of awareness and wakefulness. However, other brain-injured patients do not retain an intact peripheral motor system, so they are unable to respond to commands, even if they have the cognitive ability to perceive and understand them. Consequently, methods such as $H_2^{15}O$ PET and fMRI are used to associate specific physiological responses (i.e., changes in rCBF and changes in regional cerebral hemodynamics) with specific cognitive processes in the absence of any observable feedback (e.g., motor action or verbal responses).

The neuroimaging methods produce nervous system images *in vivo*, both in its anatomical and structural details (*morphological neuroimaging*) and in the understanding of the functional purpose of a certain brain area about a cognitive task (*functional neuroimaging*).

- **Positron Emission Tomography – PET**

PET is a method of Nuclear Medicine in the neurologic field and allows us to investigate brain functioning and its related neurochemical dynamics, both at rest and during the performance of specific mental tasks. It detects brain areas, in which metabolic-chemical processes are involved, by using radiopharmaceuticals.

The first studies in patients with DOCs used $H_2^{15}O$ PET to measure rCBF in a post-traumatic vegetative patient while the patient's mother read him a story. Compared with the non-verbal results, activation was

observed in the anterior cingulate and temporal cortices, which may reflect the emotional processing of the contents or tone of the mother's speech. In another patient diagnosed as vegetative, PET was used to study covert visual processing when the patient was presented with pictures of the faces of their family and close friends by observing robust activity in the right fusiform gyrus, the so-called human *"face area"*. In both cases, brain activation was observed in the absence of any behavioral responses to the external sensory stimuli. In one case of recovery from MCS, PET examinations showed an increased resting metabolism and clinical improvements in motor function, mapping cortical and subcortical regions [17].

$H_2^{15}O$ PET studies involve radiation, which may preclude essential follow-up studies in many patients or even an understandable examination of several cognitive processes. The power of PET studies to identify statistically significant responses is low and it is necessary to satisfy standard statistical criteria and was therefore less applicable to the clinical evaluation of heterogeneous DOCs [19].

- **Functional Magnetic Resonance Imaging – fMRI**

Given PET limitations, a significant development in this area rapidly switched emphasis from PET activations studies using $H_2^{15}O$ methodology to fMRI studies. fMRI is a functional technique for indirectly measuring brain activity. It is based on the level of blood oxygenation, named BOLD effect; the signal depends on changes in brain blood flow and metabolism, which are correlated with neuronal activity. MRI is more accessible than PET, it has increased statistical power and improved spatial and temporal resolution and does not involve radiation [19].

In recent work, *Owen et al.* (2006) have found that patients, who met all criteria to define VS, preserved language comprehension, and volitional reactions. In another latter study, *Di et al.* used *event-related* fMRI to measure the brain's hemodynamic response in patients diagnosed as VS and MCS, while a familiar pronounced the patient's name. It was found that two VS patients did not reveal any significant

activity, other VS patients revealed brain activity in primary auditory areas, as well as MCS patients, exhibited activity in higher-order associative temporal lobe areas. This is an encouraging result, only that it lacks cognitive specificity because this task was compared only with the attenuated noise of the MRI scanner. Therefore, the observed activation might be something that reflects a low-level orienting response to speech in general, an emotional response to the familiar speaker, or any one of the possible cognitive processes related to auditory stimuli. As a result, the interpretation depends on a reverse deduction, that is, a given cognitive process is only deduced from the observed activation in a specific brain area.

In VS patients, fMRI studies should be conducted hierarchically, beginning from the simplest acoustic processing to more complex aspects of language comprehension and semantics, to provide the most valid mechanism for assessing residual cognitive function.
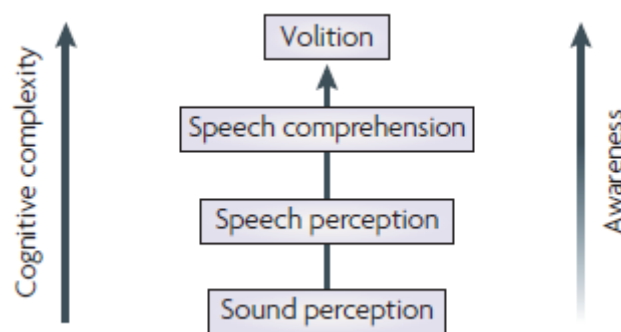
Figure 8 – A proposed hierarchical system to use fMRI for assessing residual cognitive function in VS patients [19].

Furthermore, Owen et al. have been adopted a similar principle to detect awareness in patients for whom behavioral evidence is not observable. Before doing the fMRI scan, the patient was instructed to perform two mental imagery tasks: "*imagine playing tennis*" or "*imagine visiting the rooms in his own home*". These two tasks were chosen because they involve a set of fundamental cognitive processes that reflect conscious awareness for distinguishing patterns of activation in specific regions of the brain. Indeed, an analysis of these

paradigms in healthy volunteers has permitted to identify volitional brain activity without any motor response. When the vegetative patient was asked to imagine playing tennis, a robust activity was observed in the supplementary motor area (SMA), while imagining moving from room to room in own home activated the parahippocampal gyrus (PPA), the posterior parietal lobe, and the lateral premotor cortices.

These outcomes were indistinguishable from those observed in healthy volunteers performing the same imagery tasks in the scanner [17],[18],[19].
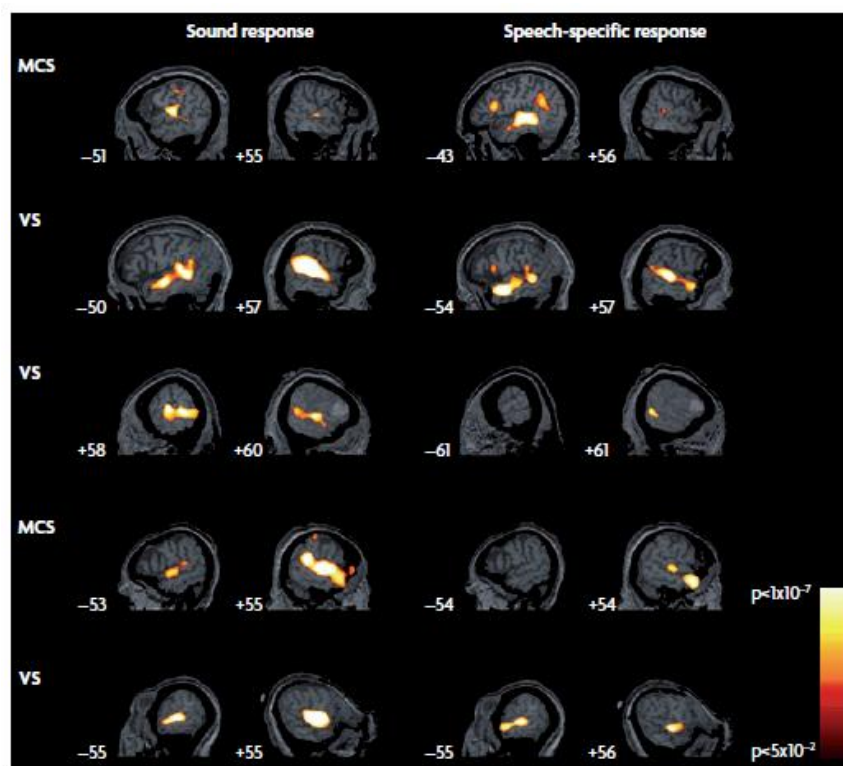
Figure 9 – It has been demonstrated that three patients with VS and two patients with MCS have residual language function both sounds and speech [19].

The future application of fMRI, as a method for evaluating patients with DOCs, is suggested to provide unambiguous evidence of the awareness preservation of self and the environment and thus to influence the diagnostic decision making [17].

- **Transcranial Magnetic Stimulation – TMS**

TMS is a non-invasive method for stimulating the cerebral cortex. In classical TMS, a plastic-coated coil of wire, placed over the scalp, generates a magnetic field, that produces a powerful and rapidly changing current. This current goes through the cranium and neuronal membrane to generate excitatory or inhibitory postsynaptic potentials.

In most experiments, stimulation is delivered to the primary motor cortex to detect motor evoked potentials (MEPs) from a muscle using surface electromyography. According to the parameters of stimulation, TMS may activate, inhibit, or interfere with the activity of cortico-cortical and cortico-subcortical networks [21].

Single-pulse TMS (spTMS) and Repetitive TMS (rTMS) are two types of stimulation, where the difference is that in the second method a train of multiple pulses at a particular frequency is applied and occur more prolonged effects on the brain. Its goal is to measure membrane excitability in corticospinal efferent neurons.

There have been very few TMS investigations in acute and chronic DOC. Until now TMS studies have focused on predicting if the patient is in a comatose state, which does not have a clear prognostic utility because of a transient absence of MEPs that can be caused by two reasons: reversible damage of motor pathways or low excitability due to treatment. While few TMS studies, to assess VS and MCS patients, are conducted in which MEP responses in most severely brain-damaged patients are revealed during the recovery period.

In conclusion, spTMS do not give sufficient information about the integrity of inhibitory and excitatory networks in DOCs, for that rTMS, particularly theta-burst, may have a therapeutic role, promoting changes in cortical excitability [21].

1.4.2 – Neurophysiological methods

Neurophysiological methods are part of electrophysiology, which is responsible for analyzing the electrical activity of different body

systems through specific instruments. Electroencephalography (EEG) is the most used neurophysiological method to record electrical brain activity, at rest, during a cognitive or sensory task, or even during sleep.

- **Electroencephalography – EEG**

Electroencephalography (EEG) is a non-invasive technique for direct measurement of brain activity and is useful in defining *critical episodes* (i.e., sleep disturbances, memory disturbances, or other transient manifestations with or without alteration of the state of consciousness); it is the essential test for making a more precise diagnosis of epilepsy. The trace is recorded through a series of surface electrodes, placed directly on the scalp, or applied through an EEG cap. In the next chapter, the characteristics of the EEG signal will be explored, while now we will focus on the usefulness of the EEG as a support technique for diagnosis in the case of patients with DOCs.

To assess awareness in patients with DOCs by using EEG-based BCI (Brain-Computer Interface), a study has been developed to occur if patients were able to modulate sensorimotor rhythms through visual feedback, auditory feedback, or both. Two motor imagery tasks (hand movement and toe wiggling) have been performed, EEG-based DOCs assessment is used to analyze Event-related desynchronization (ERD) and Event-related synchronization (ERS) distinguishing EEG patterns.

The EEG mu (8-12 Hz) and beta (13-30 Hz) bands are altered during sensorimotor processing. For that ERD is the attenuation of neuronal activity in the mu band and ERS is an increase in the beta band due to increased synchronization of neuronal activity. ERD and ERS have been analyzed for cognitive studies to provide distinct EEG pattern differences that are the basis of the left or right hand or foot sensorimotor rhythm-based BCI. During this experimental study, it has been observed a consistent activation of motor areas through sensorimotor learning session, and it has been demonstrated that BCI may provide a channel of communication for subjects, who have DOCs, in particular in patients in MCS [22].

Although the first studies conducted with the EEG instrumentation, for the assessment of DOCs, proved useless in providing support to the diagnostic process due to lack of sensitivity. The most recent work, in which sensory and cognitive evoked potentials are recorded, has been demonstrated to be more promising [23].

Short-latency evoked potentials (several milliseconds to several tens of milliseconds after a stimulus) can tell the examiner if a particular sensory pathway is working and if there is any delay in propagation of sensory signals from receptors through the ascending pathway to the cortex. When a conduction delay of the sensory path has been identified, the examiner can take advantage of this information during the evaluation, leaving, for example, more time for the patient to respond in the case of a delay along the auditory-sensory pathway.

Despite the clear utility of short-latency sensory evoked potentials and the widespread availability of EEG instrumentation in most hospitals, these simple measurements are rarely used [16].

- **Evoked-Related Potential – ERP**

Event-related potentials (ERPs) are deflections produced in the EEG trace, by calculating the means of EEG epochs, with sensory stimuli or cognitive-motor responses. The evoked potentials occur, in fact, following a sensory stimulus. ERPs are time-locked potentials to the stimulus, characterized by their amplitude and latency.

There are, however, some criticalities: first of all, the neurophysiological techniques are not standardized and therefore only allow limited comparisons with other clinical groups. Furthermore, a healthy subject sometimes does not manifest all ERP components, so even the lack of late ERP does not necessarily imply the lack of a function. The decrease in sustained attention during the test, due to length or injury to the frontal lobe, as well as serious pathologies that can increase the variability of response times, makes it difficult to detect ERPs and suggests accepting the results of new studies with caution [23].

An interesting ERP is the P300 wave which is raised through an oddball paradigm, in which there are frequent and consecutive stimuli and

some deviant or infrequent ones when a subject detects a rare and unpredictable target stimulus. The wave is defined by its peak positivity and the latency time around 300 ms and can be divided into two components: a maximum at the frontal level (P3a) and a maximum component at the parietal level (P3b). The functional significance of P300 is not yet clear, but it would reflect the termination of the cognitive period after having identified the stimulus.

Generally, it is possible to observe the P300 wave in the parietal and frontal regions, instead, its trigger originates in the brainstem structures and the thalamus. It is used in various contexts, including in the neurological-scientific field to investigate the presence of consciousness. In a recent ERP study, Schnakers and colleagues (2008) presented patients with lists of names containing their names, among others. In MCS patients, a larger P300 wave was detected in the proper name in both a passive condition and an active condition in which the patient was instructed to count the number of times he heard his name. In patients with VS, no differences were found between the active condition and the passive one [16]. The results confirmed a similar study, in which vegetative and unconscious patients exhibited a P300 component after hearing their name, albeit with higher latencies than healthy controls.

ERP studies have demonstrated some prognostic utilities for identifying patients, who might recover consciousness or progress from VS following a severe brain injury and to support diagnostic decision-making. ERPs would seem to represent an objective screening tool to spot patients who should have a cognitive function and thus would benefit from a further investigation using brain imaging techniques [16].
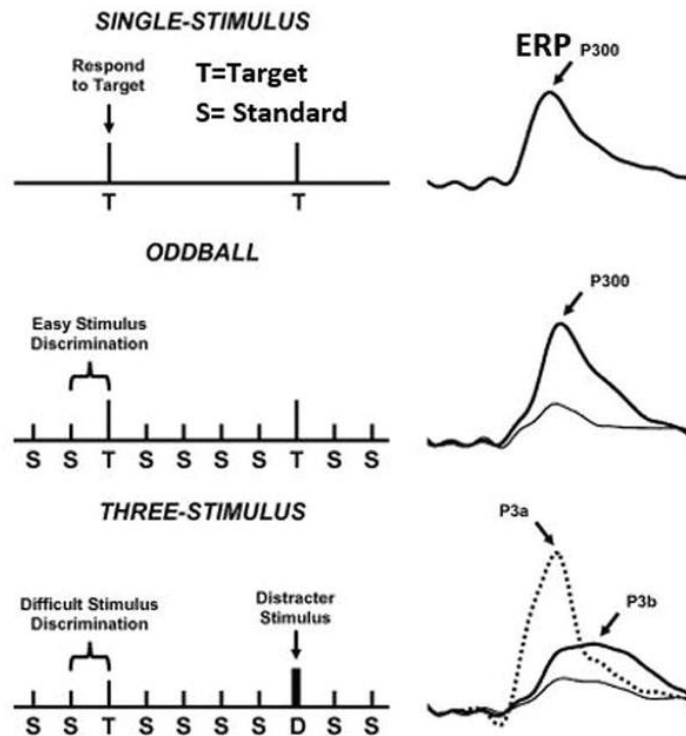
Figure 10 – Schematic account of three paradigms: single-stimulus (top), oddball (middle), and three-stimulus (bottom) with corresponding ERPs at right. The typical oddball paradigm can be presented to the subject with a computer screen or other medium to generate a sequence of events categorized into two classes: non-target and irrelevant. P3a and P3b are subcomponents of P300, in which P3a is large over the frontal/central area and P3b is maximum over the parietal area.

Chapter 2

Consciousness measurements using EEG and EMG

2.1 – Introduction

In the previous chapter, the definition of consciousness was addressed, which made it possible through the neuropsychological approach to point out the differences between the greatest global *Disorders of Consciousness* and their symptoms.

For establishing if a patient is clinically in Coma, Vegetative State or Minimally Consciousness State, clinicians have to make an appropriate diagnosis through behavioural assessment methods, that are based exclusively on the behavioural observation of the patient. Behavioural responses are essential to provide useful data to describe the patient's clinical situation but, often, these are sporadic or non-existent. However, it has been demonstrated from several studies that diagnostic errors of VS and MCS are very frequent. Therefore, differentiating the Vegetative State from Minimally Consciousness State is often one of the most difficult issues facing clinical staff involved in the care of severely brain-injured patients.

To avoid misdiagnoses and to improve clinical assessment, behavioural observations must be integrated with *neuroimaging and electrophysiological techniques* to formulate a more complete and correct diagnostic picture. Particularly to explore cognitive function in unresponsive patients through a reproducible motor command, that is a sign of awareness [25], an ERP component linked to volitional intention movement is *Readiness Potential*, on which the study of this thesis is based, to better understand its contribution during voluntary, semi-voluntary and involuntary movements acquired by electromyography (EMG), according to an experimental protocol. In

effect, there have been findings, in which they suggested EMG as a means for the awareness assessment objectively in pathologies of consciousness, through recording muscle activity below the behavioural threshold, when patients make a voluntary movement to command [24].

In *"Centro Puzzle"* of Turin, an intense research activity takes place in neuropsychological and neuroscientific fields. The project, created and described in this chapter, allows deepening the *Readiness Potentials* and its components in healthy subjects under different experimental conditions, to create a scale of measurements that allow distinguishing between voluntary, semi-voluntary, and involuntary movements. This potential is time-locked to an external stimulus due to the movement onset of the index finger acquired by the EMG signal and makes it a movement-related potential, obtained from the average of the EEG signal divided into epochs. The main purpose of the project is to develop an integrated hardware and software system Brain-Computer Interface (BCI) based on the identification of Readiness Potentials (RP) in the electroencephalographic signals to provide patients, diagnosed in VS or in MCS, an artificial communication channel to be able to communicate with the outside world.

This goal responses to a twofold need. From the diagnostic point of view, it will be possible to obtain a more precise assessment of the real state of consciousness of patients, thus being able to better identify the rehabilitation techniques; while in terms of quality of patients' life, the possibility of being able to communicate with the outside world will lead to a significant physical and psychological benefit.

2.2 – Outline of Electroencephalography

Electroencephalography (EEG) is a non-invasive technique and consists of recording the bioelectrical activity of the brain on the scalp surface through electrodes. The surface EEG can be considered as the sum of post-synaptic potentials of activated neurons synchronously. Therefore, EEG is the graphic representation of the potential difference between

an *active electrode*, detected on the site where the neural activity takes place, and a *reference electrode*, located at a certain distance from the first one [26].

Figure 6 – A typical EEG trace.

It is crucial to know the space location of electrodes exactly, to allow the right interpretation of a single recording and the comparison of results obtained between different subjects. The *10-20 International System* is the most common system to describe the location of 19 EEG electrodes through specific anatomic labels and two more electrodes are placed on earlobes (A1 and A2). This is a standardized system that refers to the fact that the distances between electrodes are always 10% or 20% of the nasion-to-inion line or the ear-to-ear distance. Each site has a letter to identify the lobe: *Pre-frontal (Fp), Frontal (F), Temporal (T), Parietal(P), Occipital (O), Central (C)*, and a number to identify the hemisphere location: *even numbers (2,4,6,8)* refers to the right side of the brain and *odd numbers (1,3,5,7)* to the left side. Electrodes in the midline are named with the letter *"z" (Fpz, Fz, Tz, Pz, Oz, Cz)*. The Cz electrode is exactly in the center between nasion and inion on the midline.
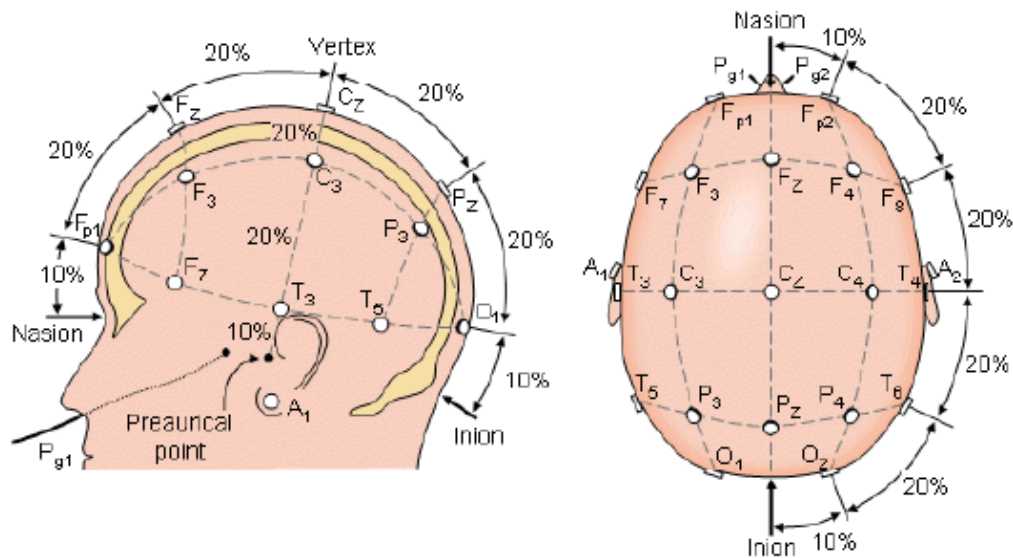
Figure 7 – 10-20 International System for electrodes' placement.

The EEG can be analyzed through *frequency-domain* analysis, also said as *spectral analysis* to obtain the frequency power distribution of a little trace of a signal. The EEG band ranges from a few Hz up to 30 Hz, indeed these rhythms can be distinguished:

Delta (δ): delta rhythm (0.1 – 4 Hz) is recorded during deep sleep and has large amplitude (75-200 μV);

Theta (θ): theta rhythm (4-8 Hz) is recorded in the state of drowsiness and some emotional states. Nevertheless, it also takes part in cognitive and working memory processes;

Alpha (α): alpha rhythm (8-13 Hz) is mainly recorded during wakefulness and is present in the posterior areas of the brain. It is more evident when the eyes are closed and in a relaxed state. **Mu** (mu) waves have the same frequency band of the alpha rhythm, connected to motor-cortex functions;

Beta (β): beta rhythm (13-30 Hz) is dominant in the states of increased arousal and concentration;

Gamma (γ): gamma rhythm (30-80 Hz) is typical of a high alert state and characterizes information processing such as the recognition of sensory stimuli and the onset of voluntary movements.

On the EEG trace, it is also possible to observe particular waves, called Event-related Potentials (ERPs), due to the administration of sensory stimuli or the performance of the motor or cognitive task.

2.3 – Evoked-Related Potential

Embedded within the EEG, however, are the neural responses related to specific sensory, cognitive, and motor events, and it is possible to extract them through an easy averaging technique. These specific responses are called *event-related potentials* because they are electrical potentials associated with specific events [27]. ERPs are, indeed, potentials because of visual, sensory, auditory, and somatosensory responses and include processes related to voluntary movement. Furthermore, the preparation of the movement produces a recognizable wave on the track before the movement performance.

ERPs provide high-resolution temporal information and ERP waveforms consist of a sequence of positive and negative voltage deflections, represented by the polarity, the amplitude, the latency, and the distribution on the scalp.

ERPs measure *time-locked* cortical function between *100* and *1000 ms* after a stimulus, represent a non-invasive technique to identify single physiological components that contribute to a selected cognitive process, and to get information about how the cortex processes signals and prepares actions.

2.4 – Readiness Potential or Bereitschaftpotential

Kornhuber and Deecke (1964) were the first authors, who discovered the slow negative electroencephalographic (EEG) activity preceding the volitional self-initiated movement on the human scalp. The experiment consisted of recording EEG, electrooculogram (EOG), and EMG simultaneously while a subject performed a repeated, voluntary flexion of the right index finger at a self-paced rate, and all data was stored on magnetic tape. Thus, by playing the tape in time reverse direction, they

performed an off-line averaging of the EEG segment that precedes the onset of EMG. In this way, Kornhuber and Deecke identified two components, one before and one after the onset of EMG: the *Bereitschaftspotential (BP)* or *Readiness Potential (RP)*, and *reafference Potential* [29].

In further investigations, they detected two more components just before EMG onset: *Pre-Motion Positivity (PMP)* and *Motor Potential (MP)*. Their finding reported that BP is slow cortical negativity and begins about *1.5 s* or more (average *800 ms*) before voluntary finger movement and it is bilateral even with unilateral movements [28]. In the last *150 ms* before the movement onset, other two potentials with different topography and polarity, PMP and MP, superimposed to BP. PMP is a bilateral potential and MP is a negative motor and the only unilateral potential before a unilateral voluntary movement.

This way, three different potentials can be distinguished before volitional finger movement: BP, PMP, and MP. The potential starts with a slow negative fluctuation (BP), which changes polarity to positivity (PMP) about *90-80 ms* before EMG onset. Over the contralateral motor cortex, additional negativity (MP) occurs about *60-50 ms* before movement onset.
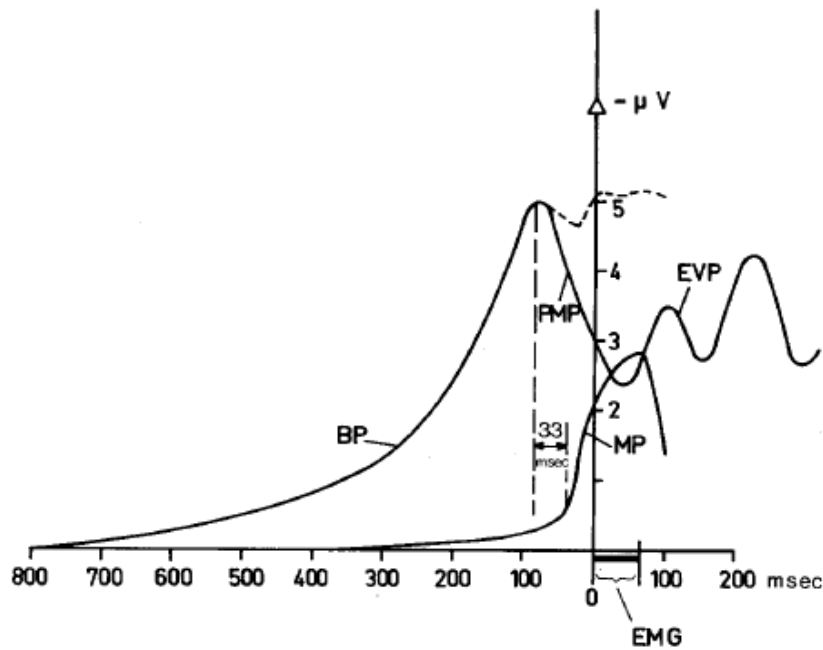
Figure 8 – Typical potential complex identifying Bereitshaftpotential (BP), Pre-Motion Potential (PMP) before EMG onset, and Proprioceptive Evoked Potentials (EVP) after EMG onset. Stippled, one of the possible variations of the contralateral potential as a superposition of PMP and additional negativity (MP-Motor Potential) before the movement onset [28].

The BP is mainly detected over the parietal and precentral areas of both sides and the midline, while over the frontal cortex it is usually absent, in most cases, or positive, but rarely negative. After *400 ms* before EMG onset, BP usually shows slightly more negative lateralization on the contralateral motor cortex than on the ipsilateral one concerning the movement side.

Since then, several studies about the *Movement-Related Cortical Potentials (MRCPs)* have been achieved about the physiological and clinical application, but it is still unknown the physiological significance of BP. Shibasaki et al. found 8 components of MRCP, before and after the movement onset, which are denominated differently: BP, NS', P-50, N-10, N+50, P+90, N+160, and P+300. Each component, except for BP and NS', was nominated as the surface polarity (P, positive; N, negative) and the mean time interval in *ms* between the peak of each component and the peak of the averaged after have rectified EMG. The interval was designed as negative or positive if the peak precedes or follows the EMG peak. The temporal position of the peak of each component, for

29

the movement onset, depending on how it was defined as the movement onset. For finger movements, EMG onset is assumed as a reference point.

Shibasaki et al. distinguished BP into two segments: the first part as *"early BP"* and the second part as "late BP".
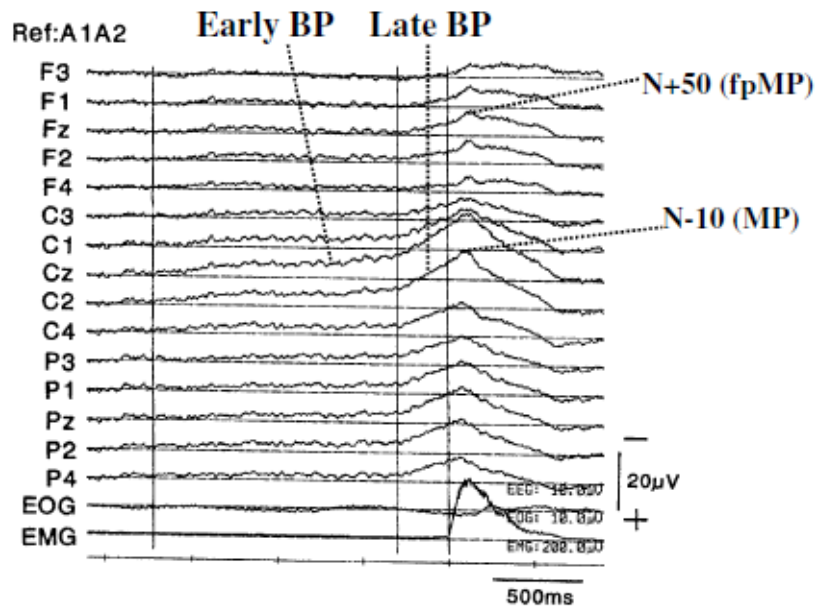
Figure 9 – Waveforms and terminology of MRCP from a single normal subject. Reference (Ref): linked ear electrodes (A1, A2). Early pre-movement negativity (early BP) begins about 1.7 s before the onset of the averaged, rectified EMG of the left wrist extensor muscle, and is maximal at the midline central electrode (Cz). Later negative deflection (late BP) starts 300 ms before EMG onset and is much larger in the contralateral region to the movement. A negative peak placed over the contralateral central area is N-10 or MP and another negative peak after N-10 is N-50 or frontal peak of motor potential (fpMP) over the midline frontal region [29].

The BP is considered an ERP as it is time-locked to an event, connected to the movement, and is an index of motor preparation. The first segment *"early BP"* reflects a set of cognitive processes such as attention, preparatory state, movement selection, intention to act which remains unconscious for a while course, whereas the second segment *"late BP"*, until getting to the *BP peak*, is influenced by the movement itself such as precision, effort, and complexity. For that, the early BP may be related to subconscious readiness for the following

movement [31] and the late BP may reflect the conscious will to act [29].

The *late BP* becomes maximum over the contralateral central area for hand movements, and at the midline for foot movements, while the early BP is bilaterally symmetrical. The asymmetric distribution of the *late BP* related to hand movements was identified by Coles [34] as Lateralized Readiness Potential (LRP), which derives from the subtraction between the potential recorded at C4 and C3, for both the left-hand movement and the right-hand movement separately.

2.4.1–The Lateralized Readiness Potential

The LRP is a measure of the lateralization of BP and reflects preferential motor preparation of one hand before the movement initiation and execution. It is derived from scalp potentials preceding limb movements. In the beginning, the RP is equally distributed over both hemispheres and becomes to lateralize before the movement onset, with larger amplitudes in the contralateral hemisphere to the movement. The lateralization is maximum over the motor cortex.

For obtaining the LRP, it is used a simple method that is, subtracting signals from the ipsilateral hemisphere to the contralateral one to the movement. For instance, in the case of the right-hand movement, the LRP is subtracting the ERP elicited in electrode C3 to the one elicited in the electrode (C4). Instead of considering C3 and C4, C3' and C4', placed *1 cm* anterior of C3 and C4, are used for the LRP recording.

Another method for calculating the LRP waveforms is the double subtraction method, in which two subtractions are performed in sequence. The first subtraction is related to both hands movements and the second one is calculated by the difference between the right-hand result and left-hand result obtained by the first subtraction. In the end, the result of double subtraction is averaged [33], [35].

2.4.2– Contingent Negative Variation

Contingent Negative Variation (CNV) is a slow negative deflection in the interval between a "Warning" and a "Go" stimulus. It is considered to reflect anticipation for the following signal and preparation to execute a command. This wave, somehow, is an index of preparation for signaled movements and expectations. The earlier segment of CNV is maximal over the frontal cortex in correspondence of "Warning" stimulus, while the latter CNV starts about *1.5 s* before the "Go" cue and reflects preparation for motor response, so it is larger over the primary motor cortex (M1). CNV is movement-preceding negativity as RP and both reflect anticipatory response, at least as far as the motor system is involved. The difference between these two signals is that CNV reflects preparation for triggered movements by sensory stimuli in a reaction time and RP reflects preparation for voluntary self-paced movements [30].

2.4.3 – Pre-movement potentials in movement disorders

The existence of BP, preceding voluntary movement, appears to have interindividual differences. In most cases, the *early BP* arises from the rostral pre-supplementary motor area (pre-SMA) without any specific site and the anterior supplementary motor area (SMA) according to the somatotopic structure and soon after in the lateral premotor cortex bilaterally with relatively clear somatotopy. While *late BP* is generated by activity in both the contralateral primary motor cortex (M1) and lateral premotor cortex with precise somatotopy. However, changes in BP can occur due to movement disorders, and the presence or the absence of a negative slope, its latency, and its amplitude, before the movement, can have diagnostic relevancy [36].

Since some part of BP originates in SMA, as said before, which receives dopaminergic input from basal ganglia through the thalamus, several investigations have been developed in patients with Parkinson's disease (PD). It has been found that the early BP was smaller in PD than in

controls over frontal electrodes, whereas there were no significant differences for the late BP. Moreover, the early BP was smaller in the off-phase of DOPA drug and normal in on-phase.

Shibasaki et al. have been studied abnormality of BP in patients with cerebellar lesions, involving the dentate-thalamic cerebellar efferent pathway. BP is usually absent in patients with degenerative diseases of dentate nucleus such as progressive ataxia with myoclonus and lipidosis, conversely, BP is much smaller or even absent for patients with cerebellar hemispheric lesions, when they move the self-paced and ipsilateral hand to the lesion.

In other researches, Kitamura and colleagues have been reported that some patients with hemiparesis due to stroke have a loss of the normal lateralization of the late BP. While during motor recovery, in other patients, the late BP is larger over the central region ipsilateral than contralateral to the movement of the paretic hand. In this way, the motor cortex of the uninjured hemisphere drives the movement of the affected hand during motor recovery. These outcomes have been also supported by fMRI and TMS studies.

Studies about BP has been applied to patients with dystonia, because of abnormalities of SMA activation and motor cortical areas. The authors demonstrated that both the early BP and the late BP were smaller for patients than control but had the same latencies, and there was not normal lateralization of the late BP.

Obeso et al. studied patients with Tourette syndrome by using the EMG onset of tics as a reference point, but they did not find pre-movement potentials, whereas normal BP before mimicking their voluntary tics was. Patients with the clinical diagnosis of psychogenic disorders have been also observed and Terada et al. found a BP like a slow negative shift of EEG before the psychogenic myoclonus, which was similar to BP before performing similar voluntary movements.

2.5 – Libet's experiment

In the early 1980s, the neurologist Benjamin Libet investigated the role of consciousness in the generation of motor action, underling the relationship between neural events and the perceived time of volitional actions or the perceived time of the start of actions.

Libet et al. measured the time when the subject was consciously aware of moving the right hand at will while he sat in front of a clock, where a spot changes direction rapidly [32]. When the clock stopped after a random interval, the subject told the position of the clock hand at the moment in which he had the first subjective experience of intending to act. This time was called *W (will)* judgment. Furthermore, he also asked to specify the time of awareness of actually moving, called *M (move)* judgment [37]. As a control, the subject was also stimulated with a skin stimulus at random times and he had to time this event *S (stimulus)*. During the experiment, EEG was recording and MRCPs were assessed to monitor the time of activity brain. They discovered an electrical potential (RP) that started about *550 ms* before the movement, but the conscious awareness of act, W judgment, occurred about *200 ms*, and M judgment occurred about *90 ms* before the EMG onset. This has been interpreted that the early slope of RP is a reflection of neuronal activity, that unconsciously prepares for the voluntary action. Therefore, our mind unconsciously plans our actions but also can afford to alter the outcome of a volitional "veto" [38].

These findings have been conducted by other authors: Haggard and Eimer observed the timing of W and compared it with the BP onset and the LRP onset moving either right hand or left hand. The LRP onset was before W judgment, and the LRP timing was similar to the late BP that indicates the beginning of asymmetry of the cortical activity according to the hand movement. It has demonstrated that the movement selection comes before the awareness [38].

The Libet clock experiment has been subject to much discussion and widely criticized. One issue is that the real voluntary action is when the participant decides to experiment, in the first place. Libet himself

discussed that his results did not negate the concept of free will. What he intended was that the movement started subconsciously but subject to veto once it reached consciousness, and this veto should be considered as free will.

Another objection is that subjective estimates of when conscious experience occurs are unreliable because the result might change as the participant divides attention between the clock and his motor preparation [39].
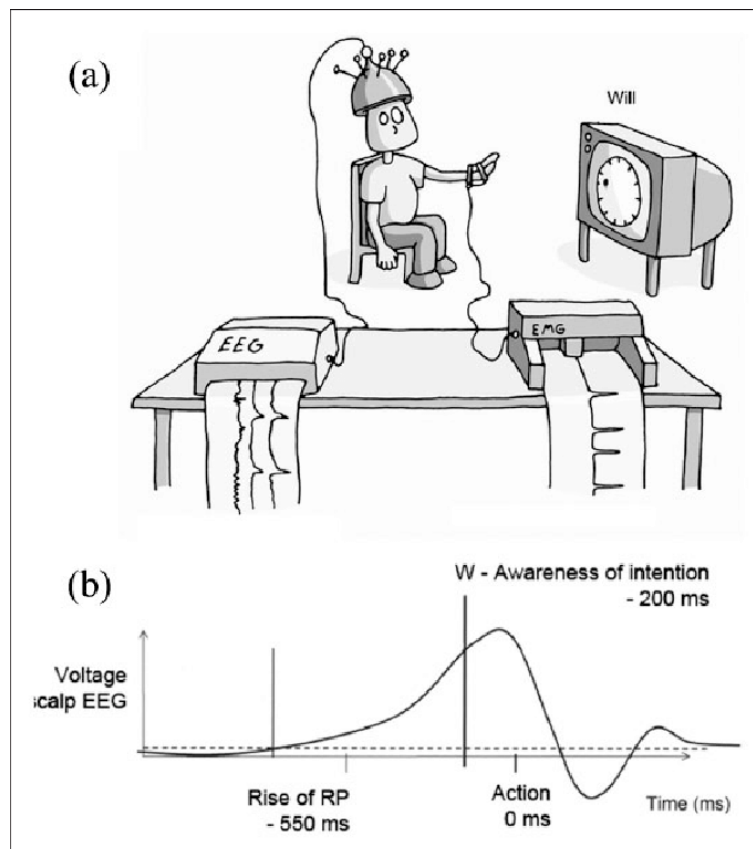
Figure 10 – (a) The Libet's experiment is represented. The participant makes a voluntary action and reports the time when he felt to move, by observing the position of the dot on the screen. EEG and EMG are acquired. (b) Readiness potential is schematized, and it begins to rise before the participant is aware of his decision to move.

2.6 – Brain areas for voluntary action

Voluntary action is viewed as a set of processes connected to specific brain areas, that therefore determine a sort of decision making. In

addition to voluntary actions, reflexes actions can also be distinguished and their difference, in how the movements originate, provides neuroscientific suggestions [32]. Voluntary actions involve the cerebral cortex, while reflexes are not cortical movements but purely spinal. Moreover, voluntary actions and are two distinct subjective experiences: the first experience concerns the planning of an act and the second one concerns the experience of agency, which is when one action is influenced by a particular external event.

The human brain has several and distinct pathways for voluntary actions. The most important component is the primary motor cortex (M1) because it is the motor and the final common track to execute commands by transmitting them to the spinal cord and muscles. Motor areas are located in the posterior side of the frontal lobe, known as the granular frontal cortex.

Before reaching M1, one input arrives at the pre-supplementary motor area (pre-SMA), which in turn receives inputs from the basal ganglia and the pre-frontal cortex. The pre-frontal areas represent the neuronal substrate, which would be at the basis of the development of the intentions, that precede and orient actions.

Several human-neuroimaging investigations have been demonstrated that the pre-SMA has more vigorous activation for self-paced actions than for triggered stimuli. The pre-SMA is a part of the frontal cognitive-network that involves premotor, the cingulate, and frontopolar cortices. In the pre-SMA, a negative and prolonged slope occurs before the volitional movement. It can be said that the RP begins with a cascade of neuronal activity that spreads from the pre-SMA to the SMA until M1, which causes the movement. Concerning SMA, M1 represents a widely complex of movements [39].

Conversely, a second cortical circuit converges on M1 and has a fundamental role for immediate sensory guidance of actions. Information from early sensory cortices is sending to intermediate representations of the parietal lobe until the lateral premotor cortex, which projects in turn to M1 [39]. In the posterior parietal areas, classified as an associative area, neuronal activity, connected to motor

acts, is observed; this means that the posterior parietal cortex has to be considered as a part of the cortical motor system. From an anatomical point of view, the parietal-frontal connections reveal a high level of specificity, and this is translated into the fact that each of these circuits appears involved in one particular sensory-motor transformation, as a description of a stimulus realized in sensory terms into one motor terms.

The frontal and the posterior parietal cortices are strongly connected and form circuits to work in parallel and integrate sensory and motor information to certain effectors. The posterior motor areas receive cortical afferents from the parietal lobe, while the anterior motor areas, from the pre-frontal cortex and the cingulate [40].

Pre-frontal and cingulate regions are important to cognitive control processes and are responsible for intentions, planning in the long term, and the choice of when to act. These regions are interconnected with medial frontal regions that are the primary source of pre-movement activity [31].
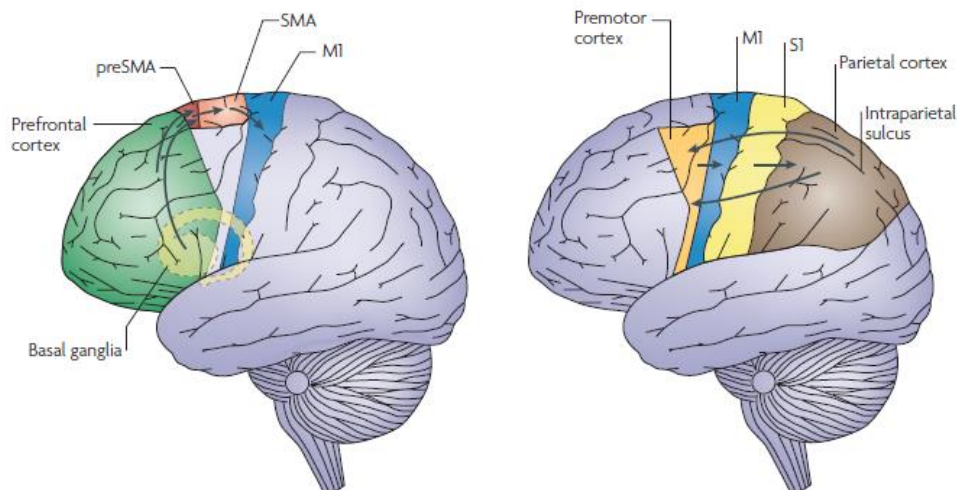
Figure 11 – The primary motor cortex (m1) receives two broad classes of inputs. First, one input reaches M1 from SMA and pre-SMA, which in turn receives inputs from basal ganglia and the pre-frontal cortex. Second, information from early sensory cortices (S1) is sent to intermediate level representations in the parietal cortex, and from there to the lateral part of the premotor cortex [39].

2.7 – Materials

During this thesis work, there has been an experimental phase performed at *"Centro Puzzle"* of Turin. The EEG recordings have been acquired on healthy volunteers, both females and males, aged between 23-26, by using *Galileo NT* and its software.

These EEG recordings were acquired by using an EEG cap with 34 passive *Ag/AgCl* electrodes, to which the two earlobes electrodes are added. The EEG datasets were recorded with a sampling frequency of *512 Hz*. During EEG acquisition it was possible to record EOG, placed two adhesive electrodes above and below each eye, to improve the removal of ocular artifacts. Inspired by the movement that Libet made in his experiment, it was decided to have the subject perform the movement of a finger by recording an EMG signal. The start of the finger movement was monitored through the placement of two adhesive electrodes on the front and the back of the second phalanx of the index finger.

2.7.1– Experimental protocol

The healthy volunteers had to perform three tasks in every experimental session:

- **Voluntary task**: the subject was instructed to bend the index finger. The firm movement had to be made during a time window of about *10 s-13 s*, started by an acoustic signal. This experiment is intended to choose the timing of the movement and not to feel the urge to move this movement is "self-paced".

- **Semi-voluntary task**: was performed a flexion of the index finger, but this time the subject has to move correspondence of an acoustic signal, as soon as it is heard. Contrary to the voluntary task, this experiment is "cue-based" because of the external trigger.

- **Involuntary task**: the patellar reflex is elicited in correspondence of the tendon with a reflex hammer. For this task, an acoustic signal is only heard by the experimenter wearing headphones, so that the subject does not expect the moment when the stimulus occurs.

  Starting from the first movement to the last, the degree of will decreases, in fact in a reflex, the control of the voluntary muscles is greatly reduced.

Every session is composed of 40 trials for each task and the acoustic signal is randomized to avoid the adaptation of the brain.

The acoustic signal is emitted by a device *LabJack* and is converted into a voltage signal through LabJack's DAQ to synchronize it with the EEG tracks. To organize the experiment, the software *OpenSesame* was used, which allowed the experimenter, through a GUI, to choose the task and the respective number of repetitions that the subject will have to perform.

2.7.2 – Experimental Setup

Figure 12 – Materials used during the experiment.

- Data Acquisition device: Galileo Suite, EB Neuro with amplifiers BE (Brain Explorer);
- The device of processing and display the EEG traces PC with Galileo software;
- The device with the stimulation system: PC with OpenSesame for the acoustic signal and the use of LabJack;
- Synchronization system: Labjack and photocoupler circuit;
- Recording tools: EEG cap, adhesive electrodes (4 for EOG signal and 2 for EMG signal), the ground electrode for EMG (for the wrist: voluntary and semi-voluntary tasks and the ankle: involuntary task), 2 earlobes reference electrodes for EEG;
- Additional accessories: TEN20 (conductive paste), NUPREP (abrasive paste), conductive EEG gel, a syringe with a blunt needle.

2.7.3– The preparation stage

The preparation stage is the longest but also the most important, as it allows to obtain a legible EEG trace.

During the experiment, two computers are used: a computer, in which is present OpenSesame software, is useful for starting the task and emitting the acoustic signal, the other one, in which there is Galileo software, is used to visualize, process, but also export subsequently, the acquired signals are connected to the EEG head.

The volunteer is made to sit on a raised chair to prevent the feet from touching the floor, to simply achieve the involuntary task, that is the patellar reflex. Furthermore, the subject is seated behind the computer, which contains Galileo software, while the second computer is placed on the table turning left from the position in which he is sitting, so as not to be influenced in any way during the experiment.

Immediately thereafter, the preparation for signal acquisition began. First of all, the electrodes for EOG and EMG recordings are placed using the TAN20 paste and then the earlobes and the wrist (or the ankle for

the involuntary task) electrodes are mounted respectively, always using the TEN20 conductive paste.

Once these electrodes are in place, the EEG cap is set on the head, trying to position the Cz electrode in the center between Nasion and Inion and also between the two earlobes reference electrodes. After placing the cap, the skin is cleaned, using the Nuprep abrasive paste, to remove sebum and dead scalp cells. Then, the inside of the cap electrodes is filled with the conductive EEG gel, through a syringe with a blunt needle.

The conductive EEG gel is used for two reasons:
- to improve signal conduction, lowering the electrode impendence to obtain a good electrode-skin contact;
- to improve adhesion with the skin, avoiding any problem of detachment caused by movement.

Before acquiring the EEG signal, the experimenter has to check that the electrodes' impendence does not exceed a certain threshold value, equal to 10 kΩ.

After finishing the experiment, the materials are cleaned, because dry gel residues on the electrodes can be a source of noise, using alcohol for earlobes and wrist (or ankle) electrodes and only water for the EEG cap.

Chapter 3

Jitter compensation

3.1 – Introduction

EEG data contains functional brain information, so EEG analysis has recently been utilized for many applications such as BCI, human cognition studies, diagnosis of diseases such as seizures, and epilepsy detection. EEG signals usually contain significant noise caused by background noise and system noise, so signal processing is necessary to improve SNR (Signal-Noise Ratio) for EEG analysis.

We dealt with typical potential RP, which is Event-related potentials, measured by averaging many trials, that represent a brain's response to the index movement. Averaging trials reduce noise power, thus enabling enhancement of the ERP signal SNR because ERP has the signal waveform in the trials if there is no time delay error in them; but the background brain activities, that are not related to the event, are independent in each of the trials. Therefore, the variable time delays, also called latency jitter, of each of the trials can cause the misalignment of them, thus affecting the ERP waveform and signal quality. Some studies have been reported that latency jitter is a problem that contaminates the averaged ERP waveform. To solve this problem, it is proposed an algorithm, based on Woody's method, which iteratively calculates the cross-correlation between each trial signal and a template or a reference signal, where the template is obtained, by averaging the trial signals whose the time delay is shifted by the delay estimated in the previous iteration.

3.2 – Software

The Galileo NT is the instrumentation software and allows to show the EEG raw data in real-time and to export in a different format, to make them usable for subsequent processing. We have chosen to save them in "*.asc*" format, with a sampling frequency of *512 Hz* and saving all acquired channels. Subsequently, the treatment was carried out using Matlab 2019a, an environment for numerical computation used for data analysis. It is based on programming language C, created by MathWorks, used for simple commands: manipulation of matrices, the creation of graphics, and, generally, data manipulation.

3.2.1– EEGLAB

It was particularly useful for EEG data analysis EEGLAB, an interactive Matlab toolbox, edited by Swartz Center for Computational Neuroscience (SCCN) [41]. EEGLAB is used for the processing of bio-potentials: continuous and event-related EEG, MEG, and other electrophysiological data. It allows to carry out analysis using a variety of functions for filters application, artifacts rejection, event-related statistics and averaging, data visualization, and other complex functions like time-frequency analysis and independent component analysis (ICA) decomposition.

Furthermore, EEGLAB provides a Graphic User Interface (GUI) for visualizing event-related brain dynamics and for storing and manipulating event-related EEG data through functions already implemented, or you can write and run scripts customized to perform the analysis in real-time and automatically.
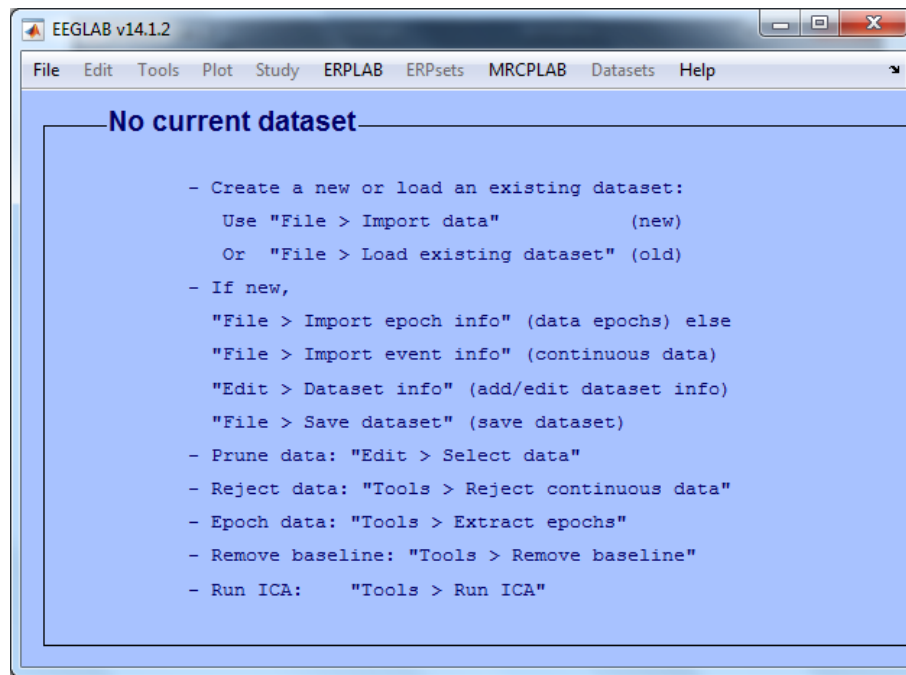
Figure 13 – EEGLAB GUI.

3.2.1– MRCPLAB

To elaborate EEG data, acquired by our software Galileo NT, a plug-in for EEGLAB has been developed. This plug-in allowed us to integrate all the algorithms employed with EEGLAB and also adding other useful functions to analyse the signal automatically, as mentioned above, aimed at a correct identification of the RP.
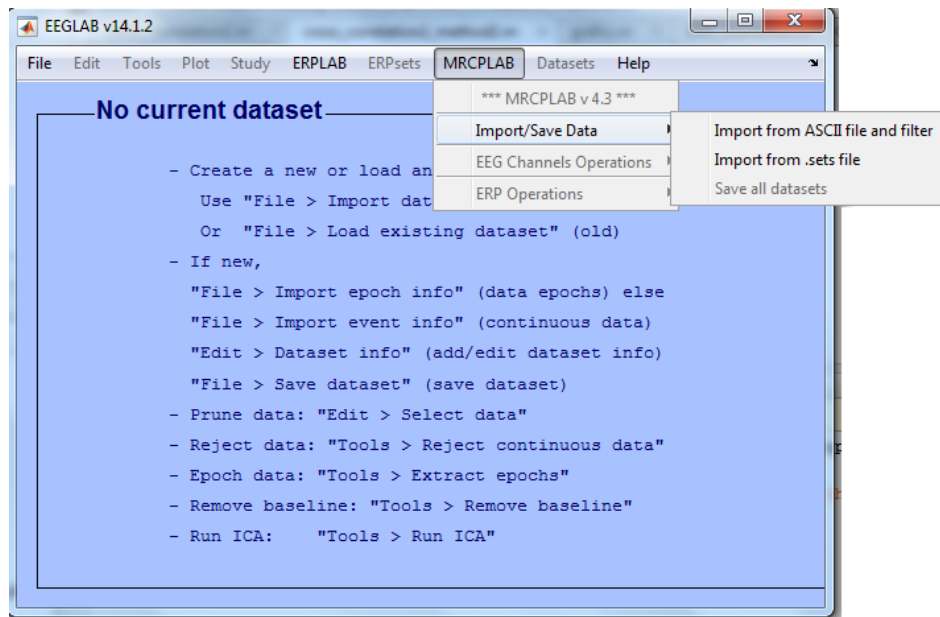
Figure 14 – MRCPLAB menus.

In particular, as you can see in figure 2, from MRCPLAB there is a drop-down menu in which the element "Import/Save Data" is used to import a dataset in the format produced by the software with the ability to save all datasets in *".set"* format and make it compatible with EEGLAB. Another element is "ERP Operations", where once the dataset is imported, through the "ERP Computing" command it is possible to compute the Event-related Potential and also to visualize them through "ERP Viewer".
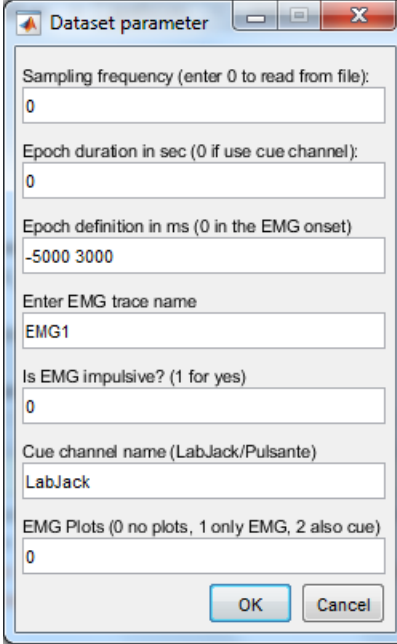
3.3 – Data Analysis

When you choose to process a dataset in *".asc"* format, an interactive window opens, which asks the user to enter some information such as:

- the sampling frequency;
- the duration of the epochs, in seconds, in which split the signal, which is to 10 s if considering datasets acquired before June 2018 or entering zero if using the cue channel (Labjack signal) for datasets acquired from June 2018;
- the definition of epochs, in milliseconds, which is already set;
- the channel on which to detect EMG signal, which will be channel 1 (EMG1) or channel 2 (EMG2). While in the experiments

conducted during this thesis, the channel "Pulsante" was used for the acquisition of the EMG signal, as there was too much noise in the two channels dedicated to EMG trace;

- the cue channel name, which is Labjack for experiments conducted on healthy volunteers;
- as the last option, we can choose whether or not to display only the EMG trace or both the EMG trace and also the cue signal.

Figure 15 – Interactive window for dataset parameter.

After selecting these parameters, data is acquired, filtered, and saved in a structure array that contains all information regarding the dataset. The information is also reported in the GUI.
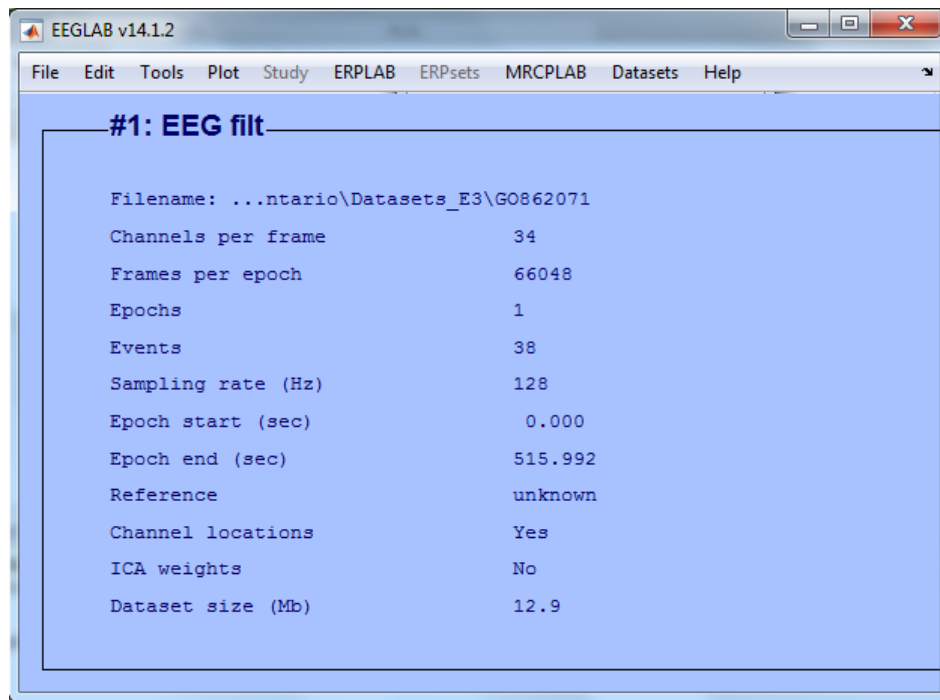
Figure 16 – GUI with the parameters of the dataset in question.

Among this information, there is also that about *channel locations*. If in a file, the dataset channel names are known, locations can be found automatically in space providing a file *Standard-10-5-Cap385.sfp*, that is a database of 385 channel labels known.

This file is already present in EEGLAB and the coordinates of each electrode are expressed in the Cartesian system.

Through this program, it is possible to view the time course of all the EEG traces, corresponding to the 34 electrodes recorded, together with the right and left EOG traces.

3.3.1– Dataset classification

During this thesis work, the datasets, present in the database, acquired from June 2018 were examined. All these acquired datasets are divided into each task (voluntary, semi-voluntary, and involuntary), performed during the experimental session.

Before processing them, a classification is made by visual inspection, based on the EMG signal and the cue signal.

In the figures, we showed both the EMG and the Labjack signals. In the plot, the EMG signal is represented by the blue curve, while the magenta one represents its variability; on the other hand, the Labjack signal is represented by black vertical lines that indicate the instant in which the temporal window begins, within which the flexion of the index is performed.

To assess the quality of the EMG signal, we looked at the variability of the signal itself and also how noisy it was. In addition to these two criteria, the movement onset was also observed, which is represented by a green dot. When the movement is performed through a wide and a determining flexion, we noted that the green dot is well seen on the plot and it is not overlapped by the rest of the signal trace; as it may happen that if the EMG signal is too noisy and the movement onset is not well done, the software may not detect the onset correctly. The Labjack signal is not always present, this is because the device Labjack, which is connected to the EEG head, produces noise caused by interference ratio such that the software fails to detect.

After having observed all plots, both the EMG signal and the Labjack signal were evaluated on a scale ranging from 0 to 3, where 0 indicates that signals have poor quality, while 3 indicates the opposite. Then all the datasets have been renamed as follows:

Name subject_AJ_task_E(0->3)_L(0->3)

- The name of the subject indicates the anonymized name of the volunteer;
- AJ indicates that the experimental session came after June 2018;
- Task is: V=voluntary, S=semi-voluntary, I=involuntary;
- E indicates the EMG signal and numbers from 0 to 3 are the scales of the quality evaluation of signal;
- L indicated the Labjack signal and numbers from 0 to 3 are the scale of the quality evaluation of the signal.

After that those datasets, which have a good quality of the EMG signal, equal to 3 on the rating scale, were taken into consideration for this thesis work carried out.

3.4 – Methods

The EEG data acquired are imported in MRCPLAB using Matlab function *importtoEEGLAB.m* and it is used the EEGLAB structure.

First of all, it is used the element ERP Computing, through the MATLAB function *epochandfilter.m.* Through this function, not only ERPs are calculated automatically, but before them, other datasets are created in which the entire EEG trace is divided into epochs, extracted using the EEGLAB function *pop_epoch*. Thus, each epoch has a time window ranging from *-5000 ms* to *3000 ms*, which has been aligned with the EMG onset as time reference at time 0. For all datasets the sampling frequency is down-sampled from *512 Hz* to *128 Hz,* to avoid the *aliasing* phenomenon, they are also filtered. First, the EEG signal was pre-processed with a 0.016–70 Hz bandpass filter (12dB/octave), with an amplifier band-pass from 0.001 to 100 Hz and a 50 Hz notch filter, then, a low-pass filter with cut-off frequency at *40 Hz* and a high-pass filter with cut-off frequency at *0.05 Hz*.

Therefore, ERPs are calculated by averaging all epochs extracted, aligned with the EMG onset. Before proceeding with the jitter compensation algorithm, all epochs with evident artifacts are discarded, because artifacts can cause an incorrect interpretation of the ERP waveform and also an incorrect delay time between an epoch and another one. This procedure is computed through EEGLAB, in which first we have been observed the time course of the entire EEG trace, and then, by using the EEGLAB *Edit menu*, through the element *Select epochs or events*, all epochs to be deleted have been selected. In this way, finally, another dataset was created, containing all epochs except those with artifacts.

Since the RP is detected over the sensorimotor cortex, including Pre-motor and Motor areas, in correspondence of the pre-SMA, the SMA,

the premotor motor cortex and M1, over the Frontal Lobe and the Somatosensory Cortex over the Parietal Lobe, 7 channels are considered: Cz, C3, C4 for the *Motor Area*; Fcz, Fc3, Fc4 for the *Pre-motor Area* and Pz for the *Somatosensory Area*.

3.4.1– Jitter compensation in computing RP: Woody's method

Woody's method was proposed by C.D. Woody in 1967 to deal with latency jitter for unknown signals. It iteratively calculates the cross-correlation between each trial signal and a template or reference signal where the template signal is the mean of all trial signals whose delay is shifted by the delay estimated in the previous iteration.

The method can be illustrated as follows [42]. Considering the signal model for an EEG channel, $x_i(n)$, that represents the amplitude of the ith iteration at time sample n ($0 < n < N$), i =1,.., I, where I is the number of trials. Each epoch contains an unknown transient template $s(n)$, delayed by d_i, as $s_{di}(n) = s(n - d_i)$, plus $e_i(n)$ epoch's noise.

$$x_i\ (n) =\ s_{di}(n) +\ e_{di}(n)$$

Thus, the delay d_i derives from iterative correlation and averaging the data signals: given an initial estimate $\hat{s}(n)$ of the template and the epochs $s_i\ (n)$, the delay d_i for ith trial is estimated as:

$$\widehat{d_\iota} = \arg\max_{d_i}\frac{1}{N}\sum_{n=1}^{N} x_i\ (n)\ \hat{s}_{d_i}\ (n)$$

where N is the number of data samples for each trial.

At 1st iteration, the initial template coincides with the signal corresponding to the 1st most correlated epoch and this epoch is not more considered among all epochs to discriminate. At 2nd iteration, the cross-correlation among epochs is computed, and then epochs are sorted again in descending order, according to the mean value of the epoch's cross-correlation. In this iteration, the maximum of cross-

correlation between the signal, corresponding to the 1st most correlated epoch, and the signal, corresponding to the 2nd most correlated epoch gives the estimation of the delay $\widehat{d_2}$. Once estimated the delay $\widehat{d_2}$, the 2nd epoch is shifted in time by its delay $\widehat{d_2}$. Thus, the new template is estimated again as the mean between the first two most correlated epochs, where the 2nd epoch is corrected in terms of delay. Note that, at 1st iteration the delay $\widehat{d_1}$ estimated was zero because it comes out from the computation of the maximum cross-correlation between the 1st most correlated epoch and epoch itself. Then, a new ith iteration from 2 to I begins computing again the cross-correlation among epochs, and sorting epochs in descending order, according to the maximum value of epoch's cross-correlation, without considering the last corrected epochs in terms of the delay.

The template at ith iteration is estimated as the mean of the most correlated epochs corrected in terms of the delay at ith iteration and the previous corrected epochs. The last template at Ith iteration is the average RP computed with Woody's method. This method is based on an iterative repetition of correlation and averaging [43].
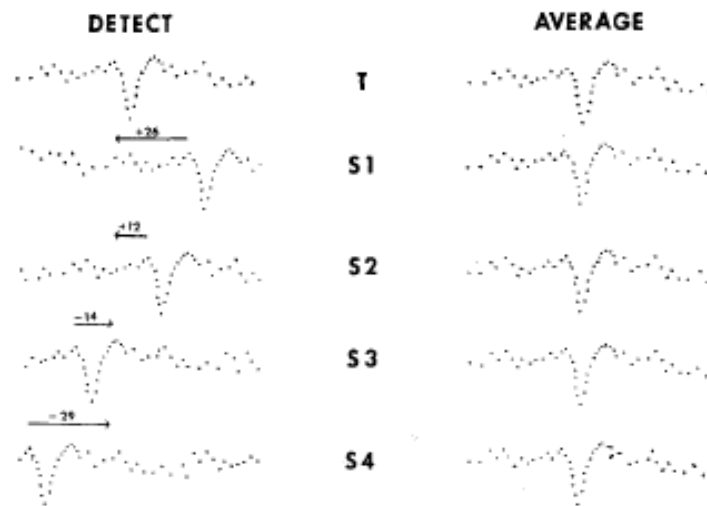
Figure 17 – Samples (S1-S4) are cross-correlated against template (T) and shifted an appropriate amount of time (arrows). After being shifted the samples are averaged [43].

3.4.2– Woody's method: Matlab function description

As described above, the algorithm is based on the correlation among the epochs. The correlation which is calculated is Pearson's linear correlation. Pearson's correlation has the advantage of being very simple and quick to calculate, while it has the disadvantage of capturing only linear relationships. So, it is assumed that somehow the brain functions as a linear system. This is a good approximation. Therefore, we calculate all possible correlations over time through the cross-correlation function.

The cross-correlation function measures the correlation between one signal and another, holding the first one still in time and shifting the second one temporally, both forward and backward in time. As mentioned above, the correlation is calculated between the epochs of a specific signal. These epochs have been created so that they are aligned with the onset of EMG. This process involves two types of problems:

1. *A computational problem*, that the epochs are aligned with the onset of the EMG, but this onset is calculated approximately by an appropriate algorithm. This algorithm consists of evaluating

52

the slope of the EMG, when the slope exceeds a certain threshold, the onset of the EMG is detected. This detection does not necessarily reflect in the same way for all epochs, what happens at the neuronal level. What we call the onset of the EMG is not necessarily the same at the neuronal level for different epochs.

To solve this problem, we hold one epoch still and we shift the other one by obtaining the correlation among the epochs in time, that is, we calculate the cross-correlation. What we are interests in is finding the shift that gives us the best correlation, that is to find the maximum of the cross-correlation function. For this reason, we define as a correlation between two epochs the maximum of the respective cross-correlation function.

2. *A biological problem* concerns the brain's response to the onset of the EMG, that is, at the onset of the movement. This response can be different from situation to situation, from movement to movement, that is, from epoch to epoch, thus obtaining different neural correlates. Also for this problem, we use the method explained above.

Since the epochs are not perfectly aligned, as a hypothesis of our problem, we calculate the cross-correlation between the two generic epochs. We take the correlation between the two generic epochs as the maximum of the cross-correlation function because this corresponds to the correlation between the two signals with the best alignment.

Therefore, from this moment on, we will call a correlation among the epochs, the maximum of the cross-correlation function among them.

The function implements Woody's method to improve the calculation of the ERP, selecting the most correlated epochs. Three methods have been implemented, which develop Woody's method but have some differences. First, let us start with the first method, which is the standard one.

The implemented Woody's method will be illustrated below, step by step.

1. First, a correlation matrix is created among all epochs. All possible correlations between the generic epoch i and the generic epoch j are calculated. The most correlated epochs are chosen because all epochs are supposed to contain more or less the signal, so on average, the epochs are correlated with each other. If instead, there are epochs with artifacts, these epochs do not correlate well with the others.

   Hence, the most correlated epochs are those that contain more signal and less noise from artifacts. Starting from the correlation matrix, we try to understand how much each epoch is correlated on average with all the others. For this reason, we associate to every epoch the median of correlations with all the other epochs. We use the median because it is an operator less sensitive to outliers than the mean.

   At the end of this step, we take the epoch with the highest median value.
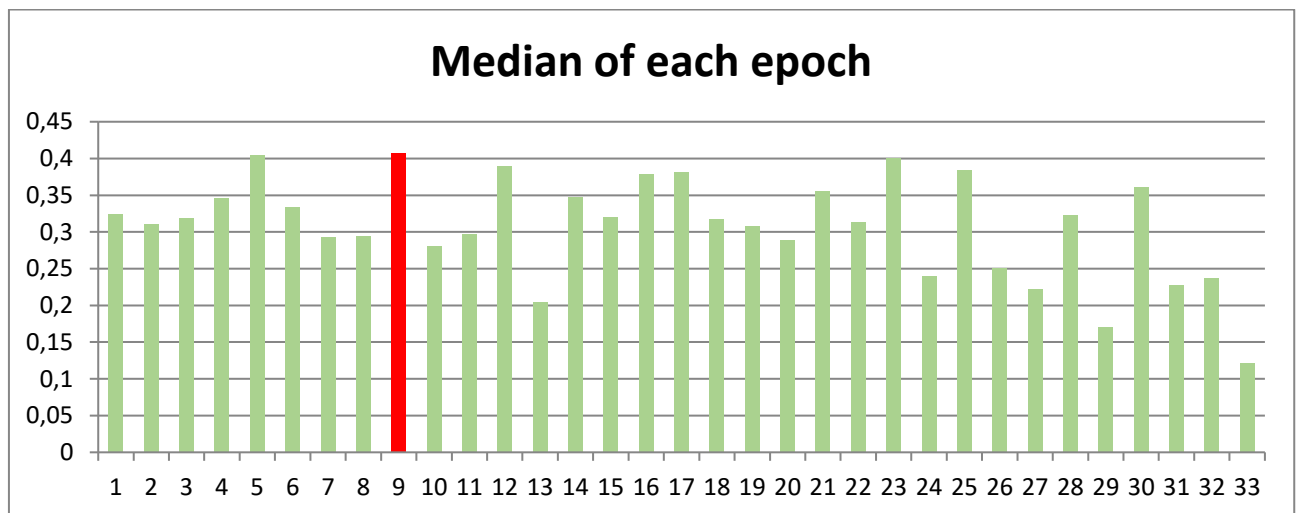

Figure 18 – It was considered a dataset consisting of 33 epochs. After having constructed the correlation matrix, in which the maximum of cross-correlation function between two generic pairs of epochs is reported, in the last column the median of each epoch is calculated. As we can see from the histogram, epoch number 9 has a median value, equal to 0.4078, higher than the other epochs.

2. The second goal of the algorithm is to find, among all the remaining epochs, the most correlated epoch with the one chosen at the previous point. This result can be obtained directly from the matrix that we have calculated previously.
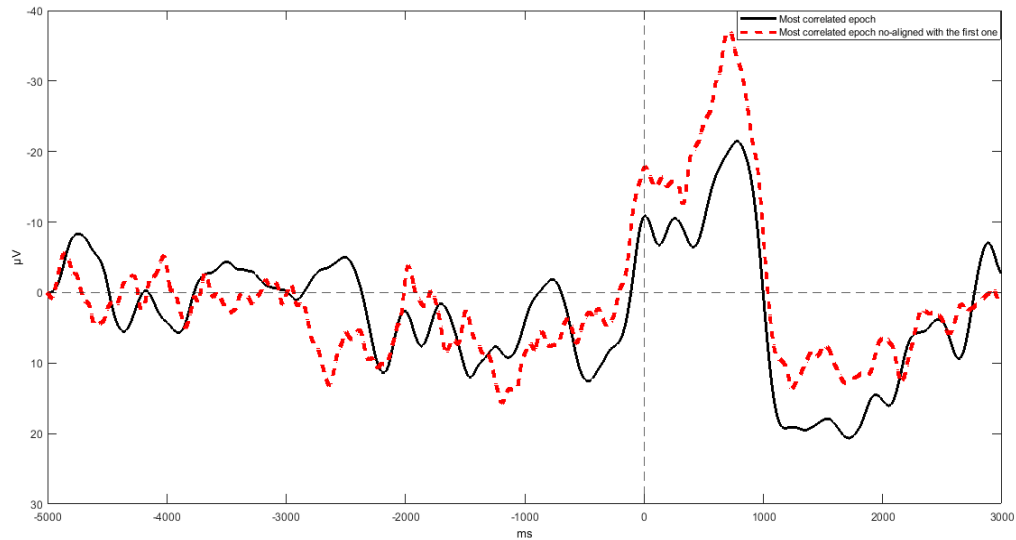

Figure 19 – The following figure shows the two signals corresponding to the first two most correlated epochs: the black signal corresponds to the most correlated epoch, while the red dashed signal corresponds to the most correlated epoch with the first one, which is the number 5. The second epoch is not aligned to the first one, it shows a delay, equal to -7.

3. At this point, we evaluate the time delay between the two epochs considered and realign them by shifting the second epoch for the first one. By computing this time shift, there will be no samples at the beginning or the end of the shifted epoch, depending on whether the shift occurs to the left or the right. In that case, we will add dummy samples equal to the value of the last sample.
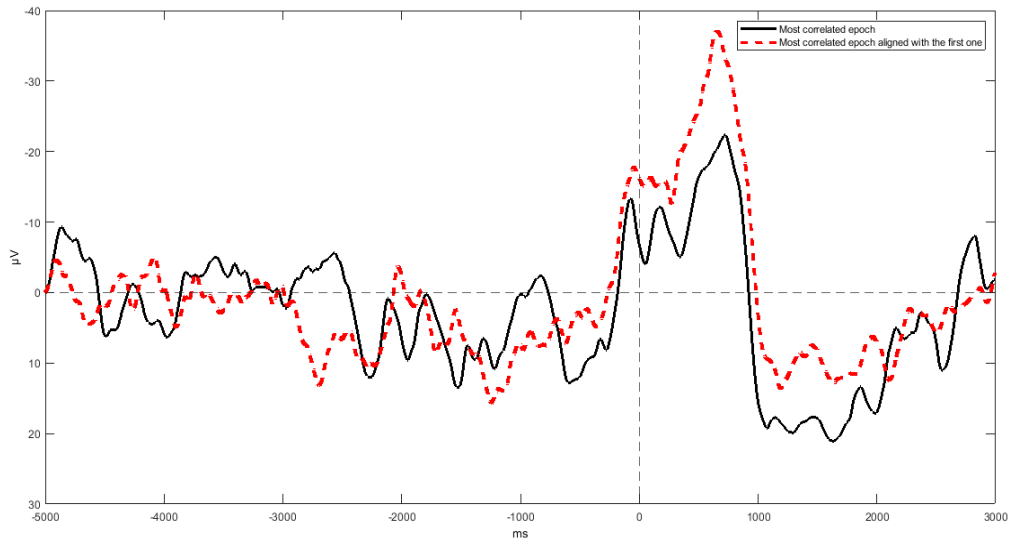
Figure 20 – The red dashed signal, corresponding to the most correlated epoch with the first one, was aligned with the signal of the most correlated epoch. Since the time delay was negative, the red signal was shifted to the left.

4. To verify if the alignment has happened correctly, the cross-correlation function is recalculated between the epochs considered, the latter must have the maximum of the cross-correlation in zero.

In practice, there may be some cases where this does not happen, as in theory, the cross-correlation function may be an increasing function towards one of the two ends of the epoch: the right one or the left one. Therefore, by aligning the epochs this *"edge effect"* could cause another non-zero delay value for which the correlation is still higher. In general, epochs with such an *edge effect* must be discarded because certainly, this correlation is spurious and probably due to some artifact. However, it is possible to have very noisy signals, so this *edge effect* is present but not particularly significant. It is verified if the maximum of the cross-correlation function, although not in zero, does not differ so much from the value in zero. If this difference is less than *10%,* the epoch is still kept. This *10%* value can be controlled by the user.

5. Once the correct alignment is verified, the average between the two epochs is calculated, thus obtaining the first template of the RP.
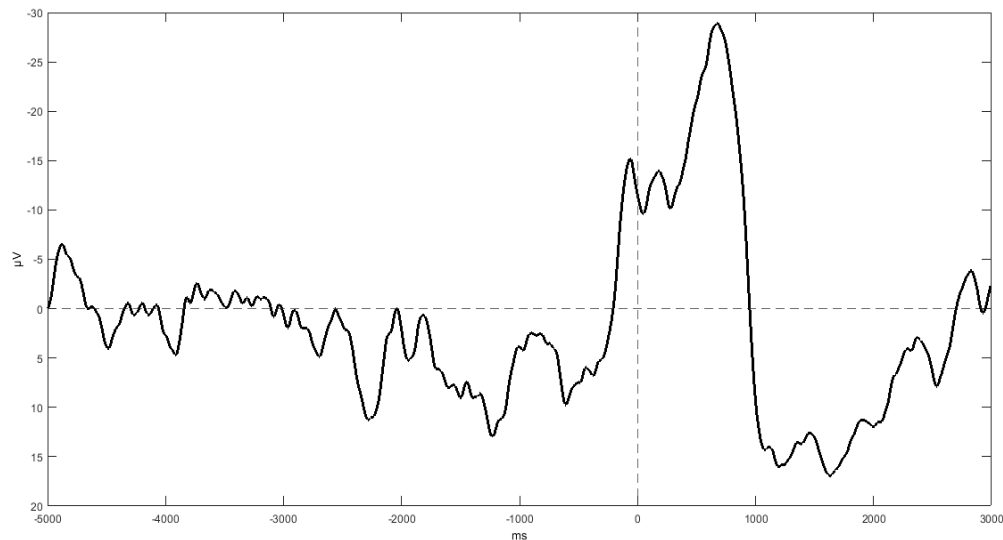

Figure 21 – In the figure, the first template of the RP is represented, obtained by averaging the two epochs.

6. At this point, we repeat the illustrated procedure, recalculating the cross-correlation function between the first template of the RP and all the remaining epochs. At each iteration, a new epoch is added to the epochs to be averaged to calculate the new template. The only case in which a new epoch is not added is obviously when such an iteration has a great edge effect, as described above. In this case, the epoch is discarded.

7. In theory, the iterations continue until the epochs are exhausted. In practice, however, if the correlation between the template and all the remaining epochs becomes too small, that is less than a certain threshold, set by the user, the iteration is interrupted. If the average correlation among the epochs is initially very low, a particularly high threshold cannot be set otherwise all the epochs would be discarded. An appropriate value of this threshold is calculated from the initial correlation matrix among all the epochs, in which we also calculated the median of the

correlations of each epoch with all the others. From the distribution of all these medians, the median and the standard deviation are, in turn, calculated. The iterations end up when the correlation is too far away from the median of this distribution. In particular, we have chosen to terminate the iterations, when the correlation between the current template and all the remaining epochs is less than the difference between the median of the distribution and its standard deviation, multiplied by *1.5*. This value of *1.5* can also be changed by the user.

8. At the end of the iterations, the definitive RP is calculated by averaging all the epochs realigned and not discarded.

9. Despite all the procedures described in this algorithm, one condition, that we want to comply with, is that the time distance between the onset of the EMG and the peak of the RP does not vary as a result of all the realignments. For this reason, after calculating the RP, we occur if this distance is identical to that which was obtained before realigning the epochs. Otherwise, we compute a shift adjustment.
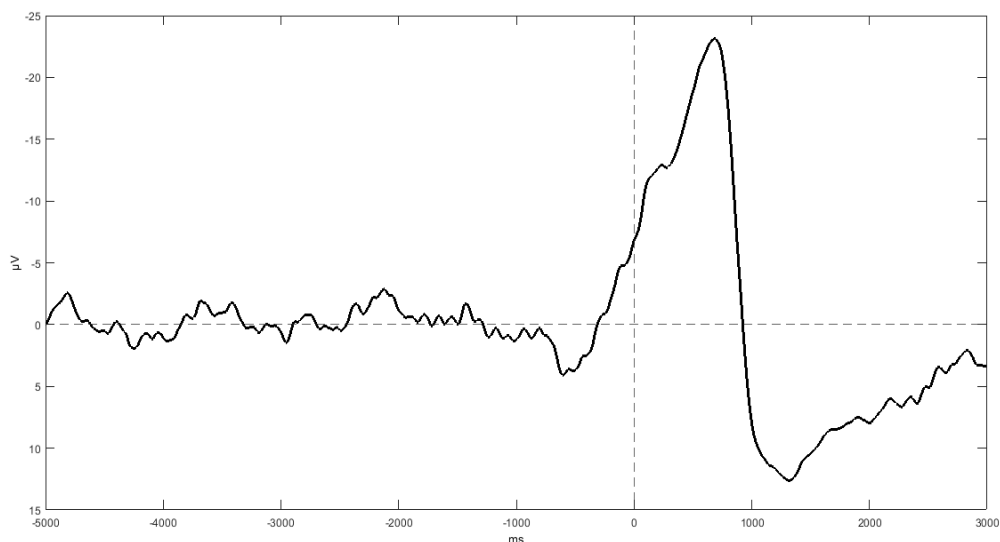

Figure 22 – In the figure, we can see the final RP, obtained by the average of the signals corresponding to the most correlated epochs and aligned with each other. In the end, a misalignment between the peak of the RP obtained and the onset of the EMG was checked. In this case, no misalignment occurred.

A problem with this method, which may arise in the presence of a large artifact, is that the epoch, which most correlates with all the others and had the highest median value of the correlations at point 1, does not contain the signal, but contains only one large artifact. In this case, the reason why it correlates very well with the others maybe because some artifact is common to all the other epochs.

Therefore, choosing as a fundamental epoch, on which to build the first template, with simply a large artifact, and not containing the signal, is not the most appropriate choice. For this reason, it is more appropriate to choose as the initial template, the RP obtained by averaging all the epochs, although they have not yet been realigned. This results in a variation to the method, which we will call the *second method*, in which the first epoch does not correspond to a real epoch, but the average of all the epochs is still not realigned. The rest of the algorithm is going the same way.

Let us make a brief digression about what can happen by using this method on patients' recordings. Although this problem is not the goal of this thesis work, we dealt with adding a further variant in the method.

The RP may be immersed in noise, in the case of recordings acquired on patients, so that the signal-to-noise ratio (SNR) is much less than what we will get on control subjects. In this case, to search for the RP within the patient track, it may help to use as an initial template a signal with the typical waveform of the RP, not obtained from the data but imposed by the user. For this reason, a *third method* has been proposed, in which the initial template has the typical waveform of the RP and has been artificially realized by the user. We do not know, if this method, in the future, can be useful for the analysis of the patients' signals, however, we will leave it available to the user.

Chapter 4

Results

4.1 – Introduction

In this chapter we will present the results about jitter compensation, based on Woody's method, to compute the RP. We noted that the best method to implement jitter compensation is the second one *(see Chapter 3)* because the algorithm starts from a good RP template to choose the most correlated epochs.

The SNR (signal-to-noise ratio), which represents how much larger the signal is than the noise, is calculated. The noise is calculated by subtracting the RP, obtained by averaging the odd aligned epochs, from the RP, obtained by averaging the even aligned epochs (or vice versa). In general, the RP is given by a component of the signal and a component of noise. Suppose we do two different estimates of the RP, in which with the first half of epochs we could have a first estimate RP_1, and with the second half of the epochs, we could have a second estimate RP_2. We calculate the two estimates as the sum between the component of the signal and the component of the noise. What differs from the two estimates, is precisely the noise. We can assume that the first estimate of the RP_1, with the first half of the epochs, is given by $s(t) + n(t)_1$, while the second estimate RP_2 is equal to $s(t) + n(t)_2$. If we take these two different estimates and subtract them, we obtain:

$$s(t) + n(t)_1 - [s(t) + n(t)_2] = n(t)_1 - n(t)_2$$

In the equation, the signal is simplified, and the difference $n(t)_1 - n(t)_2$ remains. This is possible because the signal is deterministic, so it is canceled, while the noise is a random process, so it is additive. However, in the end, we will take the power of the noise, so it is not important the order of the subtraction.

This parameter objectively demonstrates whether we get a distinguishable RP in an examined dataset. As mentioned above, *in Chapter 3*, 7 channels are analyzed: Cz, C3, C4, Fcz, Fc3, Pz. For that, we calculate five kinds of the *RPs*: the *RP* over the *Median Rosto-Caudal Area*, obtained by averaging the *RPs* over *Cz, Fcz, Pz*; the RP over the *Pre-motor Area*, obtained by averaging the RPs over *Fcz, Fc3, Fc4*; the *RP* over the *Motor Area*, obtained by averaging the *RPs* over *Cz, C3, C4*; the *RP* over the *Right Hemisphere of the Pre-Motor and the Motor Areas*, obtained by averaging the *RPs* over *Fc4, C4*, and the *RP* over the *Left Hemisphere of the Pre-motor and the Motor Areas*, obtained by averaging the *RPs* over *Fc3, C3*.

4.2 – Plots of the RPs and the SNR

The SNR is a parameter, which compares the level of the desired signal to the level of background noise. The formula of SNR is:

$$SNR = 10 * \log_{10} \frac{PWsignal}{PWnoise}$$

where the $PWsignal$ indicates the power of the signal and the $PWnoise$ is the power of all the background noise, and it is expressed in *decibel (dB)*.

The power of the signal and the power of noise are not calculated instant by instant, but we calculate the moving average power over a reasonable number of samples, that is *50* samples, so over a time window of *390 ms* to obtain a smoother value of the SNR.

While the power of the noise is the mean value of the moving average noise power on *390 ms*.

An arbitrary threshold, equal to *5 dB*, is chosen to identify the parts of the epoch in which there is the signal, then the SNR rises above a certain threshold, for example immediately after the onset of the movement. There are datasets, in which this threshold is never exceeded, because the power of the signal is lower than the power of the noise, so the signal is very noisy.

Below, we will show five plots of the SNR for each dataset, first those related to the voluntary movement task, after those of the semi-voluntary movement task, and then those of the involuntary movement task. In addition to the SNR plots, we will show the plots of the no-aligned RPs and the plots of the aligned RPs. The no-aligned RPs are obtained by averaging all the epochs without artifacts, while the aligned RPs are obtained by averaging all the aligned epochs without artifacts, computing the implemented algorithm.

The first plot is the one about the SNR, to have more ease in understanding whether or not there is the signal in a dataset. But the SNR is calculated after computing the algorithm about jitter compensation.

4.3 – Voluntary Movement Task Dataset

4.3.1 – Dataset GF892070

From the plot of the SNR, we can see that, between *1000 ms* and *2000 ms*, the power of the signal of each RP is larger than the noise power.
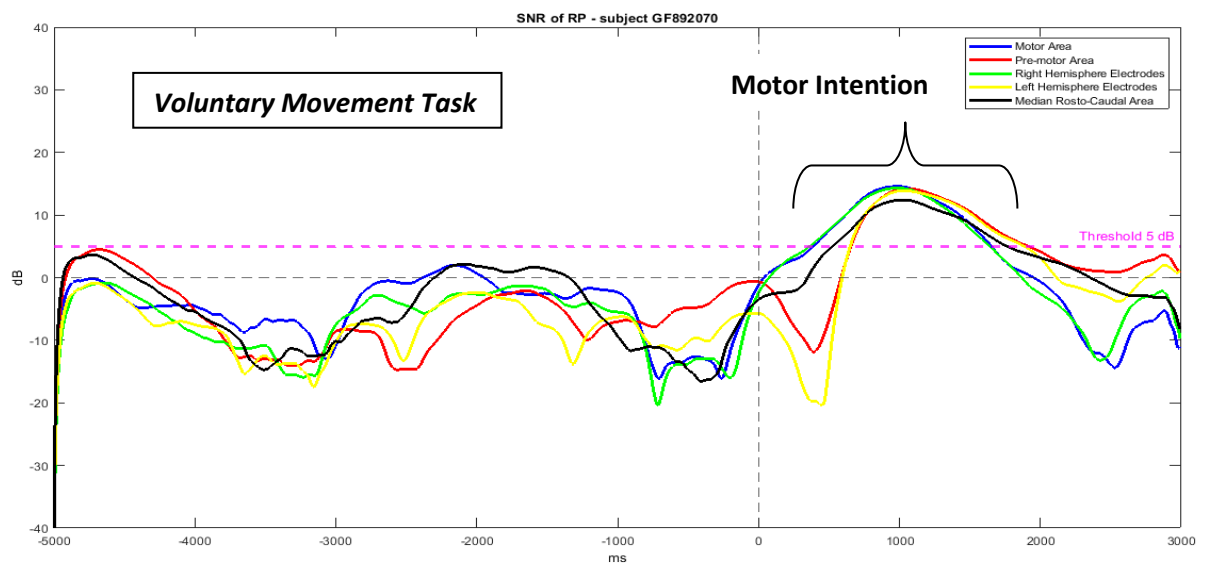
Figure 23 – SNR of RP over Motor Area, Pre-motor Area, Right Hemisphere Electrodes, Left Hemisphere Electrodes, and Median Rosto-Caudal Area.

After removing the artifacts, we calculate the no-aligned RPs. As we can see from the figure, we do not have the correct waveforms of RPs.
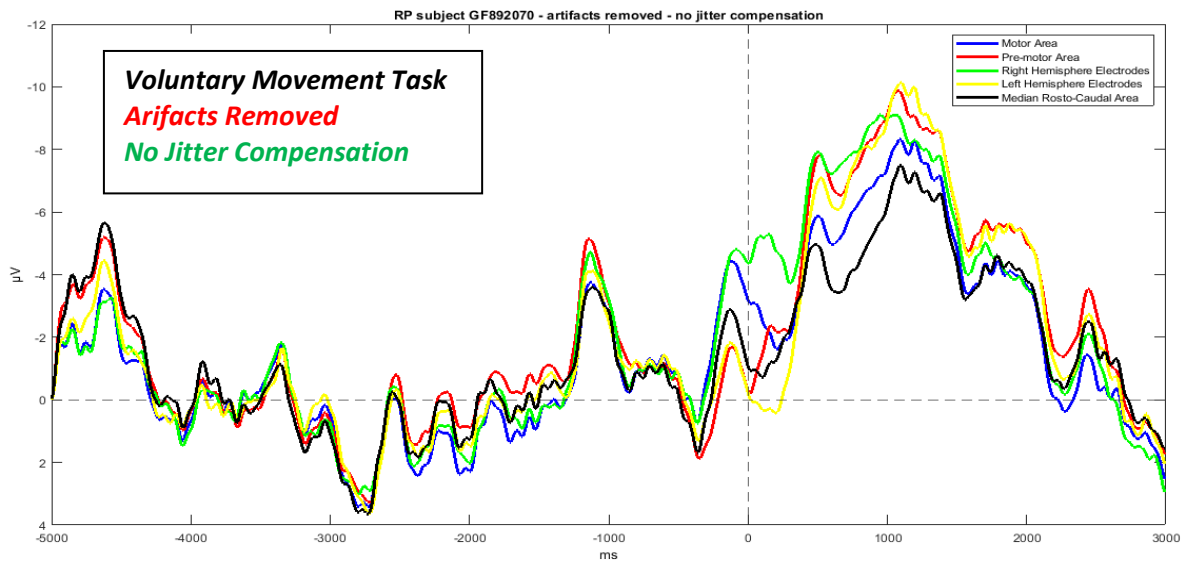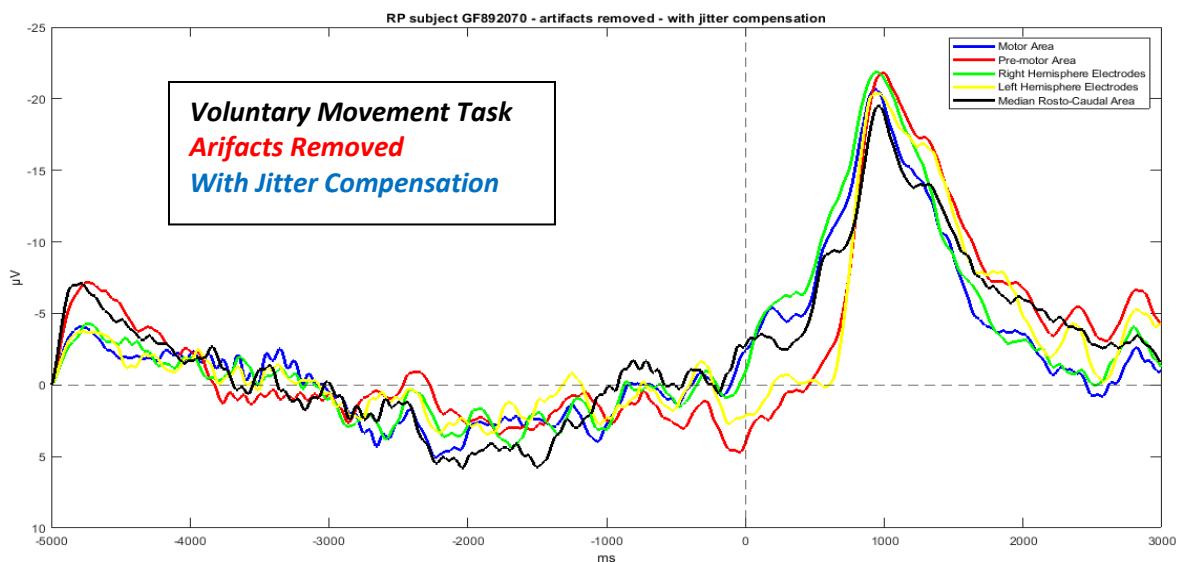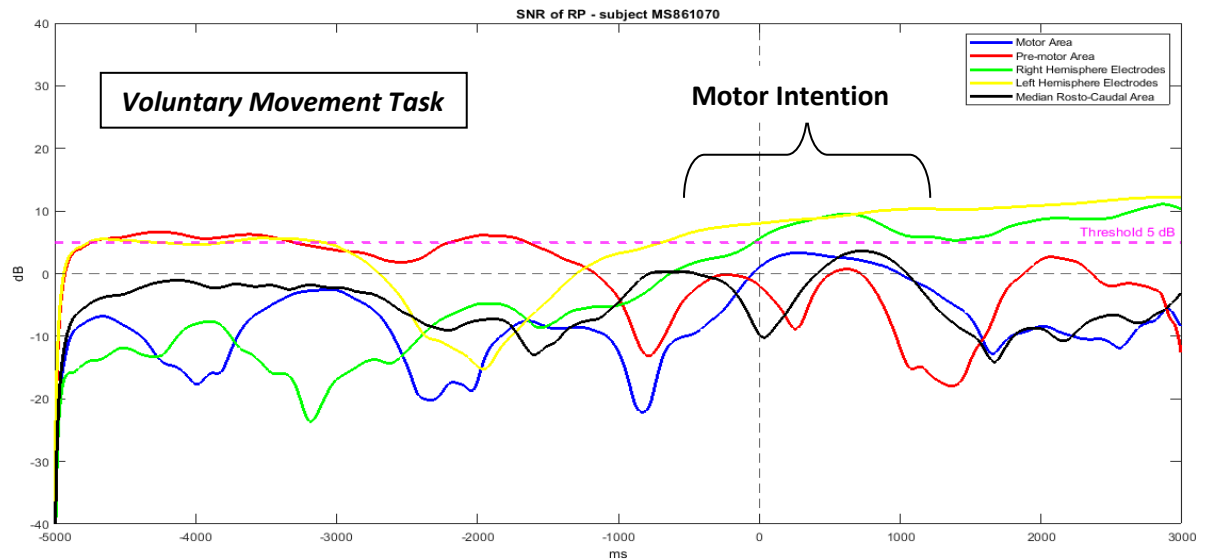

Figure 24 – RP over Motor Area, Pre-motor Area, Right Hemisphere Electrodes, Left Hemisphere Electrodes, and Median Rosto-Caudal Area – artifacts removed – no jitter compensation.

Computing the algorithm about jitter compensation, the epochs are aligned correctly so we get the correct waveforms of RPs.
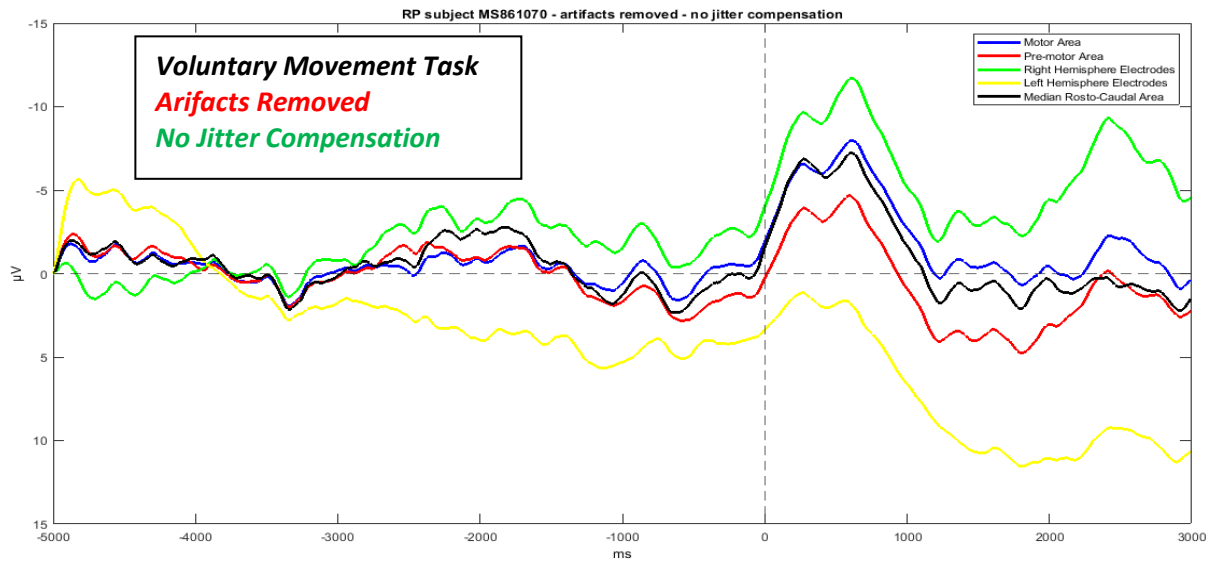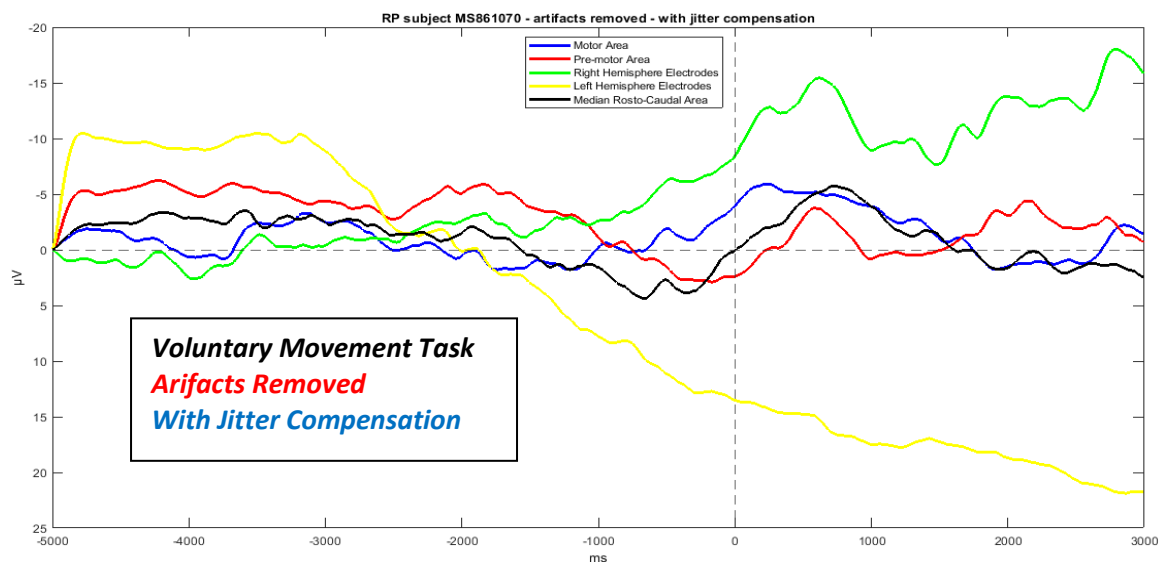

Figure 25 – RP over Motor Area, Pre-motor Area, Right Hemisphere Electrodes, Left Hemisphere Electrodes, and Median Rosto-Caudal Area – artifacts removed – with jitter compensation.

4.3.2 – Dataset MS861070

From the plot of SNR, we can see that only the SNR of the RPs corresponding to the Right hemisphere and the Left hemisphere are above the threshold, so the signal power is greater than the noise power. So the signal of this dataset is too noisy.
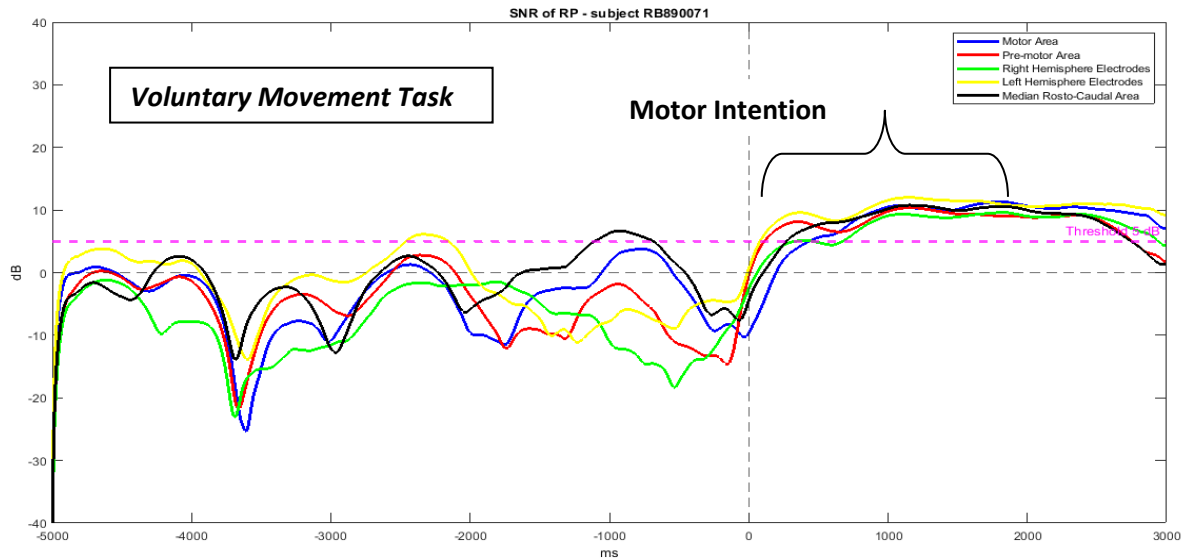

Figure 26 – SNR of RP over Motor Area, Pre-motor Area, Right Hemisphere Electrodes, Left Hemisphere Electrodes, and Median Rosto-Caudal Area.

After removing the artifacts, we calculate the no-aligned RPs. As we can see from the figure, we do not have exactly the correct waveforms of RPs.

Figure 27 – RP over Motor Area, Pre-motor Area, Right Hemisphere Electrodes, Left Hemisphere Electrodes, and Median Rosto-Caudal Area – artifacts removed – no jitter compensation.

Computing the algorithm about jitter compensation, not for all RPs we get the expected results.

Figure 28 – RP over Motor Area, Pre-motor Area, Right Hemisphere Electrodes, Left Hemisphere Electrodes, and Median Rosto-Caudal Area – artifacts removed – with jitter compensation.

4.3.3 – Dataset RS890071

From the plot of SNR, we can see that the power of the is larger than the power of noise at *1000 ms*.

Figure 29 – SNR of RP over Motor Area, Pre-motor Area, Right Hemisphere Electrodes, Left Hemisphere Electrodes, and Median Rosto-Caudal Area.

After removing the artifacts, we calculate the no-aligned RPs. As we can see from the figure, we do not have exactly the waveforms of RPs. The RPs seem to be in reverse to the conventional waveforms.
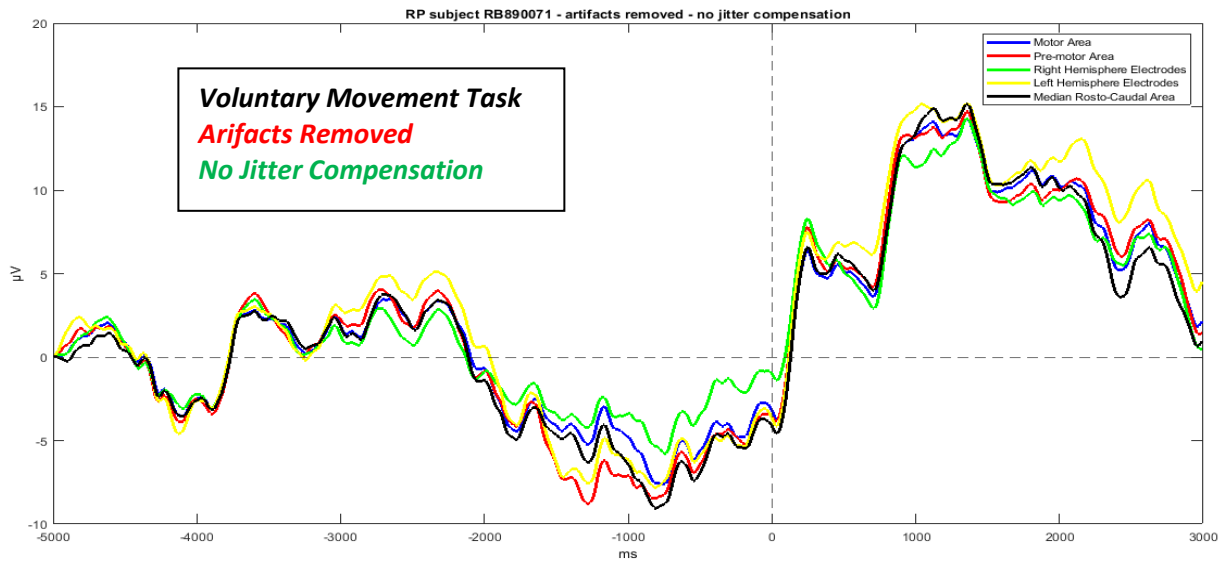
Figure 30 – RP over Motor Area, Pre-motor Area, Right Hemisphere Electrodes, Left Hemisphere Electrodes, and Median Rosto-Caudal Area – artifacts removed – no jitter compensation.

Computing jitter compensation, we do not get the correct RPs waveforms. This result can be given by the fact that the dataset contains many artifacts.
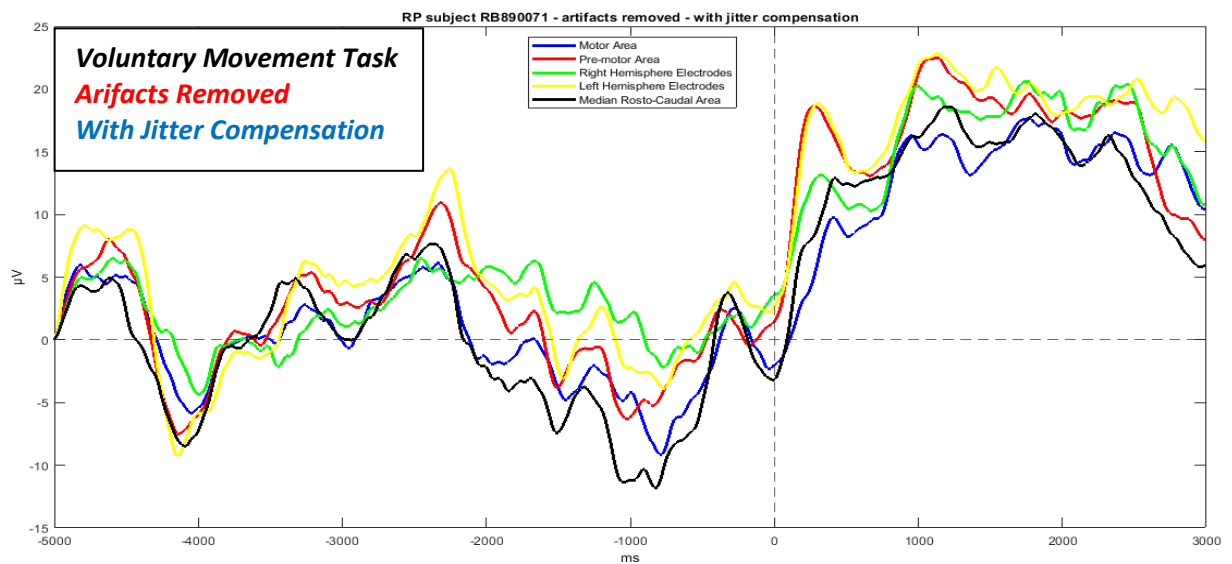

Figure 31 – RP over Motor Area, Pre-motor Area, Right Hemisphere Electrodes, Left Hemisphere Electrodes, and Median Rosto-Caudal Area – artifacts removed – with jitter compensation.

4.3.4 – Dataset TC995011

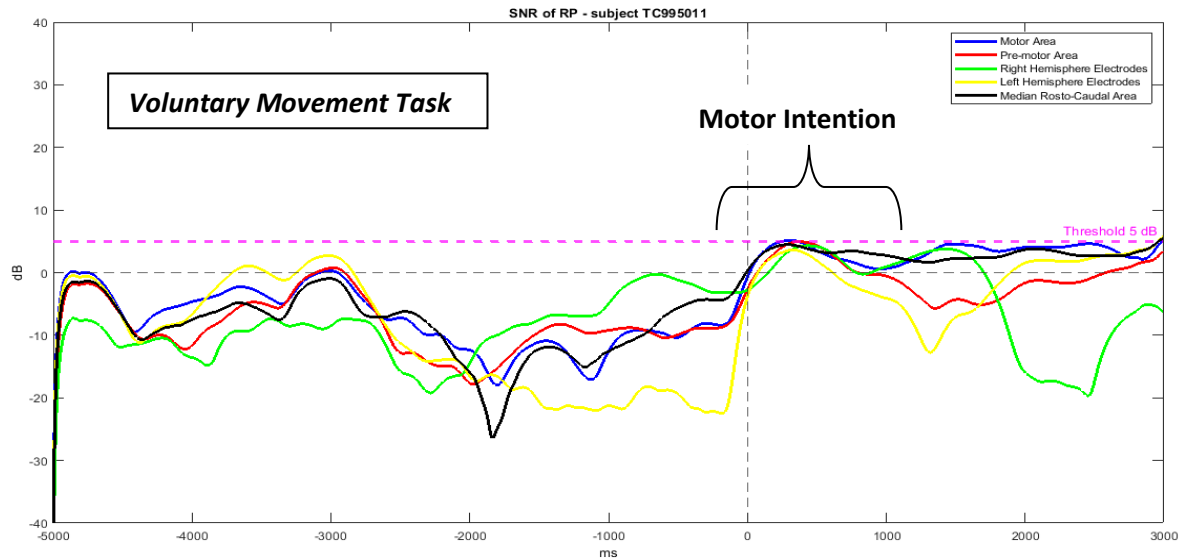We can notice, from the figure, that the SNRs of all RPs are below the threshold.

Figure 32 – SNR of RP over Motor Area, Pre-motor Area, Right Hemisphere Electrodes, Left Hemisphere Electrodes, and Median Rosto-Caudal Area.

After removing the artifacts, we calculate the no-aligned RPs. As we can see from the figure, we do not have the correct waveforms of RPs. It seems that the RPs are in reverse to the conventional waveform, so they have a positive peak.
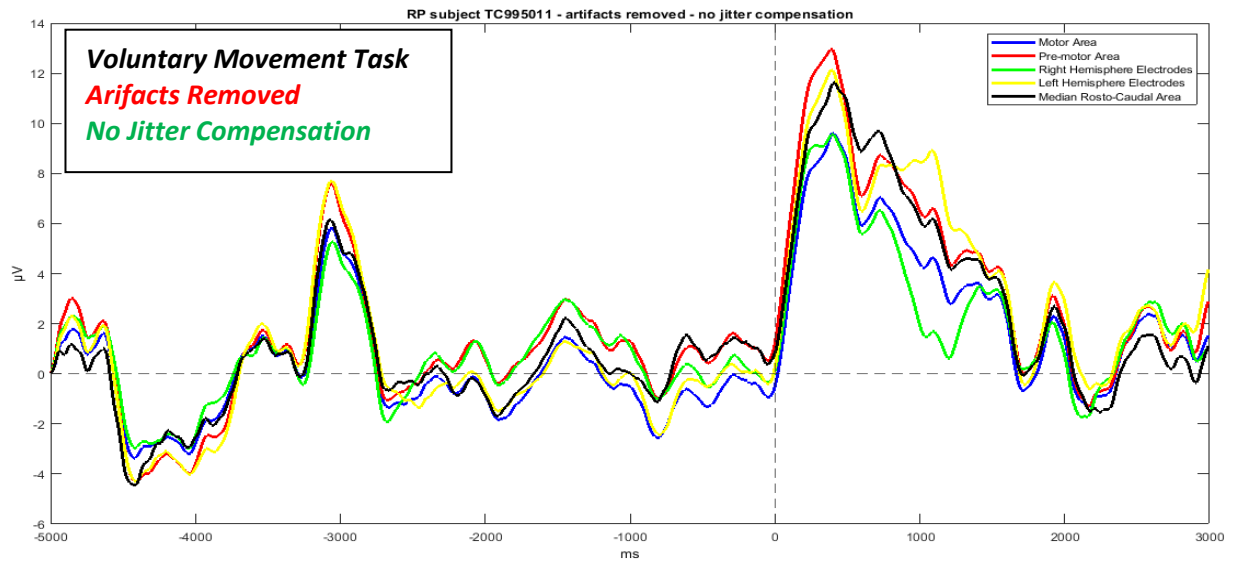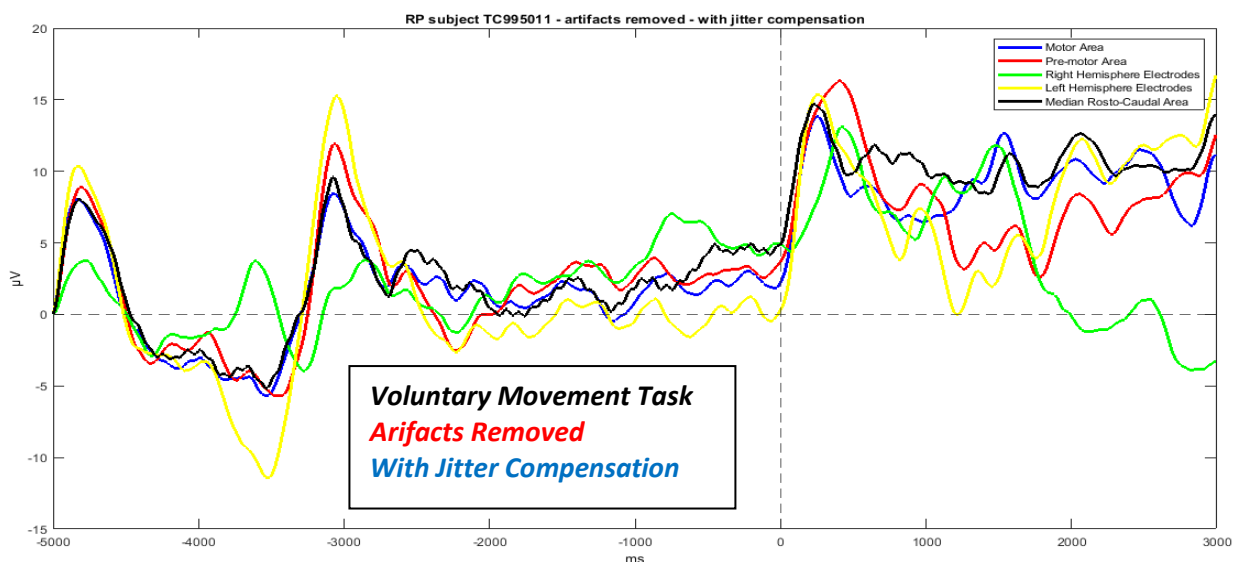
Figure 33 – RP over Motor Area, Pre-motor Area, Right Hemisphere Electrodes, Left Hemisphere Electrodes, and Median Rosto-Caudal Area – artifacts removed – no jitter compensation.

Even by computing the jitter compensation, the typical RP waveforms are not obtained.

Figure 34 – RP over Motor Area, Pre-motor Area, Right Hemisphere Electrodes, Left Hemisphere Electrodes, and Median Rosto-Caudal Area – artifacts removed – with jitter compensation.

4.4 – Semi-voluntary Movement Task Dataset

4.4.1 – Dataset AL858070

We can notice that the SNR of RP over Motor Area is below the threshold, while all the other SNRs of the remaining RPs are above the threshold.
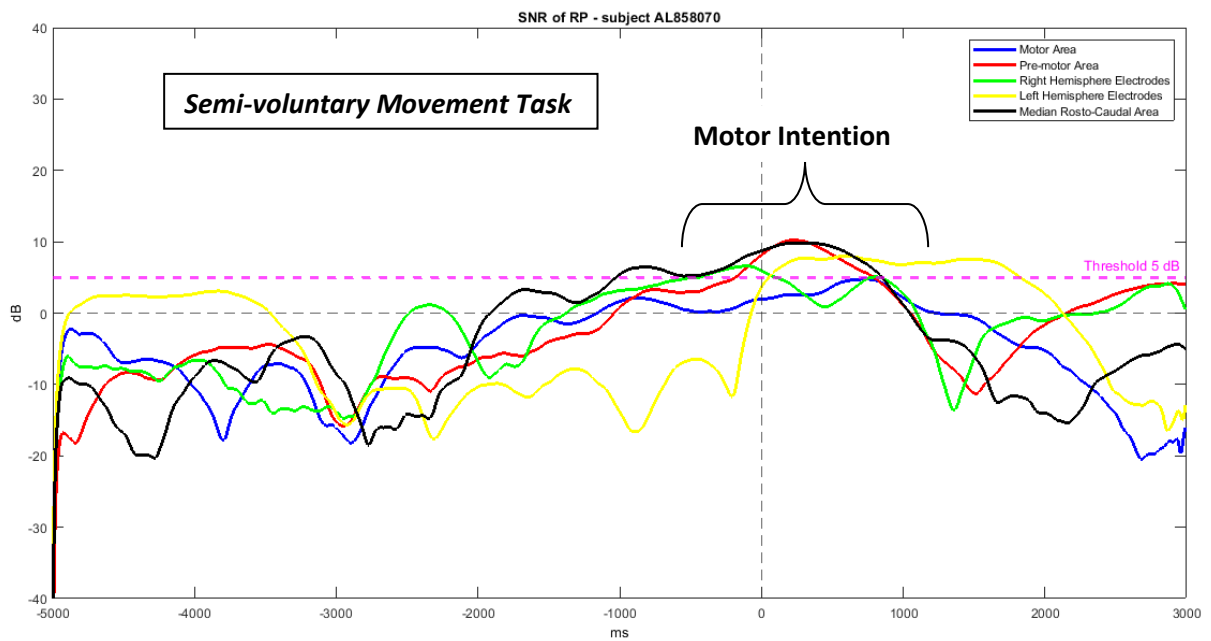

Figure 35 – SNR of RP over Motor Area, Pre-motor Area, Right Hemisphere Electrodes, Left Hemisphere Electrodes, and Median Rosto-Caudal Area.

After removing the artifacts, we calculate the no-aligned RPs. As we can see from the figure, we do not have the waveforms of RPs, that we expected.
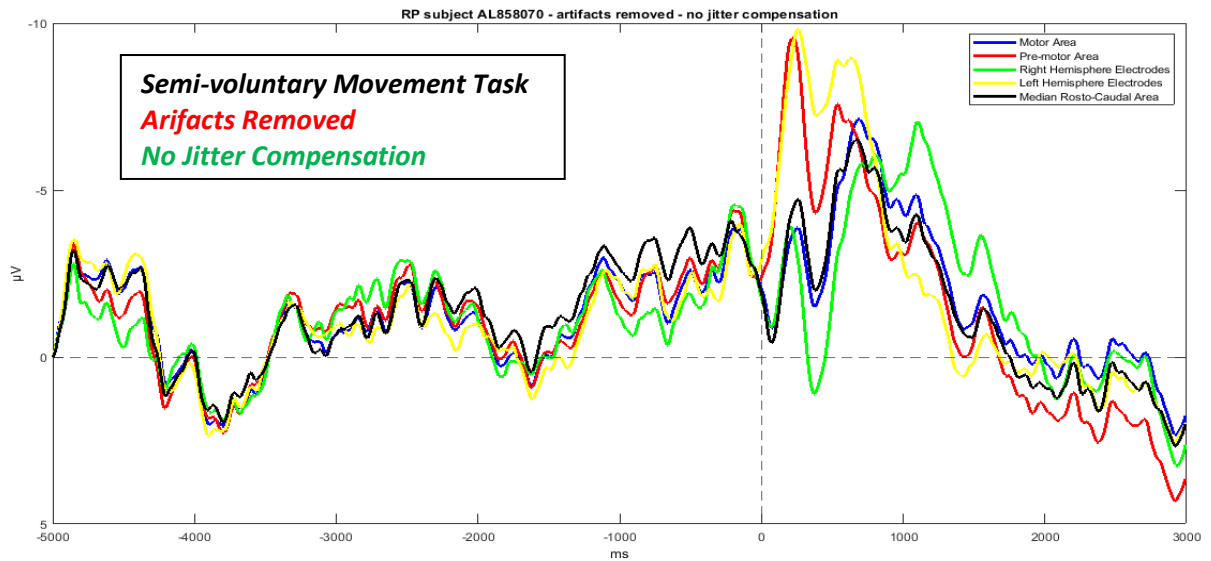
Figure 36 – RP over Motor Area, Pre-motor Area, Right Hemisphere Electrodes, Left Hemisphere Electrodes, and Median Rosto-Caudal Area – artifacts removed – no jitter compensation.

Computing jitter compensation, we can observe the good RPs waveforms.

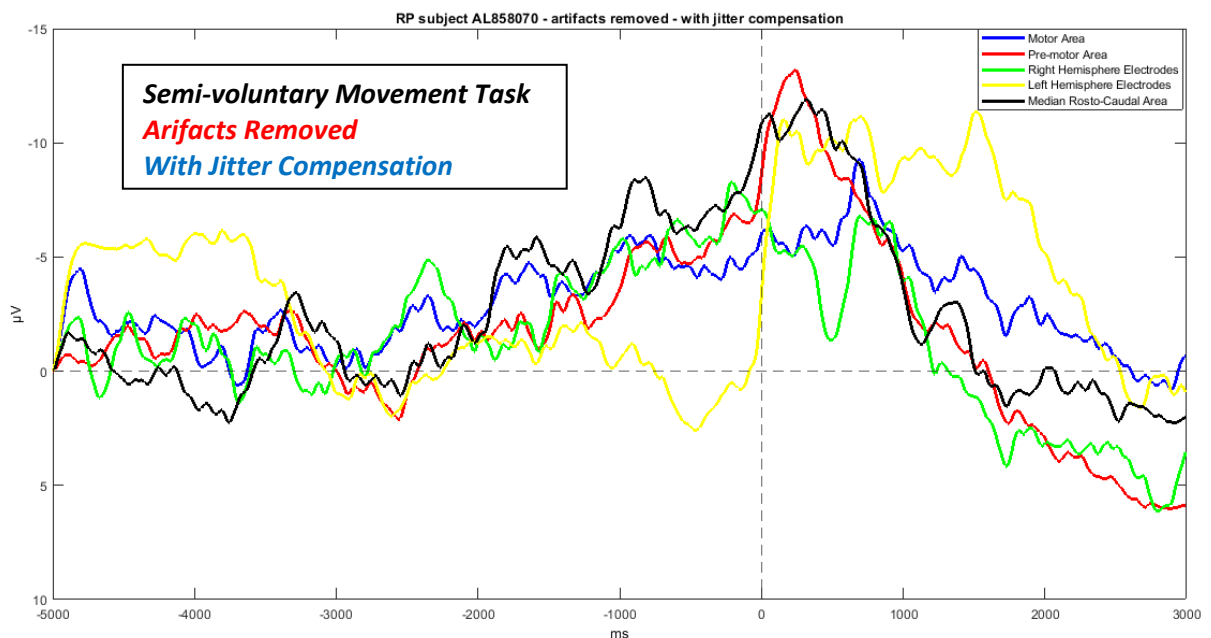**Figure 37 – RP over Motor Area, Pre-motor Area, Right Hemisphere Electrodes, Left Hemisphere Electrodes, and Median Rosto-Caudal Area – artifacts removed – with jitter compensation.**

4.4.2 – Dataset GF892070

For this dataset, only the SNR of the RP over the Pre-motor Area is above the threshold.
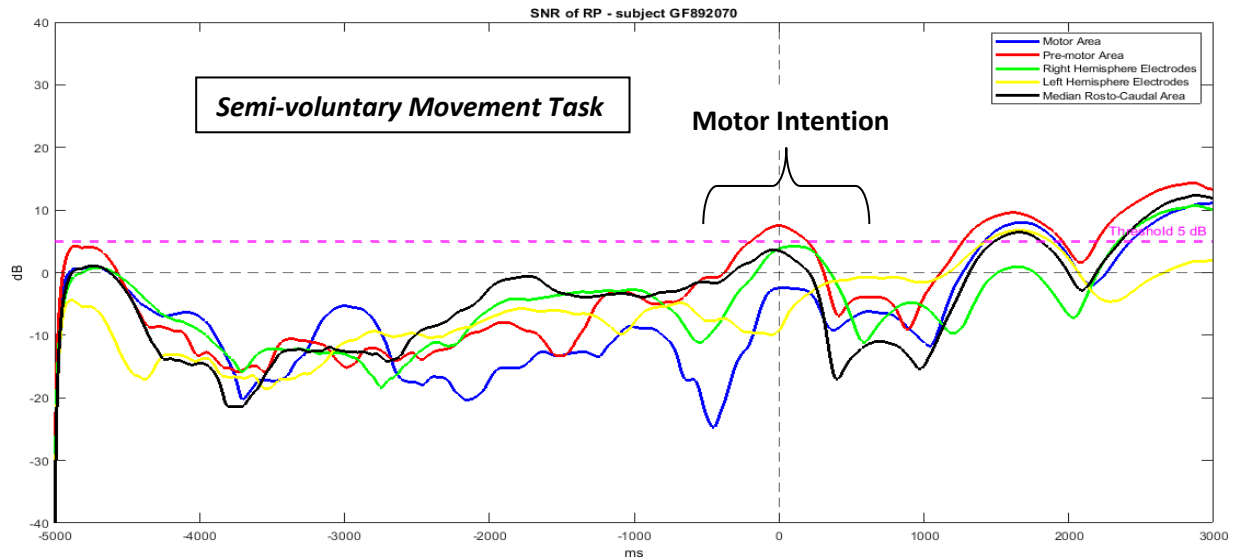

Figure 38 – SNR of RP over Motor Area, Pre-motor Area, Right Hemisphere Electrodes, Left Hemisphere Electrodes, and Median Rosto-Caudal Area.

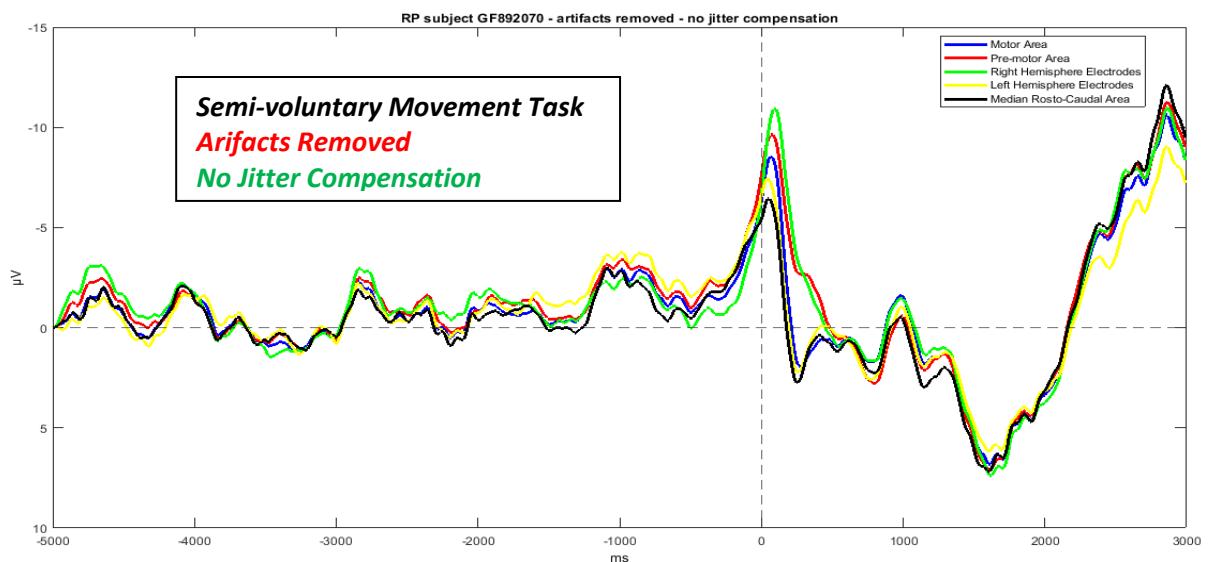After removing the artifacts, we calculate the no-aligned RPs.

Figure 39 – RP over Motor Area, Pre-motor Area, Right Hemisphere Electrodes, Left Hemisphere Electrodes, and Median Rosto-Caudal Area – artifacts removed – no jitter compensation.

As we can see from the plot, not all the RPs have a correct waveform.

Figure 40 – RP over Motor Area, Pre-motor Area, Right Hemisphere Electrodes, Left Hemisphere Electrodes, and Median Rosto-Caudal Area – artifacts removed – with jitter compensation.

4.4.3 – Dataset GO862071

From the figure, we can notice that the signal power of all the RPs, at the region where the peak of the RP is located, is larger than the power of noise.

Figure 41 – SNR of RP over Motor Area, Pre-motor Area, Right Hemisphere Electrodes, Left Hemisphere Electrodes, and Median Rosto-Caudal Area.

From the beginning, without computing the algorithm about jitter compensation, the waveform of the RPs is quite correct.
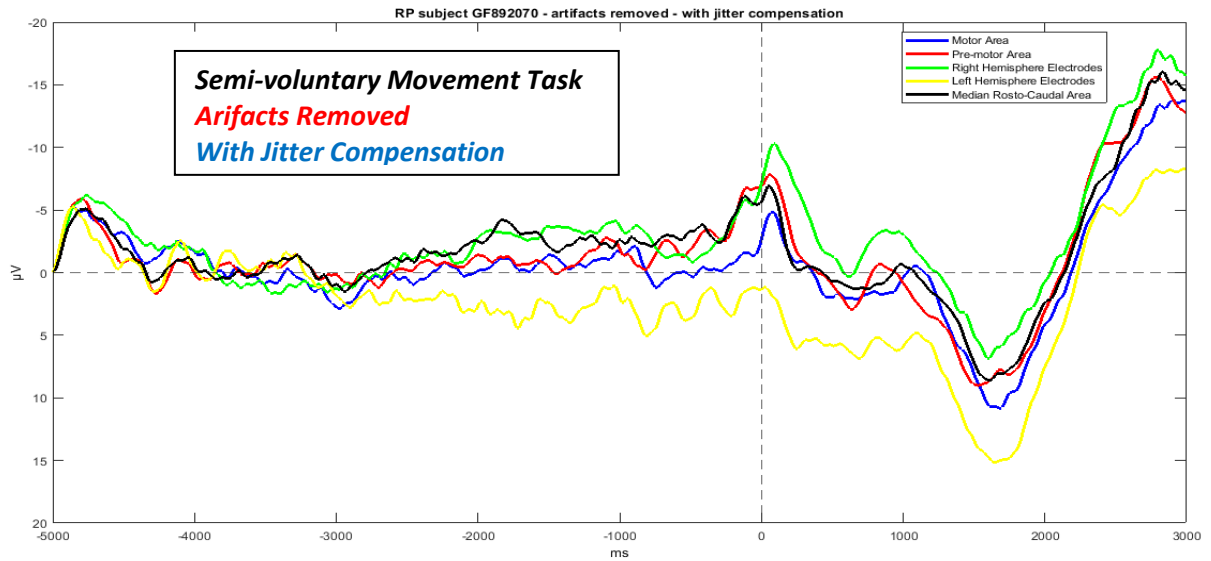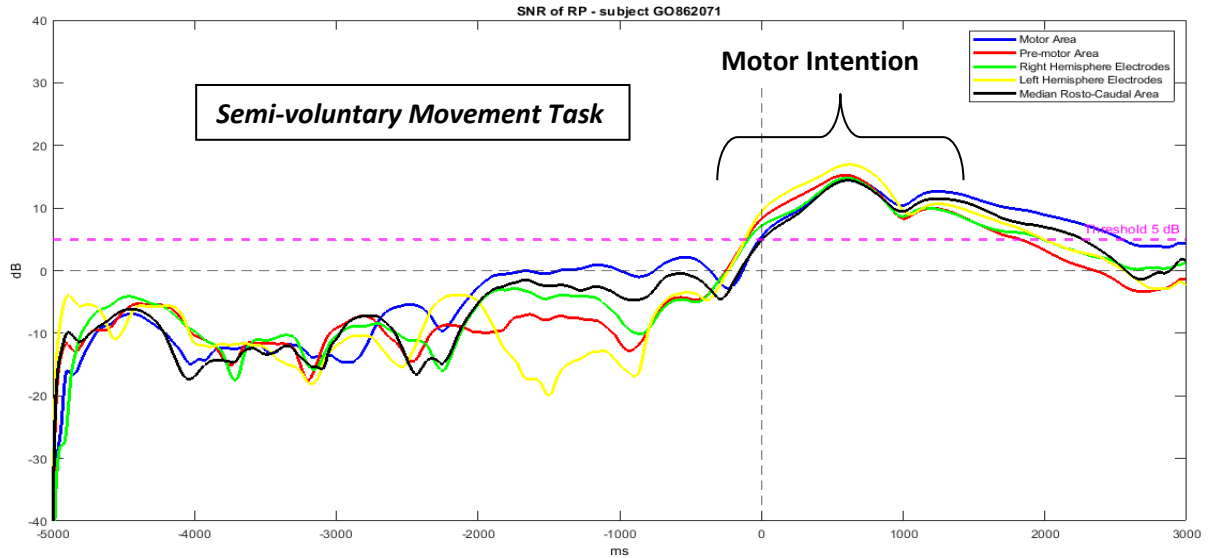

Figure 42 – RP over Motor Area, Pre-motor Area, Right Hemisphere Electrodes, Left Hemisphere Electrodes, and Median Rosto-Caudal Area – artifacts removed – no jitter compensation.

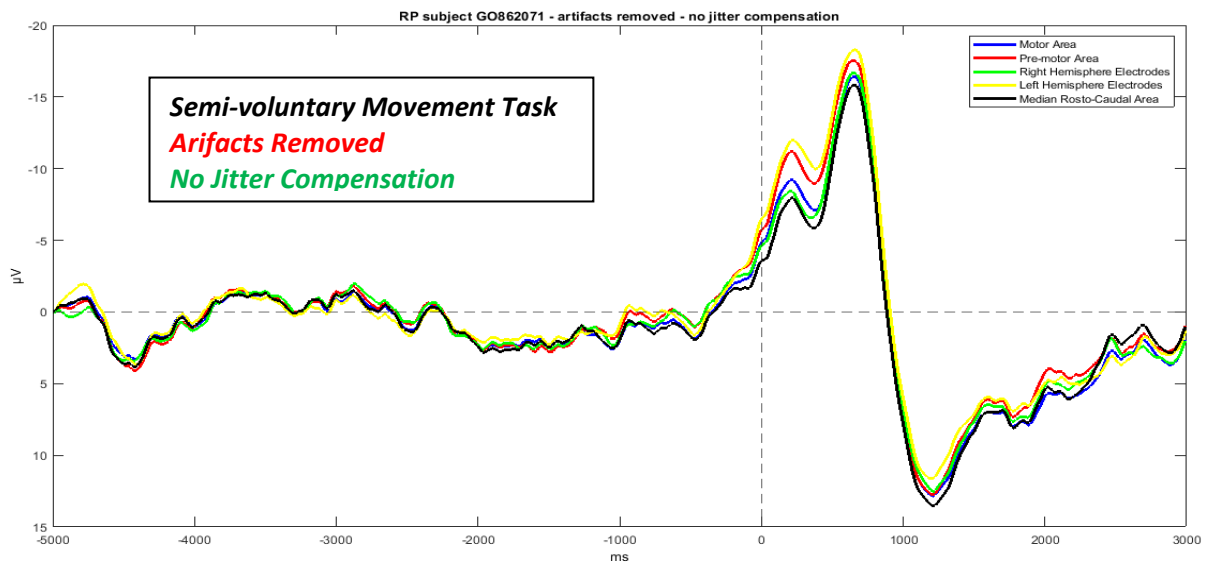With jitter compensation, the waveforms are corrected more, so this dataset is the best of all.

Figure 43 – RP over Motor Area, Pre-motor Area, Right Hemisphere Electrodes, Left Hemisphere Electrodes, and Median Rosto-Caudal Area – artifacts removed – with jitter compensation.

4.4.4 – Dataset LB892060

We can notice that the SNRs of RPs over the Pre-motor Area and the Median Rosto-Caudal Area are below the threshold, while all the other SNRs of the remaining RPs are above the threshold.

Figure 44 – SNR of RP over Motor Area, Pre-motor Area, Right Hemisphere Electrodes, Left Hemisphere Electrodes, and Median Rosto-Caudal Area.

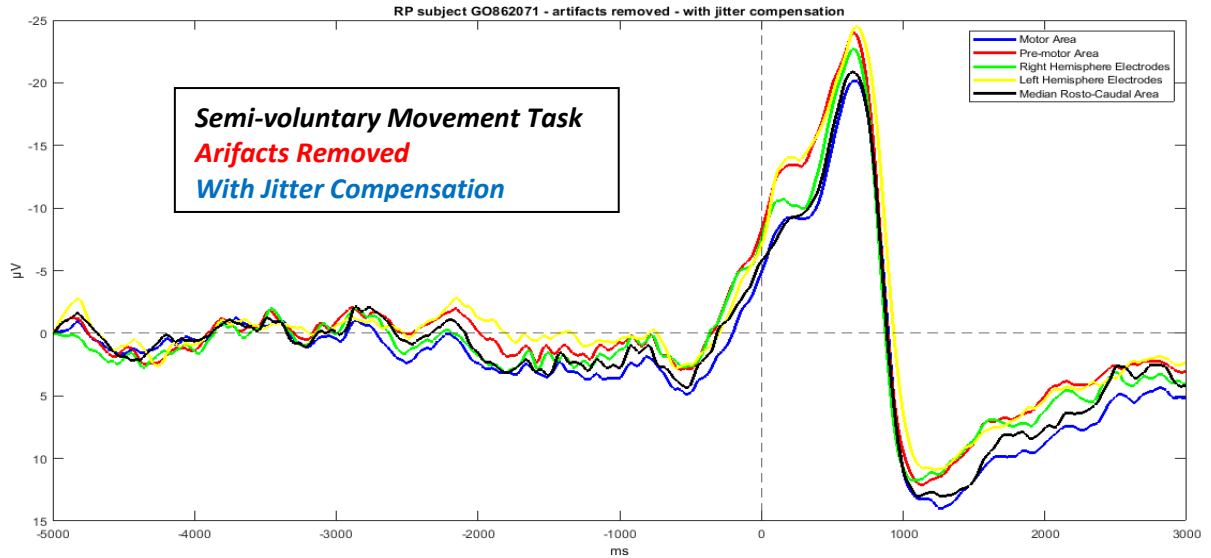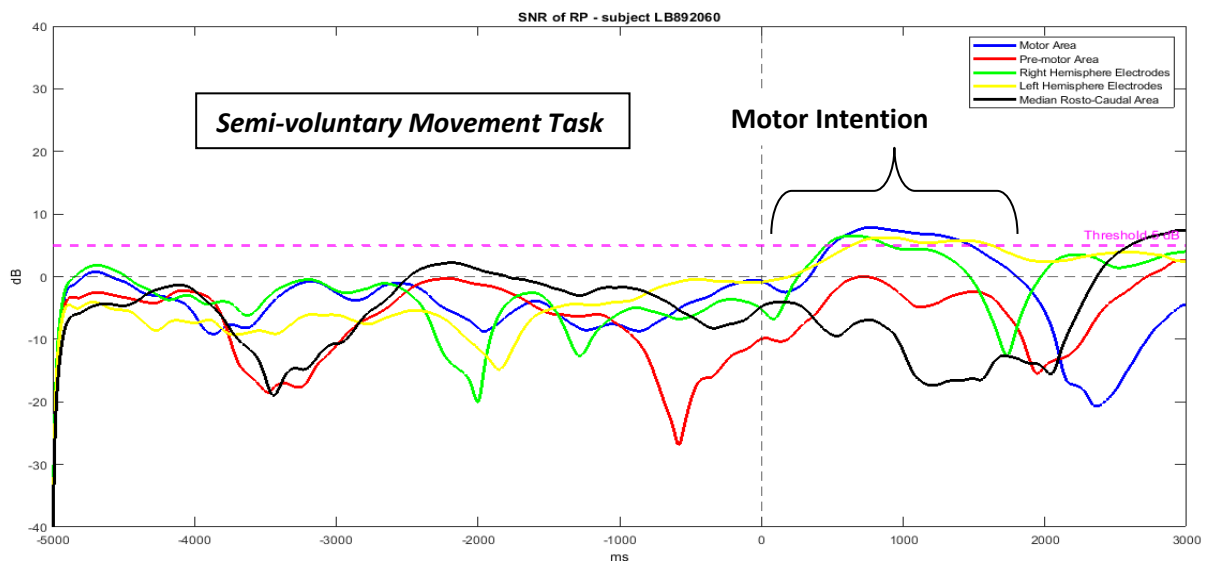After removing the artifacts, the waveforms of the RPs are reverse to the typical RP waveform.

Figure 45 – RP over Motor Area, Pre-motor Area, Right Hemisphere Electrodes, Left Hemisphere Electrodes, and Median Rosto-Caudal Area – artifacts removed – no jitter compensation.

Computing the algorithm about jitter compensation, any distinguishable RPs are obtained.

Figure 46 – RP over Motor Area, Pre-motor Area, Right Hemisphere Electrodes, Left Hemisphere Electrodes, and Median Rosto-Caudal Area – artifacts removed – with jitter compensation.

4.4.5 – Dataset RB890071

The SNRs of all the RPs are below the threshold. So, the power of the signal is lower than the power of the noise.

Figure 47 – SNR of RP over Motor Area, Pre-motor Area, Right Hemisphere Electrodes, Left Hemisphere Electrodes, and Median Rosto-Caudal Area.

After removing the artifacts, we calculate no-aligned RPs. As we can notice, from the plot, the waveforms of RPs are not correct.
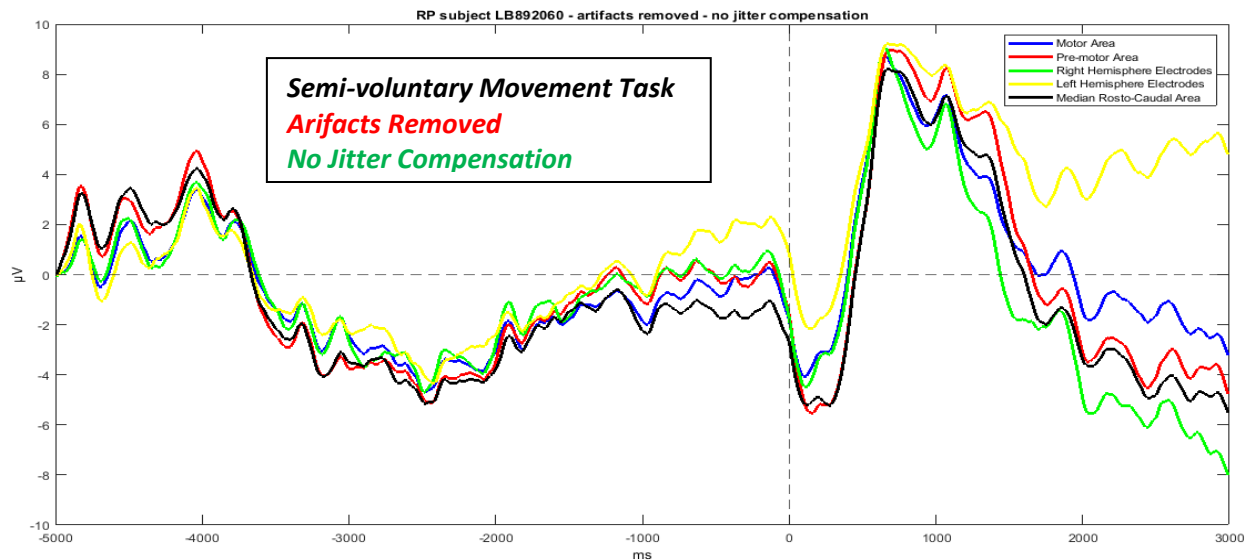
Figure 48 – RP over Motor Area, Pre-motor Area, Right Hemisphere Electrodes, Left Hemisphere Electrodes, and Median Rosto-Caudal Area – artifacts removed – no jitter compensation.

As we can see from the plot, also computing the algorithm, we do not get RPs. This is because the signal of this dataset is very noisy, and it could be an artifact.
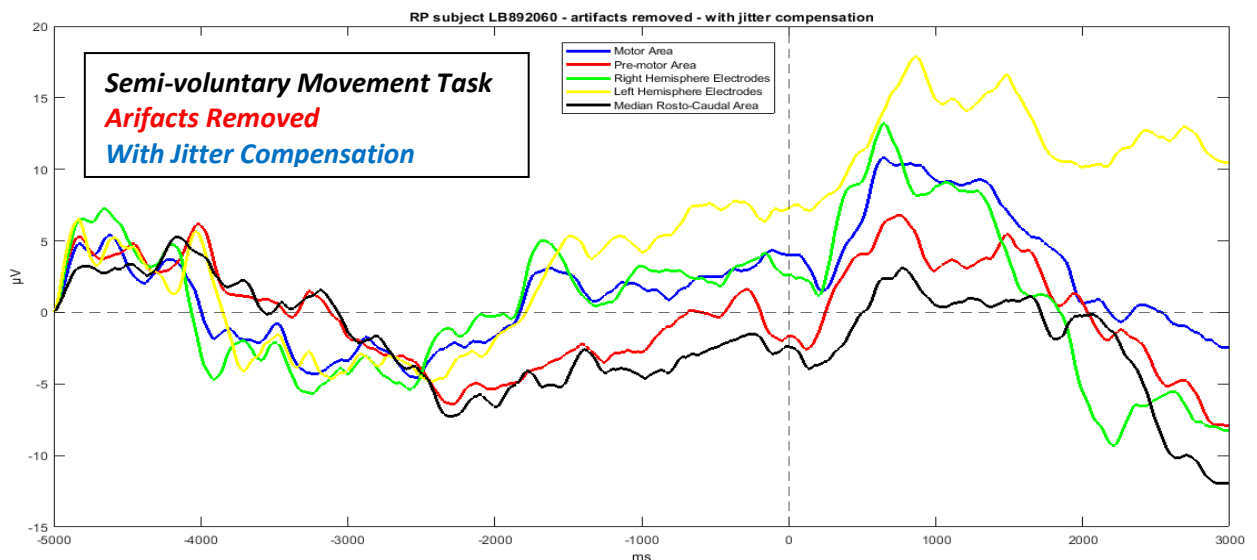

Figure 49 – RP over Motor Area, Pre-motor Area, Right Hemisphere Electrodes, Left Hemisphere Electrodes, and Median Rosto-Caudal Area – artifacts removed – with jitter compensation.

4.4.6 – Dataset SD874070

We can notice that the SNRs of RPs over the Pre-motor Area and the Right Hemisphere Area are above the threshold, while all the other SNRs of the remaining RPs are below the threshold.
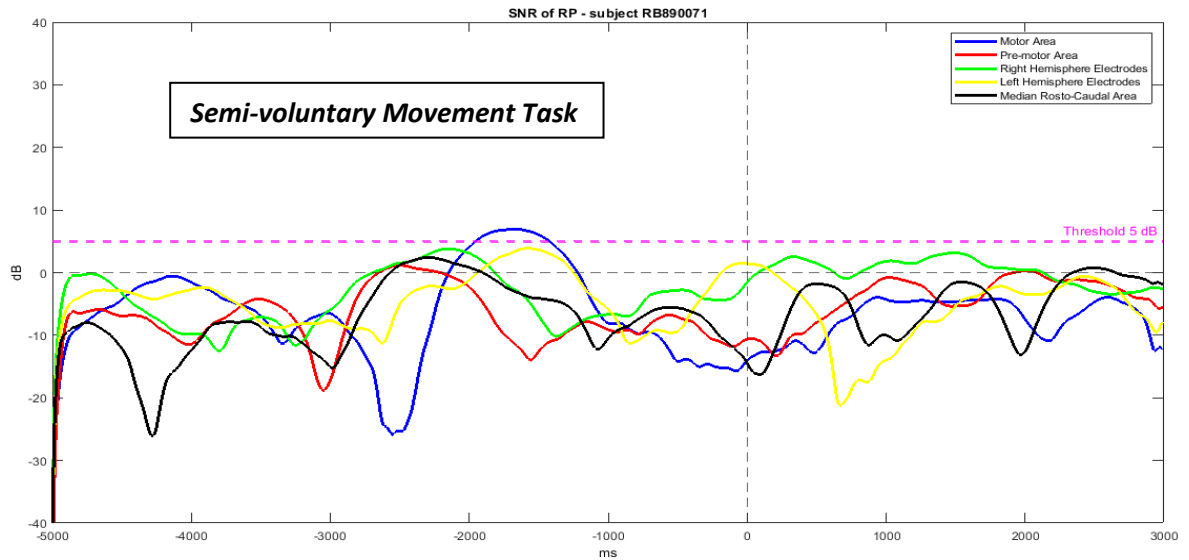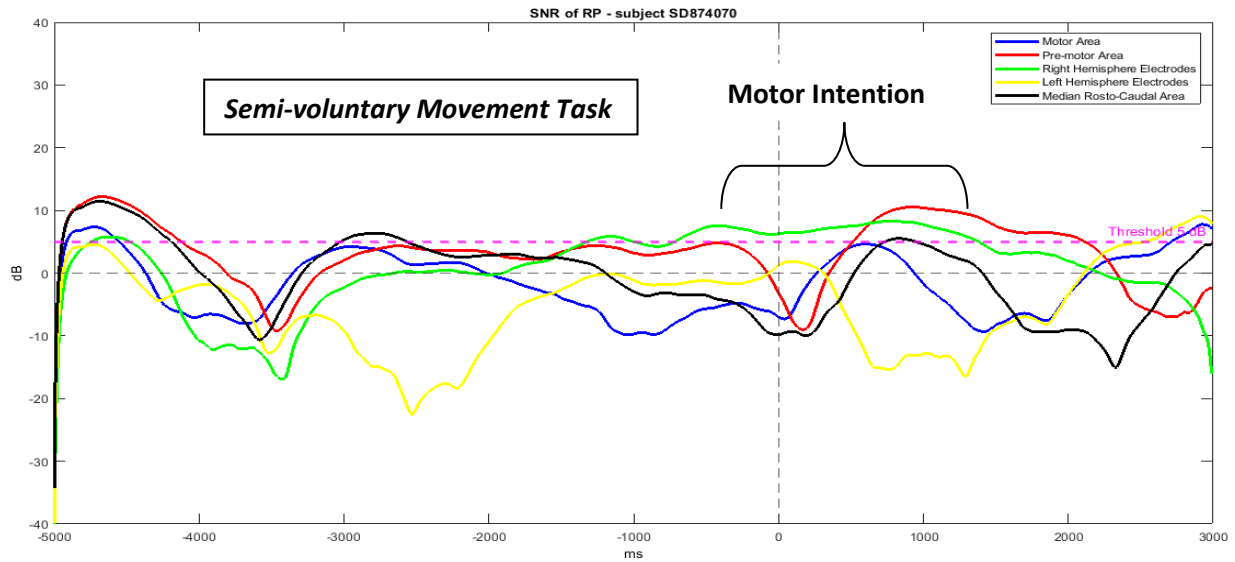

Figure 50 – SNR of RP over Motor Area, Pre-motor Area, Right Hemisphere Electrodes, Left Hemisphere Electrodes, and Median Rosto-Caudal Area.

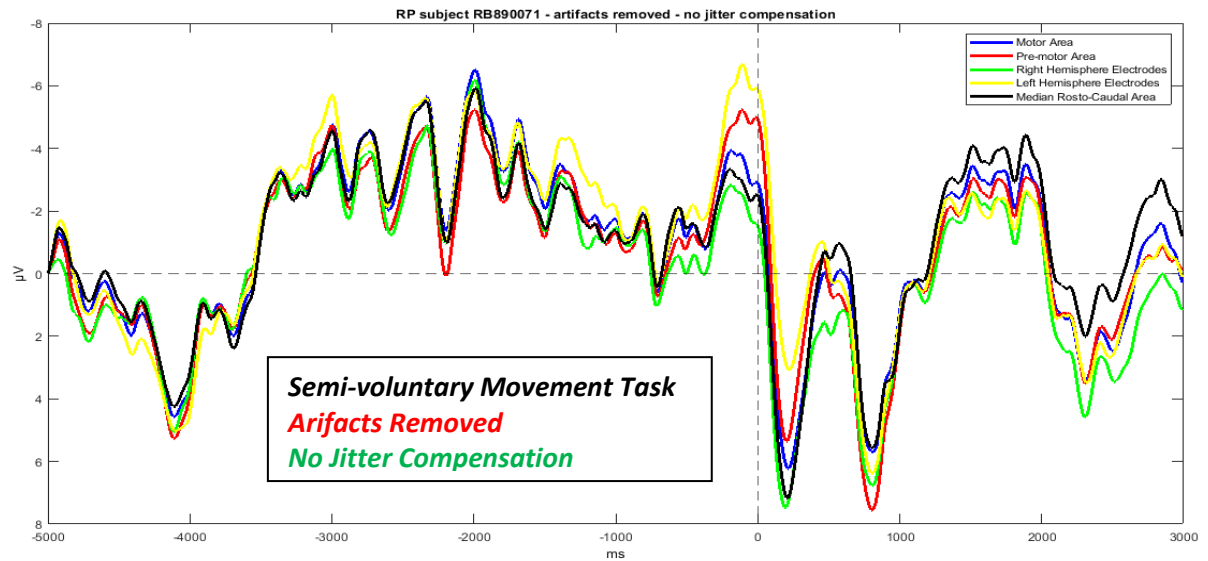After removing the artifacts, we calculate no-aligned RPs.

Figure 51 – RP over Motor Area, Pre-motor Area, Right Hemisphere Electrodes, Left Hemisphere Electrodes, and Median Rosto-Caudal Area – artifacts removed – no jitter compensation.

Computing the jitter compensation, not all the RPs have a correct waveform. Most likely this is since what we get is an artifact.
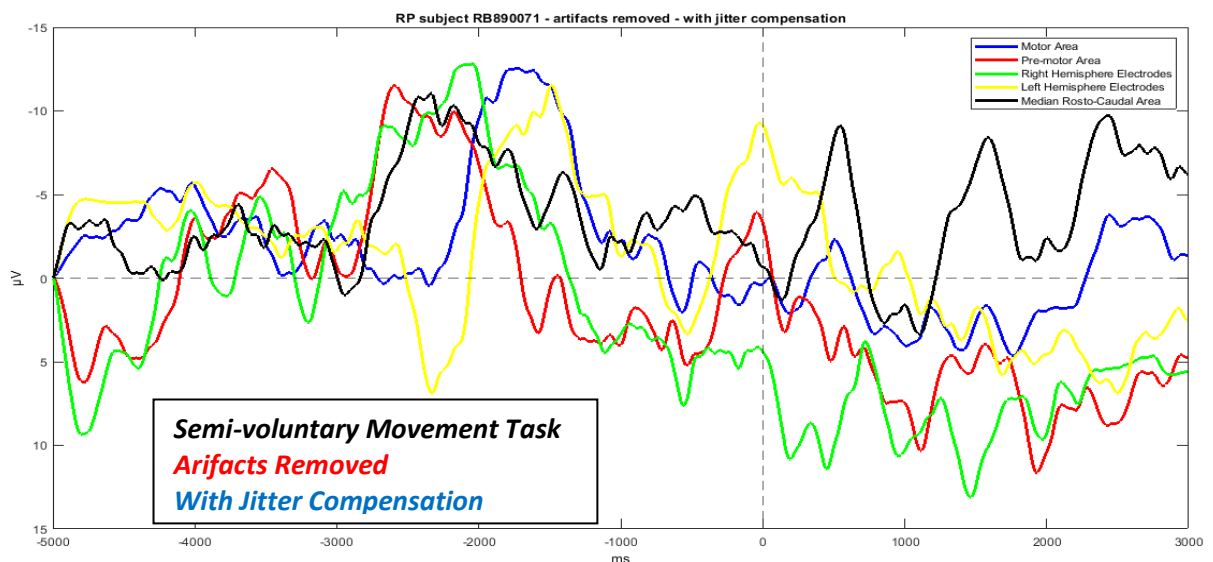

Figure 52 – RP over Motor Area, Pre-motor Area, Right Hemisphere Electrodes, Left Hemisphere Electrodes, and Median Rosto-Caudal Area – artifacts removed – with jitter compensation.

4.5 – Involuntary Movement Task Dataset

During the involuntary task, the subject does not perform a cortical movement, but only a reflex, that is the patellar reflex. Therefore, RPs should not be present.

4.5.1 – Dataset GP995111

We can notice that all the SNRs of RPs are above the threshold near the onset of the EMG.
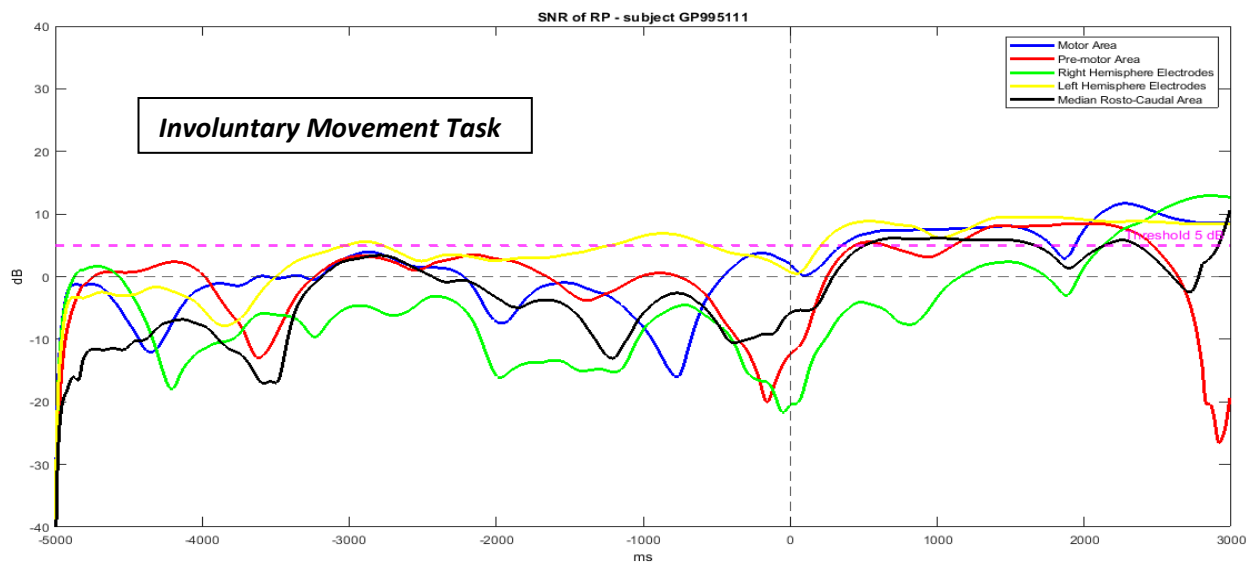
Figure 53 – SNR of RP over Motor Area, Pre-motor Area, Right Hemisphere Electrodes, Left Hemisphere Electrodes, and Median Rosto-Caudal Area.

In this dataset examined, the RPs are presented like random oscillations, without a precise waveform.

Figure 54 – RP over Motor Area, Pre-motor Area, Right Hemisphere Electrodes, Left Hemisphere Electrodes, and Median Rosto-Caudal Area – artifacts removed – no jitter compensation.

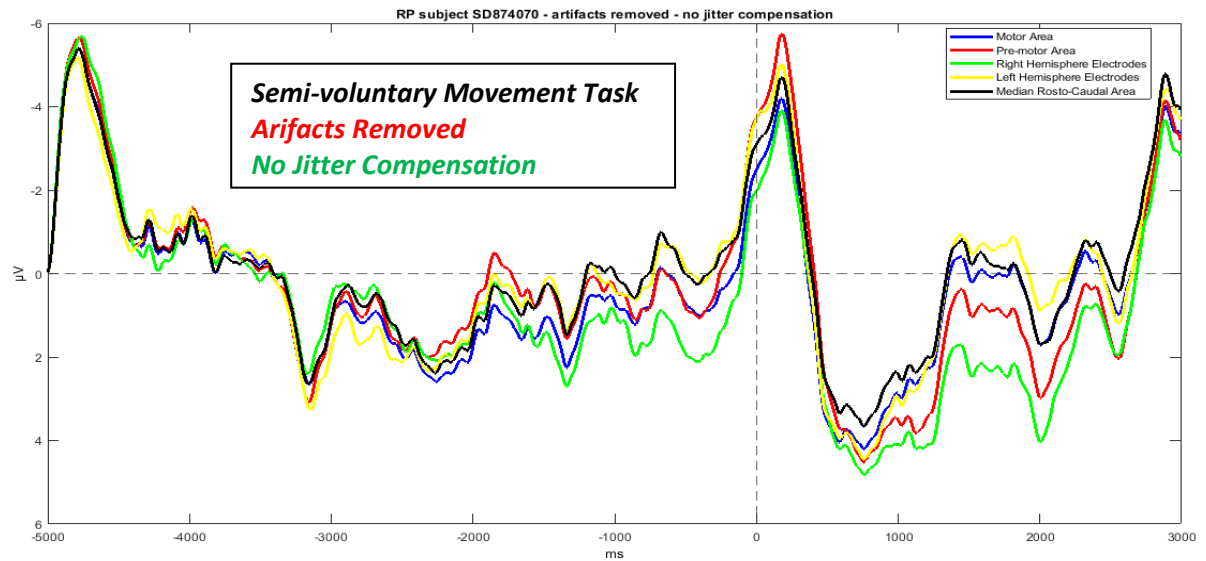Computing the algorithm, the waveforms of the RPs are completely random.

Figure 55 – RP over Motor Area, Pre-motor Area, Right Hemisphere Electrodes, Left Hemisphere Electrodes, and Median Rosto-Caudal Area – artifacts removed – with jitter compensation.

4.5.2 – Dataset LF864071

Also, for this dataset, we can see that all the SNRs of RPs are below the threshold after *1000 ms*.

Figure 56 – SNR of RP over Motor Area, Pre-motor Area, Right Hemisphere Electrodes, Left Hemisphere Electrodes, and Median Rosto-Caudal Area.

After removing the artifacts, we obtain many random oscillations with a maximum negative amplitude after the EMG onset.
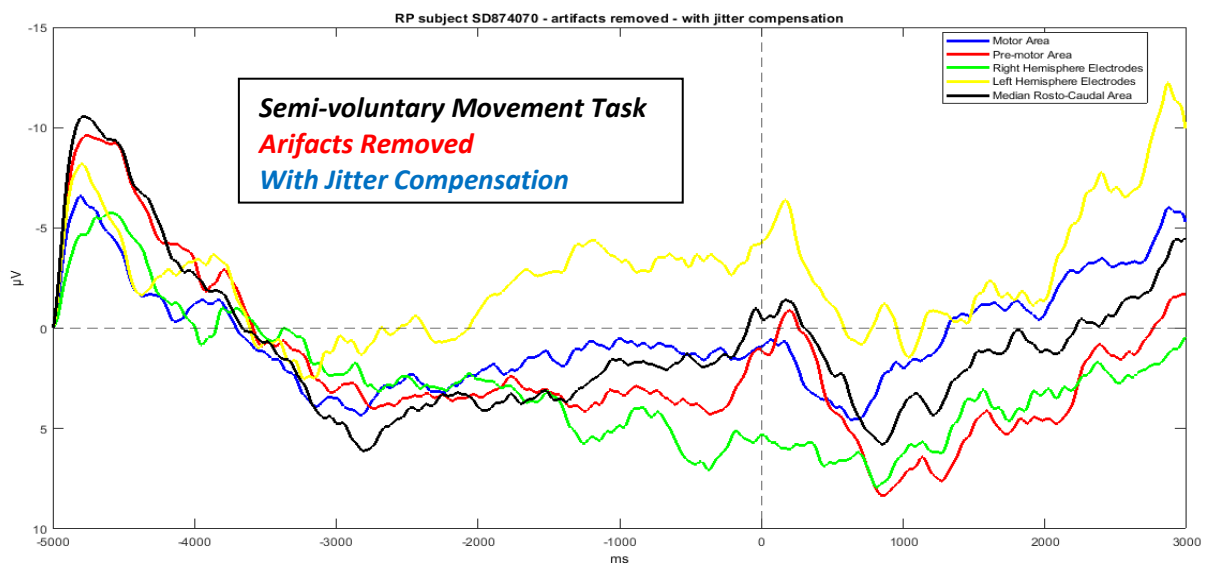
Figure 57 – RP over Motor Area, Pre-motor Area, Right Hemisphere Electrodes, Left Hemisphere Electrodes, and Median Rosto-Caudal Area – artifacts removed – no jitter compensation.

Also, in this case, computing the algorithm, none of the curves obtained corresponds to the waveform of the RP.
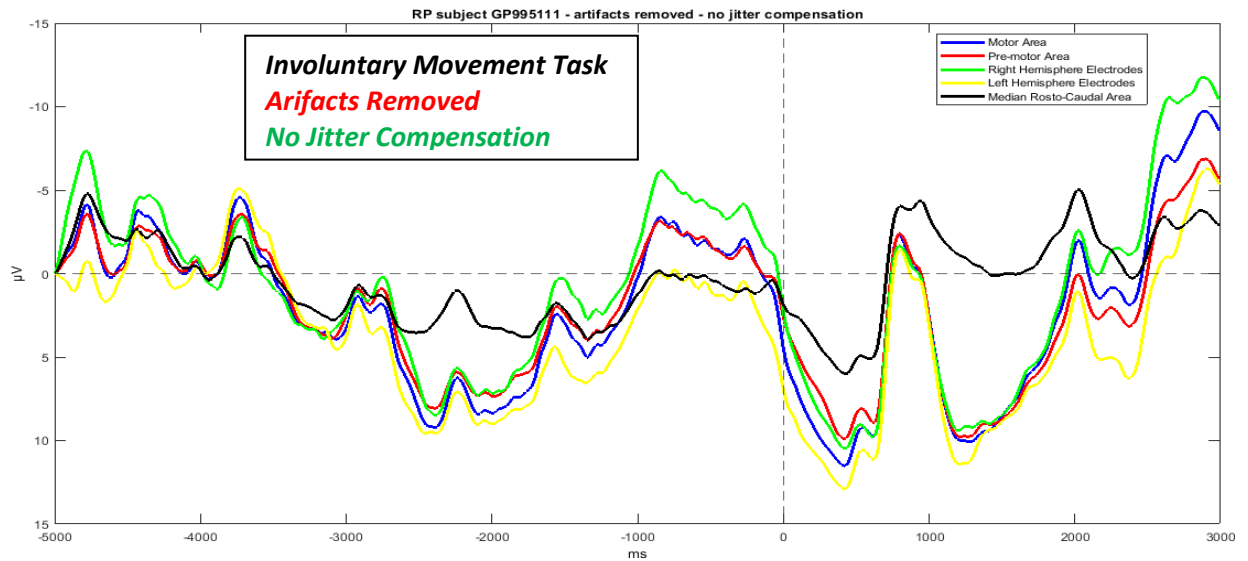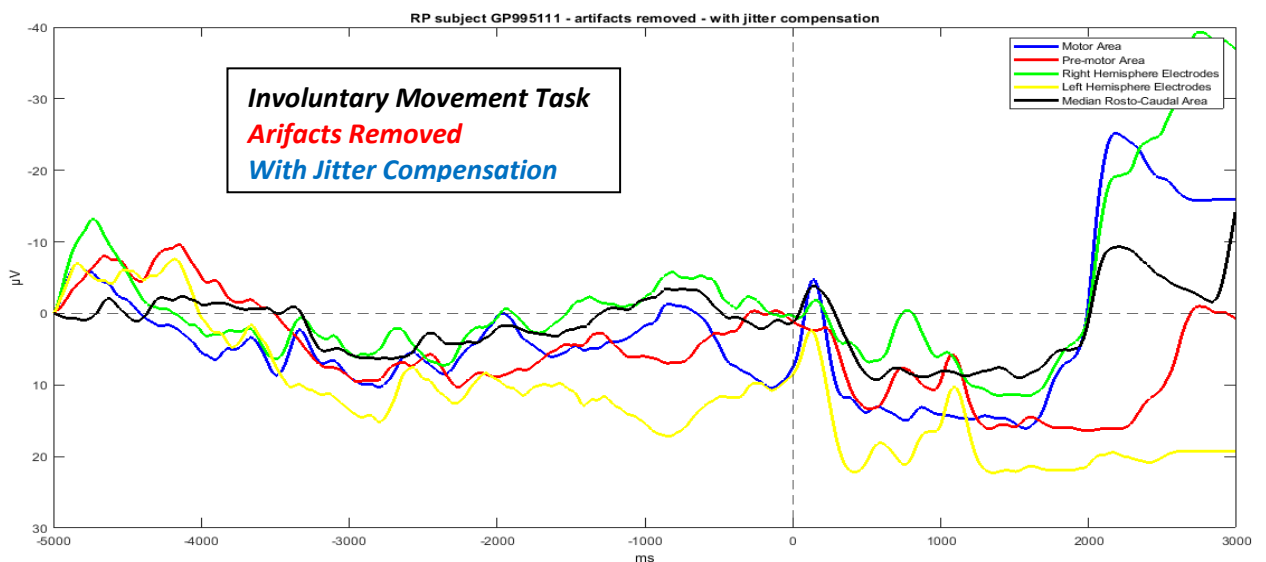

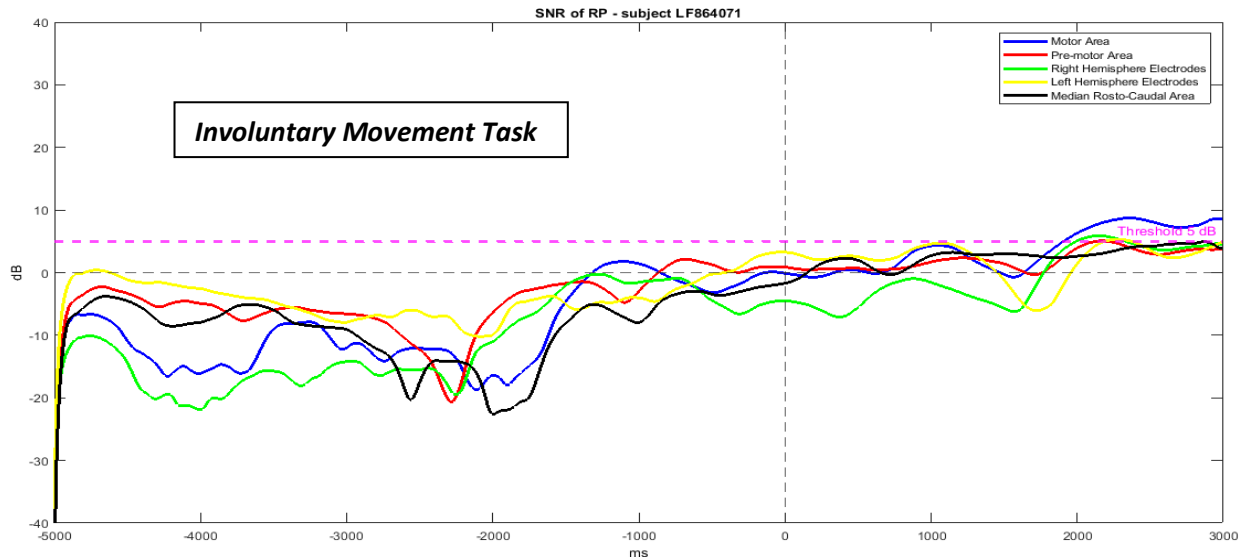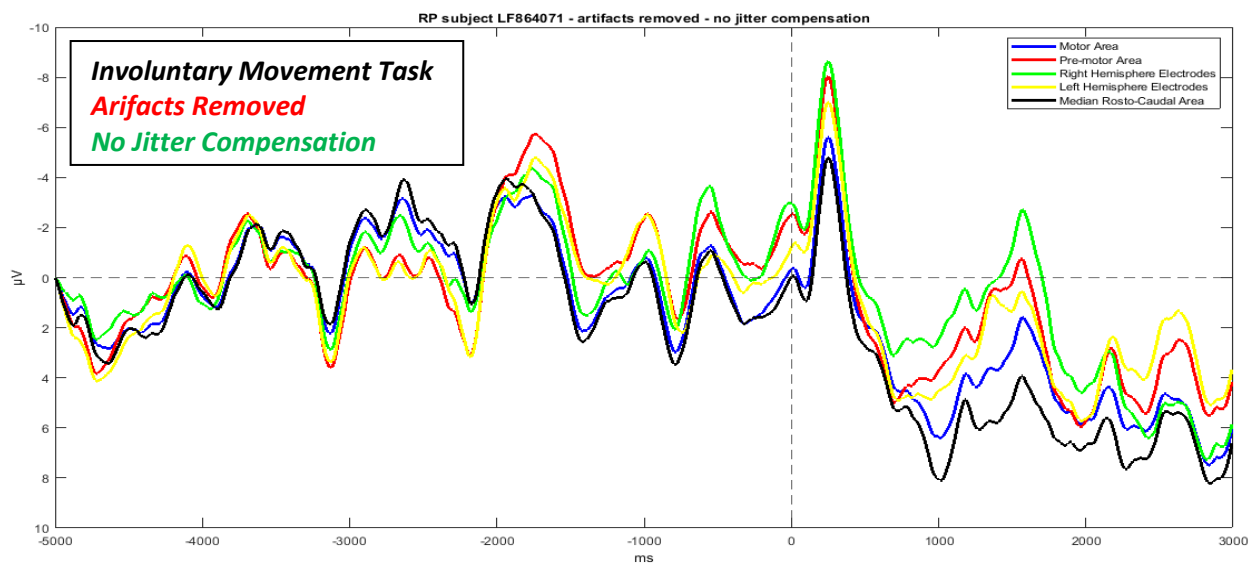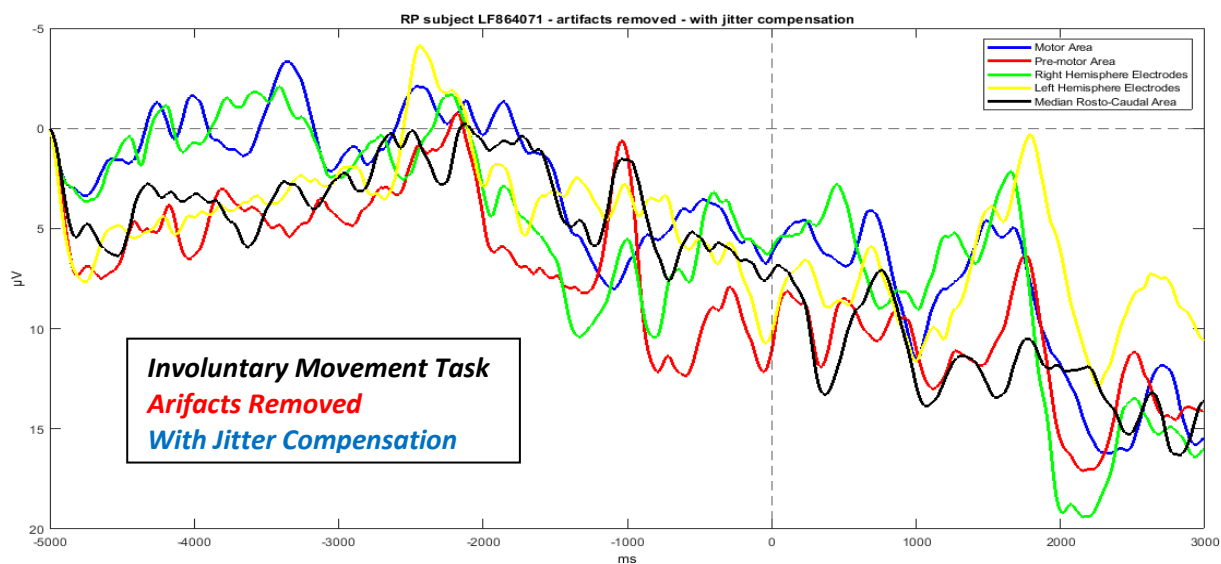**Figure 58 – RP over Motor Area, Pre-motor Area, Right Hemisphere Electrodes, Left Hemisphere Electrodes, and Median Rosto-Caudal Area – artifacts removed – with jitter compensation.**

4.6 – Discussion

As we can see from the graphs, the SNR shows us how much the signal is corrupted by the noise. From the SNR, we can see that the signal-to-noise ratio increases immediately after the onset of the EMG. Before the EMG onset, it shows that there is not much signal, then, as the onset approaches, a little better kind of signal-noise starts to be, and after that, we have only the signal. We all can this observe on the dataset GO862071, semi-voluntary task, which has the best waveforms of RPs than other datasets.

There should be a difference between the *Motor Area* and the *Pre-motor Area*, because over the *Pre-motor Area* there is more preparation for the movement, while over the *Motor Area* there is more movement. As we can note, over the *Pre-motor Area* there is a higher peak before the start of the movement.

So, this parameter allows us to say if how much larger the power of the signal is than the power of the noise. In datasets where jitter compensation works poorly, it is not because the method is incorrect, but because the signal is too much noise or has some artifact.

While what we can notice in the plots concerning the involuntary task, we do not get the RP at all, but only some random oscillations. As mentioned above, this is because the movement is not cortical, but performing the patellar reflex.

Chapter 5

Conclusions

We use the averaging technique to calculate the Readiness Potential. This technique consists of averaging the EEG signal on many trails, dividing the signal into epochs, aligning them to the onset of the movement considered as a trigger. The averaging technique is sensitive to latency jitter, which is a timing misalignment of the epochs when calculating RPs. To compensate for the unknown time jitter in computing of the RP, we implemented an algorithm, based on Woody's method, to improve the calculation of the RP by selecting the most correlated epochs, where the final RP is obtained by the average of all the realigned epochs. The algorithm is based on the correlation among the epochs so that we calculate all the possible correlations through the cross-correlation function. In this thesis work, we realigned the most correlated epochs by making a little adjustment to Woody's method.

We analysed the datasets acquired during the experimental session. Since the RP is detected over the Sensorimotor Cortex, including the Pre-motor and Motor areas, in correspondence of the pre-SMA, the SMA and M1 over the Frontal Lobe, and the Somatosensory Cortex over the Parietal Lobe. We considered 7 channels: *Cz, C3, C4* for the *Motor Area*; *Fcz, Fc3, Fc4* for the *Pre-Motor Area* and *Pz* for the *Somatosensory Area*. For that, we calculated five kinds of *RPs*: the *RP* over the *Median Rosto-Caudal Area* obtained by the average of the RPs over Cz, Fcz, Pz; the RP over the *Pre-motor Area* obtained by the average of the RPs over Fcz, Fc3, Fc4; the RP over the *Motor Area* obtained by the average of the RPs over Cz, C3, C4; the RP over the *Right Hemisphere of the Pre-Motor and the Motor Areas* obtained by the average of the RPs over Fc4, C4, and the RP over *the Left Hemisphere of the Pre-motor and the Motor Areas* obtained by the average of the RPs over Fc3, C3.

Compensating the jitter by using the algorithm, we got clear and distinguishable RPs in most of the datasets examined, both for the voluntary movement task and the semi-voluntary movement task. While in some datasets, we did not obtain RPs with a conventional waveform, this is because the signal is much noisy or contains artifacts. During the involuntary movement task performance, the subject does not do a cortical movement, but only the patellar reflex. So, we should not expect any RP. In fact, in the datasets examined, we do not get any RP but only random oscillations.

We calculated the SNR and we set an arbitrary threshold, equal to *5 dB* to identify when the power of the signal is larger than that of noise. The SNR shows us how much the signal is corrupted by the noise. From the SNR, we can notice that the signal-to-noise ratio increases immediately after the EMG onset. Before the onset of the movement, there is not much signal, then, as the onset approaches, we can see that a little kind of signal begins to be and after that, we can only observe the signal.

We have some differences between the Pre-motor Area and the Motor Area because the Pre-Motor Area denotes more preparation for the movement, instead the Motor Area indicates only the movement.

Therefore, this study demonstrates the validity of the algorithm to improve the averaging and enhance the RP signal quality.

A further advance of the study may be to investigate the level of consciousness in unresponsive patients, diagnosed in VS or MCS. So the SNR parameter should give us the *consciousness index* because the SNR shows us when the signal indicates the motor intention. Starting with the onset of the movement, where there is most of the power of the signal, we can deduce how much the subject wants to move.

Furthermore, the creation of *feature space* might be useful to classify the three types of movement: voluntary, semi-voluntary, and involuntary. The SNR parameter could be one of the components for the feature space.

Bibliography

[1] Haggard Patrick. Conscious intention and motor cognition. *Review, Trends in Cognitive Science, June 2005, Vol.9, No.6, 290-295.*

[2] Tononi Giulio. An information integration theory of consciousness. *BMC Neuroscience, 2004, Vol. 5, No. 42,5-42.*

[3] Chalmers D. J. The character of consciousness. *Oxford University Press, 2010.*

[4] Vimal R. Meanings attributed to the term "consciousness": an overview. *Journal of Consciousness Studies, 2009, 16(5), 9-27.*

[5] McGovern K., and Baars B.J. Cognitive theories of consciousness, 2007.

[6] Koch Christof. What is Consciousness? *Neuroscience, Springer Nature, 2018, Vol.557, S9-S12.*

[7] Laureys S., Majerus S., Gill-Thwaites H., and Andrews K. Behavioral evaluation of consciousness in severe brain damage. *Progress in Brain Research, 2005, Vol.150, 397-413.*

[8] Crick F., and Koch C. Are we aware of neural activity in primary visual cortex? *Nature,1995, 375 (6527), 121-123.*

[9] Abbate Carlo, and Mazzucchi Anna. La riabilitazione neuropsicologica dei disturbi globali della coscienza. *Elsevier Srl, 2012, Cap.20.*

[10] Giacino Joseph T., Schnakers C., Rodriguez-Moreno D., Kalmar K., Schiff N., and Hirsch J. Behavioral assessment in patients with disorders of consciousness: gold standard or fool's gold? *Progress in brain research, 2009, Vol. 177, Chapter 4, 33-48.*

[11] Giacino Joseph T., Ashwal S., Childs N., Cranford R., Jennett B., Katz D. I., and Zasler N.D. The minimally conscious state: definition and diagnostic criteria. *Neurology, 2002, 58(3), 349-353.*

[12] Laureyes S., Faymonville M. E., Luxen A., Lamy M., Frank G., and Maquet P., Restoration of thalamocortical connectivity after recovery from persistent vegetative state. *The Lancet, 2000, 335 (9217), 1790-1791.*

[13] Schiff N. D., Rodriguez-Moreno D., Kamal A., Kim K. H.S., Giacino J. T., Plum F., and Hirsch J. fMRI reveals large-scale network activation in minimally conscious patients. *Neurology, 2005, 64(3), 514-523.*

[14] Stender J., Kupers R., Rodell A., Thibaut A., Chatelle C., Bruno M. A., Geil M., Bernard C., Hustinx R., Laureys S., and Gjedde A. Quantitative rates of brain glucose metabolism distinguish minimally conscious from vegetative state patients. *J. Cereb Blood Flow Metabolism, January 2015,35(1), 58-65.*

[15] Laureys S., Perrin F., Brédart S. Self-consciousness in non-communicative patients. *Consciousness and Cognition, 2007, 16, 722-741.*

[16] Colman M.R., Bekinschtein T., Monti M. M., Owen A. M., and Pickard J. D. A multimodal approach to the assessment of patients with disorders of consciousness. *Progress in Brain Research, 2009, Vol. 177, Chapter 16, 231-248.*

[17] Owen A. M., and Coleman M. R. Functional MRI in disorders of consciousness: advantages and limitations. *Current Opinion in Neurology, Trauma and rehabilitation, 2007,20(6),632-637.*

[18] Coleman M. R., Rodd J. M., Davis M. H., Johnsrude I. S., Menon D. K., Pickard J. D., and Owen A. M. Do vegetative patients retain

aspects of language comprehension? Evidence from fMRI. *Brain, 2007, 130, 2494-2507.*

[19] Owen A. M., and Coleman M. R. Functional neuroimaging of the vegetative state. *Nature Reviews, Neuroscience, 2008, Vol. 9, 235-243.*

[20] Laureys S., Faymonville M. E., Degueldre C., Del Fiore G., Damas P., Lambermont B., Janssens N., Aerts J., Franck G., Luxen A., Moonen G., Lamy M., and Maquet P. Auditory processing in the vegetative state. *Brain, 2000, 123, 1589-1601.*

[21] Lapitskaya N., Coleman M. R., Nielsen J. F., Gosseries O., and Maertens de Noordhout A. Disorders of consciousness: further pathophysiological insights using motor cortex transcranial magnetic stimulation. *Progress in Brain Research, 2009, Vol. 177, 191-200.*

[22] Coyle D., Stow J., McCreadie K., McElligott J., Carroll Á. Sensorimotor Modulation Assessment and Brain-Computer Interface Training in Disorders of Consciousness. *Archives of Physical Medicine and Rehabilitation, 2015, 96 (2 Suppl 1), S62-70.*

[23] Neumann N., Kotchoubey B. Assessment of cognitive functions in severely paralysed and severely brain-damaged patients: neuropsychological and electrophysiological methods. *Brain Research Protocols, 2004, 14, 25-36.*

[24] Bekinschtein T. A., Coleman M. R., Niklison J., Pickard J.D., and Manes F. F. Can electromyography objectively detect voluntary movement in disorders of consciousness? *J. Neurol. Neurosurg. Psychiatry, 2008, 79, 826-828.*

[25] Haggard P., Clark S., and Kalogeras J. Voluntary action and conscious awareness. *Nature Publishing Group, 2002.*

[26] Macarelli O. Manuale Teorico Pratico di Elettroencefalografia. *Wolters Health Kluwer, Lippincott Williams & Wilkins. ISBN:* 9788875564278.

[27] Luck Stecen J. An introduction to the Event-Reltaed Potential Technique. *ISBN: 978026252585.*

[28] Deecke L., Grözinger B., and Kornhuber H. H. Voluntary Finger Movement in Man: Cerebral Potentials and Theory. *Biological Cybernetics, 1976, 23, 99-119.*

[29] Shibasaki H., nad Hallet M. What is the Bereitschaftpotential? *Clinical Neurophysiology, 2006, 117(11),2341-2356.*

[30] Ahmadian P., Cagnoni S., and Ascar L. How capable is non-invasive EEG data of predicting the next movement? A mini review. *Frontiers in Human Neuroscience,2013, Vol. 7, Article 124, 1-7.*

[31] Baker K. S., Mattingley J. B., Chambers C. D., and Cunnington R. Attention and the readiness for action. *Neurophycologia, 2011, 49, 3303-3313.*

[32] Jahanshahi M, and Hallett M. The Bereitschaftpotential : Movement-Reltaed Cortical Potentials. *Springer Science+Business Media, LLC, 2003, ISBN 978-1-4613-4958-7.*

[33] Eimer M. The lateralized readiness potential as an-online measure of central response activation processes. *Behavior Research Methods, Instruments & Computers, 1998, 30(1), 146-156.*

[34] Coles M.G.H. Modern Mind-Brain Reading: Psychophysiology, Physiology, and Cognition. *Psychophysiology, 1988, Vol. 26, No. 3, 251-269.*

[35] De Jong R. Use of Partial Stimulus Infromation in Response Processing. *Journal of Experimental Psychology: Human Perception and Performance, 1988, Vol.14, No. 4, 692-692.*

[36] Colebatch James G. Bereitschaftpotential and Movement- Related Potentials: Origin, Significance, and Application in Disorders of Human Movement. *Movement Disorders,2007, Vol.22, No.5, 601-610.*

[37] Haggard P., and Eimer M. On the relation between brain potentials and the awareness of voluntary movements. *Experimental Brain Research, 1999, 126, 128-133.*

[38] Hallett M. Volitional control of movement: The physiology of free will. *Clinical Neurophysiology, 2007, 118, 1179-1192.*

[39] Haggard P. Human volition: towards a neuroscience of will. *Nature Reviews-Neuroscience, 2008, 9(12), 934-946.*

[40] Rizzolatti G., and Sinigaglia C. So quel che fai – Il cervello che agisce e i neuroni specchio. *Raffaello Cortina Editore, 2006, ISBN 88-6030-002-9.*

[41]https://sccn.ucsd.edu/wiki/EEGLAB_TUTORIAL_OUTLINE#III.Advanced_Topics

[42] Cabasson A., and Meste O. Time Delay Estimation: A New Insight into the Woody's Method. *IEEE Signal Processing Letters, 2008, Vol.15, 573-576.*

[43] Woody C.D. Characterization of an adaptive filter for the analysis of variable latency neuroelectric signals. *Medical and biological engineering,1967, Vol.5,539-554.*